The Health Benefits of Solar Power Generation: Evidence from Chile

Nathaly M. Rivera*†

Elisheba Spiller‡

J. Cristobal Ruiz-Tagle§

This Version: October 2022

Abstract

Renewable energy can yield social benefits through local air quality improvements and their subsequent effects on human health. We estimate some of these benefits using data gathered during the rapid adoption of large-scale solar power generation in Chile over the last decade. Relying on exogenous variation from incremental solar generation capacity over time, we find that solar energy displaces fossil fuel generation, primarily coal-fired generation, and curtails hospital admissions, particularly those due to lower respiratory diseases. These effects are noted mostly in cities downwind of displaced fossil fuel generation and are present across the most vulnerable age groups. Our results document the existence of an additional channel through which renewable energy can increase social welfare.

Keywords: Coal-fired power plants, coal displacement, solar generation, power plants, pollution, morbidity, developing countries, Latin America
JEL classification numbers: I18, L94, Q42, Q53

*We thank Andrew Bibler, Janet Currie, Harrison Fell, Maria Harris, Sarah Jacobson, Nicolai Kuminoff, Lucija Muehlenbachs, Subhrendu K. Pattanayak, and Brett Watson for their helpful comments and suggestions. We also thank seminar participants at CAF, CERE-Umeå University, Environmental Defense Fund, FGV-EESP, Grantham Workshop, Insper, Manhattan College, Adolfo Ibañez University, North Catholic University, PUC-Chile, University of Chile, University of São Paulo, University of Talca, and workshop and conference participants at the 21st Annual CU Environmental and Resource Economics Workshop, the 25th Annual Conference of the European Association of Environmental and Resource Economists, the 2021 Association of Environmental and Resource Economists Annual Summer Conference, Camp Resources XXVI, the 7th Canadian Resource and Environmental Economics Association Workshop, the 2020 Eastern Economic Association Annual Meeting, the 2021 Empirical Methods in Energy Economics Summer Workshop, 2021 SETI Annual Meetings, Tercer Workshop Sobre Economía del Medio Ambiente y Cambio Climático, the 2021 Western Economic Association International Annual Conference, and the 2022 PDRI Conference on Climate Change the Environment, for helpful comments and suggestions. All errors are ours. A significant part of this work was written when Rivera was at the University of São Paulo and Spiller at the Environmental Defense Fund.

†Corresponding author. University of Chile, ✉: nmrivera@fen.uchile.cl.

‡Resources for the Future, ✉: bspiller@rff.org.

§London School of Economics and Political Science, ✉: j.c.ruiz-tagle@lse.ac.uk.

1 Introduction

Renewable energy is the world's fastest-growing energy source, set to become the leading source of primary energy consumption by 2050 (U.S. Energy Information Administration, 2019). It can provide several benefits to society, ranging from reductions in greenhouse gas emissions and discharges of local air pollutants to reduced dependence on imported fuels and the creation of jobs through the manufacturing and installation of these resources (U.S. Environmental Protection Agency, 2019). Yet, we still lack a good understanding of the magnitude of some of these benefits, notably those associated with reduced air pollution and health improvements. In this work, we use the rapid adoption of large-scale solar power generation in the desert region of northern Chile to empirically quantify some of the health benefits of solar energy through improvements in air quality.

Fossil fuel power generation, particularly that from coal combustion, releases large amounts of local air pollutants, including sulfur dioxide (SO_2), nitrogen oxides (NO_X), and particulate matter (PM). These pollutants are associated with several adverse health effects, along with increased hospital admissions, mortality risks, and threats to life expectancy.[1] The extent to which these emissions are curtailed with the introduction of renewables reflects the potential of alternative energy sources to offset some of the negative effects of dirty electricity generation. Nonetheless, some fossil fuel plants (e.g., natural gas plants) have consistently been dispatched to deal with the intermittency of renewables (Fell and Linn, 2013), thereby attenuating the benefits of increasing the supply of these sources. More insights on the co-benefits of renewable energy are, therefore, crucial to the cost-benefit analyses of transitioning away from fossil fuels and, in turn, for the optimal design of energy policy.

The Atacama Desert, one of the sunniest and driest deserts in the world, not only has the highest average surface solar radiation worldwide (Rondanelli et al., 2015), but also the highest solar power potential. Figure 1 shows Chile's photovoltaic power potential—a solar energy system's maximum productivity over time—relative to the rest of the world. This potential, together with the recent decline in the cost of photovoltaic (PV) technology and the country's regulations aimed at fostering the adoption of renewables, resulted in rapid market penetration of solar generation in Chile. By the end of 2012, a variety of solar plants with capacities ranging from 3 MW to 138 MW were already injecting electricity into Chile's northern electric grid. By 2017, solar accounted for 10 percent of the system's total generation. We take advantage of this surge in large-scale investments in solar energy to explore the effects of the steady expansion in solar capacity on generation from thermal

[1] For comprehensive reviews, see Currie et al. (2014) on the effects of early-life exposure to pollution, and Hoek et al. (2013) on the mortality impact of long-term air pollution exposure.

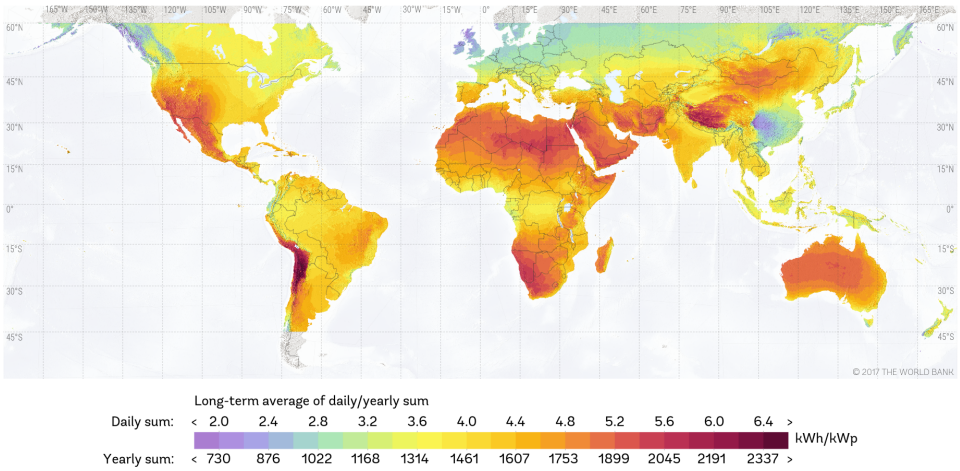

Figure 1: Chile's Photovoltaic Power Potential (kWh/kWp)

Notes: This figure shows Chile's photovoltaic power potential, which refers to how much energy (kWh) is produced per kilowatt peak (kWp) of a system. Figure retrieved from `https://globalsolaratlas.info`. Solar resource data was obtained from the *Global Solar Atlas*, owned by the World Bank Group and provided by Solargis.

plants and on human health in northern Chile. By exploring the case of Chile, we add to the scant literature on power plant pollution exposure and health impacts in emerging economies (Gupta and Spears, 2017; Barrows et al., 2018).

Our study uses data on solar generation between 2012 and 2017. To identify the effects of this increasing solar expansion, we first estimate the extent to which solar plants displace other power facilities using daily variation in plant-level power generation capacity.[2] For solar generation to have a positive effect on health outcomes, it must first displace generation by thermal plants, thereby reducing pollution levels from the baseline.[3] After identifying the set of displaced thermal power plants, we estimate a reduced form health equation on the effect of daily solar generation on daily hospital admissions. In particular, we use hospital admissions of patients with diagnoses associated with cardiovascular and respiratory diseases, conditions generally related to the combustion of fossil fuels. To reduce any potential endogeneity between power generation and health as well as to take into account the transport of pollutants, we leverage our findings on fossil fuel plant displacement and identify cities that are downwind to and near these displaced plants, and run separate regressions for this subsample of cities. In doing so, we rely on the identifying assumption that the harmful

[2]Ideally, we would use plant-level emissions data. Unfortunately, the emissions data that are collected by the government are not observed data, rather, they are engineering estimates based on generation (thus, they are a simple transformation of the kWh generated in each hour). Due to this data limitation, we utilize generation as a proxy for emissions.

[3]The alternative is that solar generation rises to meet expanding demands for electricity. In this case, there would be no displacement of fossil fuel plants, and the health impacts of the energy system would remain unchanged, although health improvements would have been seen relative to a counterfactual of increased fossil fuel generation in response to increased loads.

effects of local air pollution exposure are stronger downwind of the pollution source and decrease with distance. Finally, to attribute the health effects to air quality improvements, we use additional (but limited) data on fine PM concentrations for a subset of our cities and estimate an instrumental variable approach that uses solar as an instrument for pollution in our health regressions.

Our results show that increased solar generation in Chile led to a displacement of daily thermal generation, particularly of coal- and gas-fired power generation. This displacement is robust to leveraging variation in daily solar capacity factor, suggesting that increased solar capacity over time is driving the results. Subsequently, we find that, through this displacement, solar generation reduces respiratory admissions, particularly admissions due to lower respiratory diseases in all cities included in our sample. We find these reductions to be predominantly in cities downwind of and in close proximity to these displaced facilities. Specifically, we find that one additional GWh of solar generation led to a 10.8% reduction in hospital admissions due to lower respiratory conditions across all cities, and to a 14.5% reduction across downwind cities within $10km$ of distance from displaced fossil fuel plants. Our analysis by age group indicates that these reductions are mostly observed among infants (less than 1 year old) and toddlers (ages 1–5), the most vulnerable age groups, and occur primarily after short-term exposure to abated pollution from displaced thermal plants. These results remain unchanged after several robustness checks, which include the use of predicted displacement, alternative estimation methods, the use of cities upwind of displaced facilities and those downwind of non-displaced units, and the use of hospital admissions of patients with diseases presumably not related to air pollution as alternative outcomes. An alternative analysis using limited air pollution monitoring data also corroborates these results.

Several reasons lead us to consider our findings as a lower bound on the true health benefits of solar generation, particularly in developing countries. First, our area of study (Chile's northern region) has limited healthcare infrastructure. Therefore, any reduction in hospitalizations may have a beneficial spillover effect by increasing the number of hospital beds available in turn helping reduce the number of untreated unrelated injuries and illnesses. Second, reductions in air pollution exposure for young children and infants have a lifelong benefit in terms of reduced illnesses and improved economic outcomes (Currie et al., 2014). Third, communities with greater shares of low-income households and minorities may live closer to large air polluters in Chile, as has been demonstrated in both the U.S. and India (Banzhaf et al., 2019; Kopas et al., 2020).[4] In this case, improvements in air quality may

[4]Previous evidence shows indications that lower-income populations in Chile are more likely to live near environmental disamenities, such as mining. For example, Rivera (2020) finds that residential properties near mining sites in northern Chile have lower values and that these values are particularly salient for new residents in the area, suggesting an environmental-based sorting. These inequities may also be caused by

not only bring greater long-term benefits to populations experiencing uneven exposure to air pollution but also help to reduce inequities caused by pollution exposure.[5]

A wide number of papers document the displacement of coal-fired power plants, either through a decline in the price of natural gas (Linn et al., 2014; Knittel et al., 2015; Cullen and Mansur, 2017; Holladay and LaRiviere, 2017; Linn and Muehlenbachs, 2018; Johnsen et al., 2019), through the expansion in renewable generation capacity (Kaffine et al., 2013; Cullen, 2013; Novan, 2015; Callaway et al., 2018; Fell et al., 2021; Bushnell and Novan, 2021), or through interactions between the two (Holladay and LaRiviere, 2017; Fell and Kaffine, 2018). These studies also document significant interactions among competing renewables, whereby solar generation can lead to a shift in the supply of hydropower. To the extent that renewables offset and displace one another, the injection of new renewable sources into the grid may lead to ambiguous environmental impacts. One of the benefits of conducting this analysis in northern Chile is the small amount of non-solar renewables on the grid during the study period (contributing only 6% of total capacity in 2017, combined). This allows us to effectively isolate the impact of solar generation on fossil fuel displacement more clearly.

We extend this previous literature by empirically documenting some of the consequences of thermal displacement on morbidity outcomes. A small subset of literature estimates the effect of changes in the power sector on health. For example, Burney (2020) estimates the health benefits associated with the shift from coal to natural gas combustion in the U.S., finding that the exit of coal-fired plants between 2005 and 2016 saved approximately 26,000 lives. Along those lines, Casey et al. (2018a) find that coal and oil power plant retirement in the U.S. led to improvements in fertility outcomes, and Casey et al. (2018b) show the link between these retirements and a decrease in preterm births among nearby populations. Our work adds to this literature, presenting new evidence on the benefits that curtailing coal-fired generation has on morbidity. Moreover, we estimate this impact even without coal plant retirement; rather, we can identify the health benefits of having a large amount of solar generation at the intensive margin, even if it does not lead to coal plant shutdowns. In doing so, we contribute to the literature by quantifying the value of curtailing coal-fired generation.

The analysis of solar generation also represents an advantage in evaluating the health benefits of renewables relative to other similar sources such as wind. Increases in wind power generation may be associated with reduced pollution due to higher wind speeds and

housing siting decisions; for example, Rau et al. (2015) shows evidence of government housing projects built in close proximity to mining waste sites in the city of Arica, also located in northern Chile.

[5]There are additional benefits from power plants' emission reductions that go beyond the health and emissions dimensions. For instance, see Rivera and Loveridge (2022) and Mei et al. (2021) on the property value impacts of fuel switching in the U.S. and China, respectively.

greater dispersion, hampering the identification of health impacts. One exception, however, is Fell and Morrill (2022) which find fewer emergency room visits in Texas due to day-to-day variation in wind energy and a subsequent curbing of thermal generation. An alternative body of work identifies the health benefits of a cleaner grid (Spiller et al., 2021; Anenberg et al., 2012; Muller and Mendelsohn, 2009) or the addition of new utility-scale solar capacity (Sergi et al., 2020) in integrated assessment frameworks. These studies employ cutting-edge air transport and chemical transformation models but use existing epidemiological literature and underlying health and population statistics to calculate the impact of policies on health. To the best of our knowledge, we are the first to *empirically* test the impact of increased large-scale solar generation on health. Therefore, our work also adds to the growing literature on the co-benefits of renewable generation (Siler-Evans et al., 2013; Barbose et al., 2016; Buonocore et al., 2016; Spiller et al., 2017; Millstein et al., 2017; Fell and Morrill, 2022), a key aspect in evaluating the economic potential of renewable energy portfolios (Edenhofer et al., 2013; Wiser et al., 2017; Hollingsworth and Rudik, 2019), and in the design of health-based air quality regulations (Abel et al., 2018; Thakrar et al., 2020).

The remainder of our work proceeds as follows. We review the literature on the health effects of power plant emissions in Section 2, demonstrating that emissions from thermal power generation can cause a variety of different negative health impacts, with major morbidity impacts on respiratory and cardiovascular outcomes—the two health outcomes on which we focus. In Section 3, we describe the power sector in Chile detailing the aspects of the independent northern grid we are studying in this paper as well as describing how plants are dispatched, which helps inform our displacement analysis. We present the data in Section 4, including data on health outcomes, power plant generation, wind directions, and control variables such as demographic information. In Section 5, we lay out our empirical strategy as well as our identification approach, which relies upon wind direction and the results from our displacement analysis to identify downwind cities. The results and robustness checks are in Sections 6 and 7, respectively, where we show that solar can effectively displace thermal power generation and improve health outcomes, particularly in downwind cities, and that our results are robust across different methodologies and approaches. Finally, we conclude in Section 8 with a discussion about the policy implications of our findings.

2 Power Plants' Emissions and Health Consequences

Fossil-fuel electricity generation accounts for a large share of greenhouse gas emissions, particularly carbon dioxide (CO_2). The sector is also a major driver of outdoor air pollution, primarily due to the burning of coal, which releases important amounts of airborne pollutants

such as sulfur dioxide (SO_2), nitrogen oxides (NO_X), mercury (Hg), and particulate matter (PM). All of these pollutants are associated with adverse health effects, mortality risks, and threats to life expectancy (Chay and Greenstone, 2003a,b; Currie and Neidell, 2005; Currie et al., 2009; Chen et al., 2013; Arceo et al., 2016; Knittel et al., 2016; Schlenker and Walker, 2016; Lavaine and Neidell, 2017). Here, we briefly summarize the evidence on the detrimental health impact of exposure to the main pollutants from coal combustion. Evidence suggests its displacement by solar generation is expected to curtail mostly SO_2, NO_X, and PM emissions.

SO_2 is an invisible gas, part of the sulfur oxide (SO_X) family of gases, formed when fuel containing sulfur (e.g., coal, oil) is burned (U.S. Environmental Protection Agency, 2014). Exposure to high concentrations of SO_2 is associated with eye, nose, and throat irritation, infectious complications of chronic obstructive pulmonary disease, and increases in hospital admissions due to obstructions of the lower airway (e.g., asthma) (World Health Organization, 2006). SO_2 reacts with other compounds in the atmosphere to form fine PM. PM is the general term used to describe solid particles, dust, and drops found in the air, all with different compositions and sizes. Evidence on the health impact of exposure to coarse PM (PM_{10}) and fine PM ($PM_{2.5}$) suggests detrimental effects on a variety of health outcomes, including respiratory diseases (Schwartz, 1996), cardiovascular diseases (Schwartz and Morris, 1995; Brook et al., 2010; Franklin et al., 2015), low birth weight (Currie et al., 2009; Currie and Walker, 2011), and infant mortality (Chay and Greenstone, 2003a,b; Arceo et al., 2016; Knittel et al., 2016).

NO_X are reactive gases and include nitrogen dioxide (NO_2), nitrous acid (HNO_2), and nitric acid (HNO_3). Although mobile sources may contribute to greater releases of NO_X into the atmosphere, stationary fossil fuel combustion represents a significant portion of annual domestic NO_X emissions. Outdoor exposure to NO_X has been found to increase asthma and bronchitis diagnoses in children (Pershagen et al., 1995; Chauhan et al., 2003; Gauderman et al., 2005), and on older populations (Schlenker and Walker, 2016). This pollutant can also react in the presence of heat and sunlight in the atmosphere to create ground-level ozone, a harmful chemical associated with lung diseases and premature deaths (Bell et al., 2004, 2005).

3 The Power Sector in Chile

The electricity sector in Chile is composed of three different segments: generation, transmission, and distribution, all 100% privately owned. Before 2018, Chile's electricity market featured four different electric systems (see Appendix Figure A1): two major interconnected

systems, the Northern Interconnected System (SING) and the Central Interconnected System (SIC); and two additional minor grids, the Aysen Electric System (SEA) and the Magallanes Electric System (SEM). The SING system, located in Chile's northern region, has 5 GW of installed capacity, 2.5 GW of peak load, and more than 85% reliance on fossil fuel generation (i.e., coal, natural gas, and diesel). Although the northern region of Chile is relatively unpopulated, with SING serving only 7% of the country's total population, this region hosts most of the large-scale copper mining companies that operate in the country, a sector characterized by its electricity-intensive production activities.[6]

3.1 The Generation Segment

Electricity generation in Chile is produced in a competitive market, though the transmission and distribution sectors are regulated. Generation at SING is characterized by a spot market, long-term forward contracts, and capacity payments. The spot market relies upon merit-order dispatch under the coordination of the Economic Load Dispatch Center (CDEC), which, to meet the system's load, dispatches generators at every hour based strictly on their marginal cost. Thus, the hourly marginal cost of the system equals the cost of the most expensive unit being dispatched (Galetovic and Muñoz, 2011).[7] This dispatch, determined by CDEC based on fuel costs, informs our methodology in estimating the displacement of fossil fuel plants by solar generation. Specifically, we incorporate the relative costs of fossil fuels into our dispatch equation to control for the market forces that will play a large role in determining dispatch and the ability of solar to displace fossil fuel plants (see Section 5.1).

On the Increase in Solar Generation. Although numerous PV systems have existed in Chile since 2007, they were mostly in the form of small-scale stand-alone systems and part of rural electrification programs (Haas et al., 2018). In 2008, however, the Chilean government established a quota system for renewable energies ("Ley de Energías Renovables No Convencionales"—ERNC); this currently requires these sources to account for 20% of participation in the energy mix by 2025 (Ministry of Energy, 2013). The ERNC policy, in combination with decreasing costs in PV technology, led to the installation in 2012 of the first large-scale solar plant in northern Chile, La Huayca, adding 25.05 MW of gross capacity

[6]Conversely, the SIC system, located in central-south Chile and with 17 GW of total installed capacity and 7 GW of peak load, relies heavily on hydro generation (around 35%) and serves 90% of the country's population. These two major grids, SING and SIC, began an interconnection process in November 2017 that resulted in a full integration by May 2019, thereby creating Chile's National Electric System (SEN). In this paper, we focus on the period before November 2017, thus avoiding any potentially confounding factors that may be associated with the interconnection itself.

[7]Regardless of whether generators are dispatched, each of these agents receives a monthly capacity payment aimed at guaranteeing enough generation capacity to supply energy during times of peak demand.

to SING. By 2015, solar participation at SING reached 119 MW, equivalent to 2% of the total daily system generation (≈.376 GWh). By the end of 2017, this participation had grown to 655 MW, equivalent to 10% of total daily system generation (≈1.5 GWh).[8]

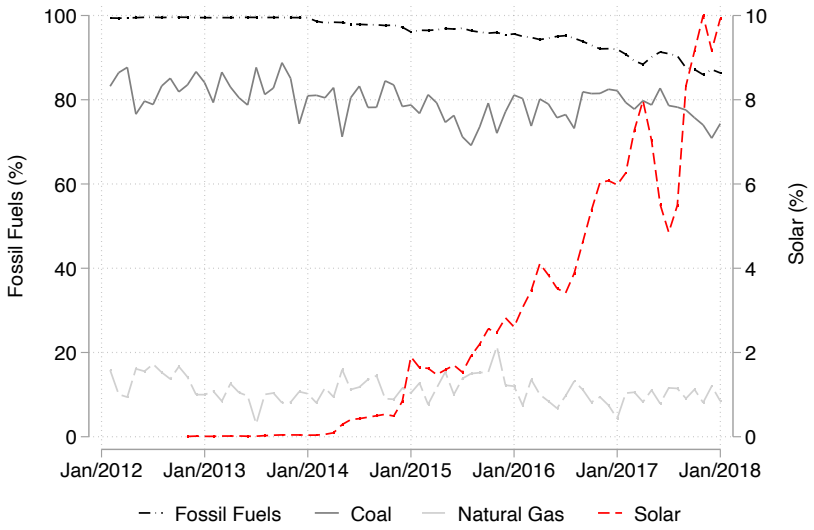

Figure 2: SING's Monthly Fossil Fueled and Solar Power Generation

Notes: This figure shows monthly power generation at Chile's northern grid, SING, by fuel source from 2012 to 2017. Data are reported in percentages relative to SING's monthly generation. Fossil fuels' monthly generation is shown in the main y-axis. Solar monthly generation is shown in the secondary y-axis. Data come from the National Electricity Coordinator from 2012 to 2017.

This can be seen clearly in Figure 2, which depicts the share of SING's monthly power generation by both fossil fuel and solar facilities during the sample period. At the start of the period, power generation at SING was (almost fully) coming from fossil fuels, with coal alone representing around 85% and natural gas roughly covering the other 15%. The increase in solar over time coincides with the persistent decrease in fossil fuel power generation over the same period. By the end of 2017, coal-generated electricity represented around 77% of SING's monthly generation, while natural gas use was equivalent to less than 10%.[9]

3.2 Power Plants' Emissions

The power sector accounts for roughly 40% of Chile's total greenhouse gas emissions. It produces 34,568.2 kt and 1.6 kt of carbon dioxide equivalent emissions (CO_2e) due to

[8]Data retrieved from the annual reports of Chile's National Energy Commission (CNE), https://www.cne.cl/nuestros-servicios/reportes/informacion-y-estadisticas/

[9]Appendix Figure A4 shows SING's total monthly load over the sample period (dashed line). The increasing trend in demand over time indicated in this graph rules out a demand-driven reduction in fossil fuel power generation. The figure also shows that SING's total monthly solar generation (solid line) has increased at a faster rate than demand over the same period.

CO_2 and methane (CH_4) discharges, respectively (Chile Environmental Ministry, 2018). In terms of criteria air pollutants, the sector is responsible for more than 30% of the country's total NO_X and SO_2 emissions, a situation that is aggravated by the longevity of some fossil fuel power plants, as older plants generally emit more. In SING, for instance, some coal-fired generators are the oldest in the country, with ages that in some cases exceed 50 years (Programa Chile Sustentable, 2017). Annual discharges from the sector comprise 57% and 40% of the northern grid's total SO_2 and NO_X emissions, respectively (Chile Environmental Ministry, 2017). Regarding PM, the country generally registers high levels of daily average $PM_{2.5}$ concentrations, and in northern Chile, these levels are largely due to the region's dependence on fossil fuel power generation (Chile Environmental Ministry, 2017).[10]

Air pollution monitoring at the city level is limited in the country. For the cities in our analysis, only four of them have monitoring stations that record $PM_{2.5}$, and only one of them records NO_X and SO_2 concentrations. Appendix Figure A2 depicts monthly average $PM_{2.5}$ concentrations from 2012 to 2017 across the four cities in our sample with available $PM_{2.5}$ daily data. We include in solid gray the date (month and year) of connection of the solar plants in our sample and in dashed red the WHO's air quality standard of 15 $\mu g/m^3$ for 24-hour averages as a reference. As shown, monthly average concentrations have decreased over time but still exceed air quality standards during certain times of the year. This situation highlights the importance that solar-powered electricity can play in reducing environmental-related health concerns in areas with a heavy reliance on fossil fuels.

Figure 3 illustrates hourly average SO_2 (3(a)), NO_X (3(b)) and $PM_2.5$ (3(c)) concentrations in one of these cities, Tocopilla, the city with the highest number of coal-fired plants in SING. We see the distribution of hourly pollution 30 days before the first solar connection in our sample (black line), and 30 days after the last one (gray line). Relative to the situation before the first solar connection, Figure 3(a) depicts a statistically significant decrease in hourly SO_2 concentrations right after all solar plants were connected to the system, particularly during the hours in which solar panels are at peak capacity (between 10 am and 3 pm). We see a similar trend in panel (b) for NO_X, although the difference in concentrations before and after seems to lack statistical significance. Finally, panel (c) shows that $PM_{2.5}$ significantly decreased during hours of morning sunshine: from 8 am to 11 am. The extent to which these reductions are effectively due to the entry of new solar installations anticipates the potential positive health impact of a cleaner grid.

[10]Previous studies have documented some of the harmful effects of PM exposure in Chile. For instance, Dardati et al. (2021) show that increases in $PM_{2.5}$ lead to a rise in respiratory emergency room visits, Bonilla et al. (2021) document a positive association between long-term $PM_{2.5}$ exposure and incidence of COVID-19 mortality, and Bharadwaj et al. (2017) expose some of the long-term harmful effects of early-life exposure to CO (and PM) on cognitive performance.

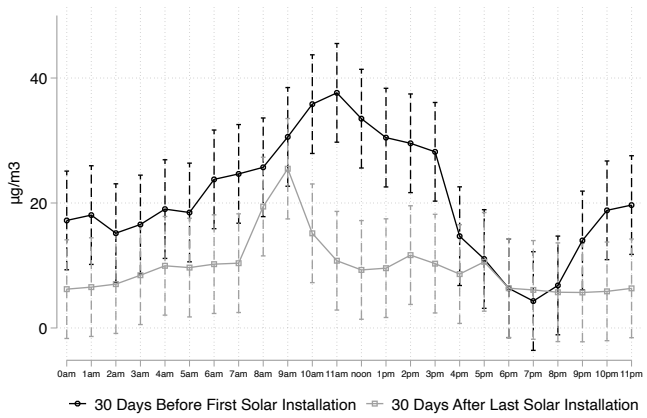

(a) SO_2

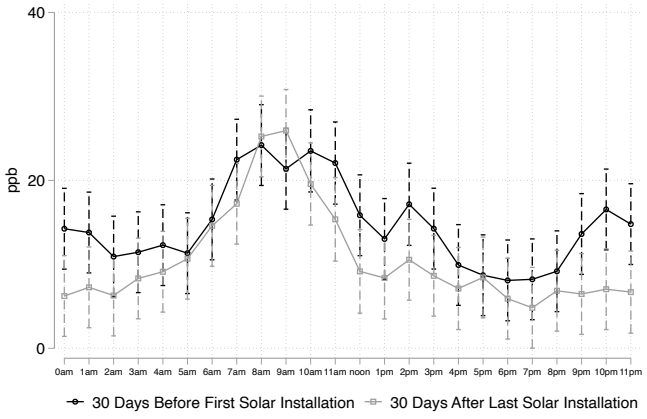

(b) NO_X

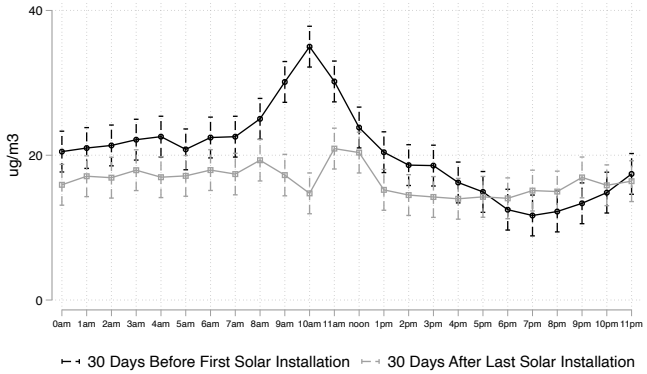

(c) $PM_{2.5}$

Figure 3: Hourly Sulfur Dioxide (SO_2), Nitrogen Oxide (NO_X), and Fine Particulate Matter ($PM_{2.5}$) Average Concentrations in Tocopilla Before and After the First Solar Connection

Notes: This figure shows point estimates and 95% confidence intervals for hourly average concentrations in the city of Tocopilla 30 days before and 30 days after the first and last solar power connections. Point estimates are obtained after regressing hourly concentrations averaged across stations on dummies for hours interacted with an indicator taking the value of 1 for observations after the last solar connection, and 0 for observations before the first solar connection. Hourly predictions "30 days before the first solar connection" correspond to observations before October 1st, 2012. Hourly predictions "30 days after the last solar connection" correspond to observations after July 21st, 2017. SO_2 and $PM_{2.5}$ are measured in micrograms per cubic meter of air ($\mu g/m^3$), and NO_X in parts per billion (ppb). Data come from the Ministry of Environment through the National Air Quality Information System (SINCA). From the original data, we trim the top and bottom 1% of all observations.

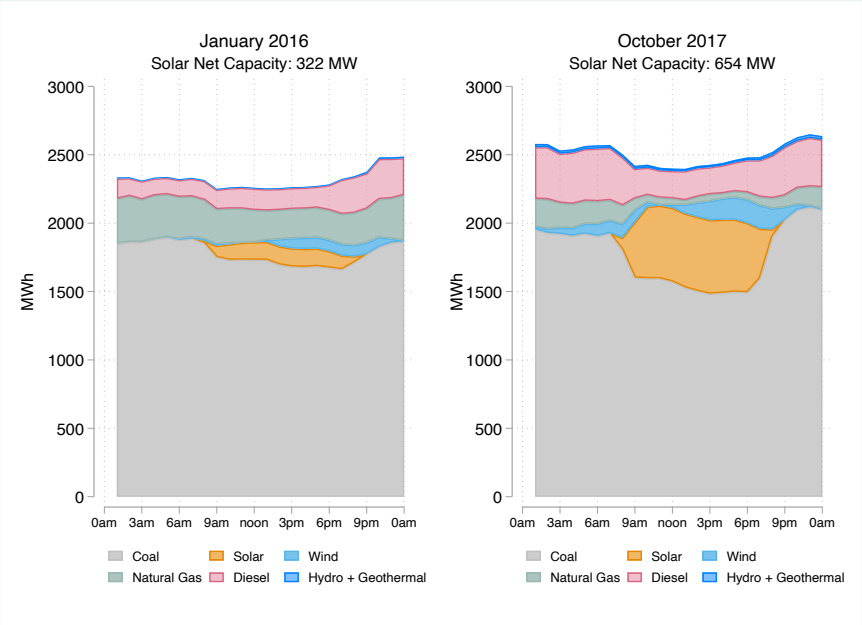

Figure 4: SING's Hourly Generation by Fuel Before and After Large-Scale Solar Installations

Notes: This figure shows SING's total hourly generation by fuel source before and after large-scale solar power generation investments. The left-hand side graph shows hourly generation (in MWh) by fuel averaged over the first week of January 2016 (with 322 MW of net solar capacity). The right-hand side graph shows hourly generation (in MWh) by fuel averaged over the last week of October 2017 (with 654 MW of net solar capacity). Data come from the National Electricity Coordinator from 2016 to 2017.

Notwithstanding, reductions in pollution over time could potentially be explained by other factors such as improvements in emissions intensity from coal and natural gas plants, or the retirement of dirty, old fossil fuel plants during this time period. In this case, we would expect to see reductions across all hours, particularly those hours in which coal and natural gas were on the margin. However, Figure 4 on SING's hourly generation by fuel source suggests otherwise. This figure illustrates hourly generation averaged over the first week of January 2016 (left-hand side, total of 332 MW of solar capacity), and the last week of October 2017 (right-hand side, total of 654 MW of solar capacity), just before the SING–SIC interconnection.[11] When comparing these two periods in Figure 4, we observe increased solar capacity largely displaced hourly coal- and gas-fired combustion during Atacama's sunlight hours (7 a.m.–7 p.m.). Additionally, it demonstrates a relatively flat load. Thus, improvements in emissions intensity and/or exit of dirty fossil fuel plants would most likely lead to an overall reduction in emissions across all hours and would unlikely have a particularly large effect during sunshine hours. Thus, Figure 3 and Figure 4 together suggest solar is leading to drops in air pollution during the sunshine hours as it displaces fossil fuel generation, mostly coal-fired generation.

Preferably, we would test the main hypothesis of this paper using data similar to those in

[11] Unfortunately, publicly available hourly generation data start only in 2016.

Figures 3 and A2. As mentioned earlier, however, we lack comprehensive city-level data on airborne pollution concentrations for all the cities in our sample, as air quality monitoring stations in Chile are scarce for cities other than Santiago. We address this limitation with our displacement analysis, effectively proxying for changes in emissions due to changes in fossil fuel-based generation. Later in the paper, we employ the available data on $PM_{2.5}$ concentrations for the four cities in our sample as an additional test on our results (see Section 6.2.2).

4 Data

4.1 Plant-Level Data

We obtain comprehensive plant-level data on daily power generation from the National Electricity Coordinator (Coordinador Eléctrico Nacional — CEN), the national body in charge of SING. Along with the information on generation, the data include specifics on plant-level technology and capacity, which we later merge with data on fuel use and prices obtained from the National Energy Commission (Comisión Nacional de Energía — CNE). As November 2017 was the month in which SING and SIC were first connected, our study period goes from 2012 until 2017. Descriptive statistics for daily generation by energy source are presented in Table 1, while fuel use and prices are in panels A and B, respectively, of Appendix Table A1.

Table 1: Daily SING Generation (GWh) by Plant Primary Fuel Source

Energy Source	Obs.	Mean	Std. Dev.	Min.	Max.	Initial Year: 2012		Final Year: 2017	
						#EGUs	Cap. (MW)	#EGUs	Cap. (MW)
Coal	2,192	39.36	3.68	17.62	49.04	13	1,959	15	2,449
Diesel	2,192	.12	.19	0	1.99	12	117	13	117
Fuel oil	1,187	0.07	0.12	0	0.63	3	36	3	36
Fuel oil #6	2,192	0.37	0.49	0	2.30	4	177	7	50
Natural gas	2,192	5.03	2.18	0	17.29	5	1,368	6	1,925
Hydro	2,192	0.21	0.03	0.07	0.33	4	16	5	17
Geothermal	306	0.21	0.20	0	0.73	-	-	2	79
Wind	1,492	.84	.47	0	2.78	-	-	2	200
Solar	1,918	1.46	1.60	0	6.09	1	25	18	655

Notes: This table displays the main descriptive statistics on daily power generation at Chile's northern grid, SING, from 2012 to 2017. The information is displayed by the primary fuel source. Observations are plant-days. EGUs are electric generating units. Capacity (cap.) is the average net capacity for the given year. All gas-fired power plants are combined-cycle (CC) plants that also run with diesel. Data come from the National Electricity Coordinator from 2012 to 2017.

Table 1 shows that coal-fired electric generating units (EGUs) are SING's main source of power generation, with an average of 39.36 GWh per day, followed by gas-fired units

with 5.03 GWh, and solar units with 1.46 GWh. This is consistent with the amount of fuel used by these sources, as coal and gas plants report the greatest usage in Table A1. From Table 1, we also observe that coal-fired and hydroelectric plants are always dispatching in our sample, as revealed by the positive minimum daily generation. Furthermore, solar generation experienced the highest growth in terms of the number of new units and capacity installed into the system, as shown in the last four columns of Table 1.[12]

4.2 Health Outcomes

We use data from the Department of Health Statistics and Information (Departamento de Estadísticas e Información de Salud — DEIS), part of Chile's Ministry of Health, from 2012 to 2017. DEIS provides data on each patient that has been discharged from any hospital in the country, together with information on their date of admission, age, and the physician's diagnosis of the leading cause of disease based on the International Standard Classification (ICD-10). Although the data are compiled at the hospital or urgent care center level, they include a variable on each patient's city of origin. This allows us to construct a panel of city-level daily hospital admissions, which constitutes our main health outcome. We focus on hospital admissions due to cardiovascular (codes I00/I999) and respiratory conditions (codes J00/J999), and, within respiratory conditions, we further examine upper and lower respiratory infections.[13] Descriptive statistics on the daily rate of hospital admissions by admission condition are presented in panel A of Table 2 for the 19 cities in the sample.

In addition to constructing health outcomes by disease, we also compile health outcomes across age groups using the patient's age. In particular, we examine morbidity outcomes across infants (< 1-year-old), toddlers (between 1-5 years old), kids (between 6-14 years old), adults (between 15-64 years old), and seniors (65-years old or more). Descriptive

[12]Notice in Table 1 that the total net capacity of plants running with fuel oil #6 decreased from 177 MW in 2012 to 50 MW in 2017. This is due to the closure of two main generators, units U10 and U11, part of Termoelectrica Tocopilla, a power plant in operation since 1960. Four generators indeed were closed during the sample period. Although solar generation may also displace fossil fuel generation at the extensive margin, our main analysis is conservative as it is centered around the effects of displacement at the intensive margin only. If these shutdowns were a consequence of the injection of solar power into the system, our estimates would thus constitute a lower bound of the true effect of solar power generation on improved health outcomes.

[13]Specifically, we use codes J00/J069 and J30/J399 for upper respiratory and codes J09/J189 J20/J229 J40/J479 J60/J709 J80/J869 for lower respiratory diseases. Upper respiratory infections affect the nose and throat, causing symptoms such as sneezing and coughing. Among the most frequent upper respiratory infections are the common cold, sinusitis (sinus inflammation), epiglottitis (trachea inflammation), and laryngitis (infection of the voice box). Lower respiratory infections affect the lungs and lower airways. Common lower respiratory infections are bronchitis (bronchial tube inflammation), bronchiolitis (an infection of the small airways, affecting children), pneumonia (a lung infection), asthma (long-term disease of the lungs), influenza, and tuberculosis (bacterial lung infection).

Table 2: Summary Statistics on the Daily Rate of Hospital Admissions

Disease	Mean	Std. Dev.	Min.	Max.	Obs.
Panel A. All Cities					
Cardiovascular	1.044	4.848	0	409.84	41,648
All respiratory	1.204	5.636	0	409.84	41,648
Upper respiratory	0.274	2.002	0	168.35	41,648
Lower respiratory	0.787	4.363	0	319.49	41,648
Panel B. Downwind Cities $\leq$ 10km of Displaced Plants					
Cardiovascular	2.253	3.114	0	21.75	4,384
All respiratory	2.552	4.069	0	57.92	4,384
Upper respiratory	0.482	2.550	0	57.15	4,384
Lower respiratory	1.854	2.893	0	24.13	4,384
Panel C. Downwind Cities $\leq$ 50km of Displaced Plants					
Cardiovascular	1.818	3.002	0	21.75	6,576
All respiratory	2.029	3.707	0	57.92	6,576
Upper respiratory	0.379	2.175	0	57.15	6,576
Lower respiratory	1.478	2.737	0	24.13	6,576
Panel D. Downwind Cities $\leq$ 100km of Displaced Plants					
Cardiovascular	1.545	3.082	0	30.13	8,768
All respiratory	1.692	3.635	0	57.92	8,768
Upper respiratory	0.314	2.009	0	57.15	8,768
Lower respiratory	1.244	2.784	0	30.18	8,768

Notes: This table displays the main descriptive statistics on the daily rate of hospital admissions (all ages) by disease from 2012 to 2017. Hospital admission rates are per 100,000 people. We separate out the sample by all cities, and then specifically for those cities downwind of displaced thermal plants (identified in Section 6.1), at different distances. Data come from the Ministry of Health, through the Department of Health Statistics and Information (DEIS) from 2012 to 2017.

statistics on the daily rate of hospital admissions by age group are in Appendix Table A2.

4.3 Wind Direction

Our data on wind direction come from Chile's Meteorological Service and Air Quality System from 2012 to 2017. The data cover four cities that host fossil fuel power plants, namely Arica, Iquique, Tocopilla, and Antofagasta.[14] The eight-wind compass roses for these cities are displayed in Figure A3 for daytime (dashed line) and nighttime (solid line) wind patterns for all cities except for the city of Iquique (in Figure 3(b)), for which we

[14]Mejillones is another city with fossil fuel power plants but no available wind data; instead, we rely on information from the nearest available city, Antofagasta, 62 km away.

only have nighttime wind direction. In the definition of downwind cities, we approximate daytime wind patterns for Iquique using nighttime information. Although wind speed is generally higher at night, we use daytime information given our focus on the daily thermal displacement by solar energy sources. Considering that solar installations produce at peak capacity around midday, we expect daytime wind direction patterns to be more informative of a population's true exposure to reduced emissions from the displacement of fossil fuel generation during solar availability.

4.4 Other Covariates

We also obtain information on other factors potentially correlated to hospital admissions. First, we obtain data on city-level demographic characteristics such as population, density, poverty, and fertility rates as a proxy for socioeconomic factors known to affect health outcomes.[15] We gather this information from the National System of Municipal Information (Sistema Nacional de Información Municipal — SINIM). The demographic data are updated every two years, and therefore we can include these variables in our estimation regressions jointly with city-fixed effects.

Data on weather come from two different sources. First, we gather information on maximum and minimum temperatures from the National System on Water Information (Sistema Nacional de Información del Agua — SNIA) for several monitoring stations located in remote areas in northern Chile. Although we obtain this information for almost all cities in our dataset, there are some incomplete entries, which we replace with daily regional averages. The second source is Solar Explorer, an initiative of the Chilean Ministry of Energy (Ministerio de Energía) that contains humidity data for all the cities in our sample. Descriptive statistics for these covariates are in Panel A of Table A3 in the Appendix.

5 Methods

5.1 Displacement

We begin by econometrically identifying the effect of solar adoption on the power generation of existing power plants from 2012 to 2017.[16] To that end, we categorize all the plants in the system by their primary fuel type (e.g., coal, diesel, natural gas, fuel oil) and then define a set of linear models of daily generation to estimate which types of plant decrease

[15] Unfortunately, city-level data on indicators such as unemployment and income are not publicly available.

[16] Our displacement analysis is a short- to medium-term analysis given that it takes SING's infrastructure as given during our sample period (Baker et al., 2013).

or increase their production with the introduction of solar generation. Given our interest in the overall effect of solar power generation on health, we use daily-level variation in power generation to identify effects because total daily generation (and thus emissions) is more directly related to health outcomes than, say, hourly shifts. We define our baseline aggregated generation displacement equation as follows:

$$G_d^f = \gamma_0 + \gamma_1 S_d + \sum_{j \neq f} \delta^j \left(FuelUse_m^f * \frac{P_m^f}{P_m^j} \right) + \gamma_2 Load_d + \omega_d + \tau + \epsilon_d^f, \quad (1)$$

where G_d^f is the system's generation by fuel f during day d, and ω_d is a vector of daily weather covariates. It is important to include these weather controls as renewable generation is highly dependent on weather conditions (e.g., wind and hydro). We also include τ, a vector of time-fixed effects, and ϵ_d^f is an error term. We consider two options of τ. The first, τ_1, includes year, month, and weekend fixed effects, while a stronger version, τ_2, includes year, seasons, year $\times$ seasons, and weekend fixed effects.

Equation (1) also includes the variable $Load_d$ that represents the system load during day d to control for increases in demand over time, as demonstrated by Appendix Figure A4.[17] In addition, Equation (1) considers a term that models SING's dispatch of generators to control for differences in input prices that may affect daily dispatch conditions. This term is given by the interaction between aggregate use of fuel f during month m, $FuelUse_m^f$, and the relative international (exogenous) monthly prices of the fuels in the system, P_m^f/P_m^j, where $f \neq j$. Here, one concern may be that, in the eventuality of a displacement of fuel f, $FuelUse_m^f$ may be also affected by solar generation. We test the robustness of including $FuelUse_m^f$ in specification (1) by first using fuel use in month $m-1$, that is, $FuelUse_{m-1}^f$, and second, by removing $FuelUse_m^f$ from Equation (1). These alternative approaches result in qualitatively similar results; see Section 6.1 for a discussion. Importantly, we do not include relative prices with respect to solar energy or other renewables, given their zero marginal cost.

The key variable in Equation (1) is S_d, which represents the system's total solar generation during day d. The idea behind this is that, after controlling for plant-level (fuel use) and system-specific covariates (prices, load), weather, and time fixed effects, residual variation in generation by fuel f can be explained by variation in the system's total solar power. To ensure that any potential outcome effect is attributable to variation in solar generation, we run an alternative specification to Equation (1) in which we replace S_d by a daily solar capacity factor CF_d^{solar} (defined as total daily solar generation on day d weighted by solar net capacity on day d). Because solar comes online sporadically throughout the sample period,

[17] As the large-scale copper mining industry is an important agent in the demand for energy at SING, variations in daily load should also capture similar variations in copper production.

utilizing capacity factors instead of generation can capture the more long-run effects of solar entry while still capturing daily variation in solar generation. In both cases, the parameter γ_1 reflects whether, and to what extent, daily solar power induces a significant change in daily generation by non-solar sources. A negative (positive) γ_1 signals a solar-induced displacement (ramp-up) of non-solar sources.

We estimate Equation (1) with an ordinary least square (OLS) estimator, bootstrapping standard errors to account for any heterogeneity and serial correlation in the generation data. To take into account the heterogeneous capacity across fuel types, we also estimate an alternative specification of Equation (1) in which we replace the outcome G_d^f by capacity factors CF_d^f, defined as the total daily generation by fuel f weighted by its net capacity. Given that CF_d^f takes values between 0 and 1, we estimate this version of Equation (1) using a generalized least-squares (GLM) estimator assuming a logit distribution.

Additionally, we run a plant-level version of Equation (1) to individually identify the set of plants displaced by solar generation and those that are not. Later on, in our health analysis, we use this plant-level displacement analysis as the main input to classify cities based on their exposure and proximity to displaced plants. We modify Equation (1) to include generation G_{id}^f by plant i, and plant i's corresponding fuel use $FuelUse_{im}^f$, as follows:

$$G_{id}^f = \gamma_0 + \gamma_1 S_d + \sum_{j \neq f} \delta^j \Big(FuelUse_{im}^f * \frac{P_m^f}{P_m^j} \Big) + \gamma_2 Load_d + \omega_d + \tau + \epsilon_{id}^f. \tag{2}$$

5.2 Solar Generation and Health

Once we have identified whether solar power generation induced a displacement of fossil-fueled plants, our next step is to estimate the effect of solar power generation on hospital admissions. We define our baseline health equation as follows:

$$Health_{jd} = \delta_0 + \delta_1 S_d + \omega_{jd} + \zeta + \tau + \nu_{jd}, \tag{3}$$

where $Health_{jd}$ represents the rate of hospital admissions (per 100,000 people) in city j during day d; ω_{jd} is a vector of daily city-level weather covariates that may affect morbidity outcomes such as daily maximum and minimum temperatures and humidity; ζ is a vector of city-fixed effects (or city $\times$ year fixed effects); τ is a vector of time-fixed effects, and ν_{jd} is an idiosyncratic effect. Unlike Equation (1), here we use the strongest specification of time-fixed effects, which includes year, seasons, year $\times$ seasons, and weekends (that is, vector τ_2). Including time-fixed effects, year $\times$ seasons fixed effects, or year $\times$ city fixed effects is important to take into account potential improvements in fossil fuel plants' emissions factors that could have taken place over time and confound the effect of interest.

The main variable in Equation (3) is S_d, which measures SING's total solar generation on day d. Given the specification of Equation (3), we leverage daily within-quarter variation in total solar generation to identify health effects. Because we construct this variable utilizing generation from all solar plants in the system, daily variation in S is exogenous to any day-to-day variation in hospital admissions in a given city j, and thus, our parameter of interest, δ_1, gives us an unbiased marginal effect of daily solar generation on the daily rate of hospital admissions. We estimate Equation (3) with an OLS estimator. However, given that we have a large number of zeros in the outcomes (count variables) and a clear overdispersion of these outcomes across cities in our sample, we check the robustness of this estimator with alternative count regression models in Section 7.[18]

There are potential drawbacks in the estimation of Equation (3). First, fossil fuel plants may not be randomly placed across the region, so cities with and without fossil fuel plants may be observably different. Indeed, this is the case exhibited in panels B and C of Appendix Table A3, which show that cities without fossil fuel plants (panel C) are smaller, less dense, and with higher poverty rates than those with fossil fuel plants (panel B) (all of these differences are statistically significant).[19] Thus, in addition to including city-fixed effects, we also control for time-varying (biennial) demographic characteristics (e.g., population, poverty rate, density, fertility rate) in the estimation of Equation (3). Second, large copper mines are important energy consumers in northern Chile, and also a significant air pollution emitter. For this reason, we also include monthly large-scale copper production by city in the estimation of Equation (3).[20] Third, there may be substantive dynamic effects of daily avoided fossil-fueled pollution on health outcomes. As air pollution gathers and accumulates in the atmosphere over time, we would expect to see a lagged impact of daily improvements in air quality on health.[21] In particular, air quality improvements over three or four days may very well lead to more significant health benefits today than contemporaneous improvements in air quality. In that case, Equation (3) would give us an incomplete picture of the actual health effect of a cleaner grid.

There is precedent in the literature for testing the effect of lagged exposure to air pollution on health. For instance, Neidell (2009) includes up to six days of lags (with only four days of lags in their preferred specification), while Schlenker and Walker (2016) opt for three

[18] See Appendix Figure A5 for an example of overdispersion and the pile-up-at-zero in our data.

[19] Statistical tests are omitted for simplicity.

[20] Large-scale copper mining operations roughly represent 96% of the industry's total production. We obtain monthly large-scale copper production from the Chilean Copper Corporation (COCHILCO). We would much rather use data on daily variation in production, but this information is unavailable.

[21] Indeed, there is evidence that certain air pollutants can have an extended effect on health. For instance, U.S. Environmental Protection Agency (2006) find ozone can have an effect on health for up to four days after exposure.

days of lags. Although these two studies are looking at *degradation* of air quality while we look at *improvements* in air quality, we could potentially identify a dynamic effect by including lags in our health equation. However, this is not straightforward in our setting because our variable of interest (solar generation) is highly colinear across days.[22] Thus, including lags and leads would result in unstable estimates due to the multicollinearity of the variables. Instead, we take a slightly different approach by testing whether there is a cumulative impact of longer-term solar generation (and thus, longer periods of exposure to reduced fossil fuel-related pollution) on health. We do this by estimating the impact of average weekly, monthly, and yearly solar generation on health outcomes, as depicted by Equation (4) where $T = \{7, 30, 365\}$. Expressed in this way, δ_{1T} approximates the average weekly, monthly, or yearly effect of solar generation on daily hospital admissions:

$$Health_{jd} = \delta_0 + \delta_{1T} T^{-1} \sum_{t=1}^{T} S_{d-t} + \omega_{jd} + \zeta + \tau + \nu_{jd}. \tag{4}$$

5.2.1 Identifying Assumptions

The validity of our empirical specifications in Equations (1), (2), (3), and (4) relies on, first, the identifying assumption that large-scale investments in solar power generation are exogenous to day-to-day variation in fossil-fuel generation once we control for plant-level characteristics, daily load, demographics, and time fixed-effects. This is a reasonable assumption given the massive large-scale investments in renewables were encouraged by the ERNC policy, which we use as a natural experiment (see Section 3.1). In this case, the total variation in solar generation in SING is as good as randomly assigned.

One concern to identification is the possibility that day-to-day variation in solar generation may be insufficient to identify any health effects. This concern could be amplified with the inclusion of year $\times$ season fixed effects in our health estimation equation, as we may be soaking up the variation in solar generation over time. To rule out this concern, Figure 5 illustrates significant across- and within-quarter variation in solar generation (black dots) over time. Two main reasons explain these variations. First, as mentioned before, there is increasing solar capacity (gray bars) over time in our setting. Second, solar plants generally operate with reduced capacity due to the intermittent nature of the sun over the course of the day. In our sample, average solar capacity factor is 19.67%, and maximum capacity is 42% (see Appendix Figure A6). Thus, using solar generation provides us with sufficient variation over time to be able to accurately identify its effect on health. In any case, we also

[22] Our multicollinearity tests between $Solar_d$ and $Solar_{d-l}$ for $l = \{1, 2, 3\}$ reveal variance inflation factors (VIFs) of magnitudes close to a 100.

estimate Equation (3) using CF_d^{solar} instead of S_d for added robustness.

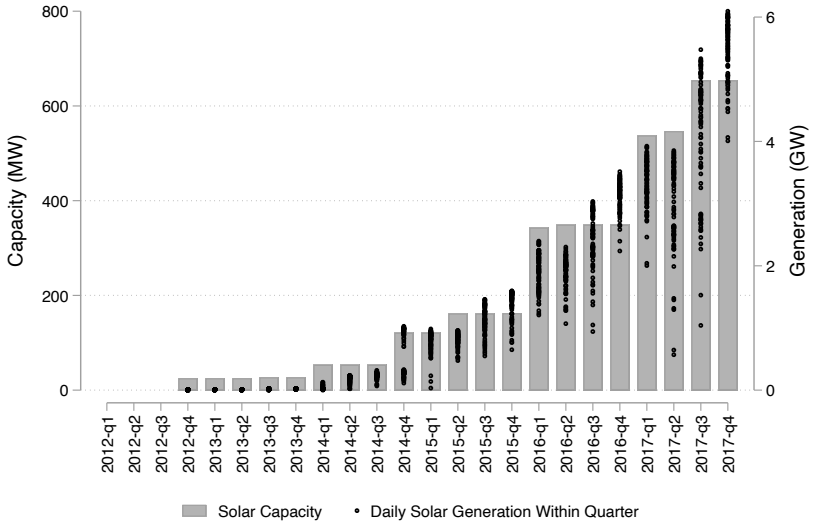

Figure 5: Within-Quarter Solar Capacity and Daily Solar Generation Over Time

Notes: The figure shows variation in solar generation and solar capacity within quarters. Bars show accumulated solar net capacity (in MW) within quarters. Dots indicate the daily average solar generation (in GW) within quarters. Data come from the National Electricity Coordinator from 2012 to 2017.

An additional concern is a potential endogeneity between power generation and health outcomes. For instance, power plant locations can be correlated with local income, as local employment and wages may be associated with power plant output. At the same time, higher (lower) wages can correlate with better (worse) health outcomes, and thus, identification of the main parameters in our health equations may be threatened. We argue that, by using system-level daily solar generation, we can avoid any localized endogeneity concerns as solar generators are scattered across the entire SING system and far from demand centers (see Figure A7) instead of being concentrated in certain cities as in the case of thermal generation.

However, to guarantee identification, we pair information on average city-level wind direction (see Figure A3) with the results from our plant-level displacement analysis, which allows us to distinguish cities downwind of displaced fossil fuel plants.[23] To the extent that large-scale daily solar generation displaces thermal generation, the reduction in emissions from these displaced thermal plants is likely to benefit cities that are located downwind of these units.[24] Additionally, we identify cities upwind of displaced plants and downwind of

[23]We obtain the average wind direction by drawing a pie slice with an angle of $\pi/4$ radians (i.e. 45 degrees) bisected by the average daytime wind direction in each location. The resulting average wind direction is: 1.15π radians (206.9 degrees) in Arica (Figure 3(a)), 1.57π radians (282.7 degrees) in Iquique (Figure 3(b)), 1.33π radians (238.6 degrees) in Tocopilla (Figure 3(c)) and 1.09π radians (196 degrees) in Antofagasta (Figure 3(d)).

[24]In classifying downwind cities, we acknowledge the simplicity of our approach when it comes to un-

non-displaced plants to use later in a robustness analysis. We enrich this wind analysis with the calculation of distances to the displaced thermal plants and construct an indicator for whether a city is downwind of and near a displaced plant. Thus, when estimating our health equations for all cities, we also do so for cities downwind of displaced fossil fuel plants that are located within $10km$, $50km$, or $100km$ of their boundaries. In doing so, we rely on the identifying assumption that harmful effects of pollution are stronger downwind of and closer to displaced thermal plants.

6 Results

6.1 Fossil Fuel Displacement

Panel A of Table 3 (Appendix Table A5) presents the results of estimating Equation (1) on the effect of 1-GWh of daily solar generation (Solar_d) on daily aggregated generation (panel A) and on daily capacity factors (panel B) of fossil fuels (renewable sources). To verify that any finding is attributable to more solar plants coming online, we also include the results of the effect of a 1-percentage-point (pp) increase in solar capacity factor ($\text{Solar Cap Factor}_d$) on the same outcomes; thus, each row in Table 3 represents a different regression. Columns labeled (2) include more time-fixed effects than columns labeled (1); further results follow a similar format.

Our findings in Table 3 (and Appendix Table A5, which estimates the displacement of renewables by solar) show that solar-generated electricity displaces other fuel sources, particularly dirty sources. We observe that an extra 1-GWh of daily solar generation reduces the day-to-day generation of plants running with coal and with natural gas by 0.48 and 0.27 GWh, respectively (panel A, columns (2)).[25] Considering the descriptive statistics in Table 1, we observe that this displacement is roughly equivalent to 1.22% and 5.36% of the daily average electricity generated by these fossil fuels. Qualitatively similar effects are found in panel B on capacity factors of thermal plants. An extra 1-GWh of solar generation displaces in 1.4 percentage points capacity factors of coal-fired plants and in 4.9 percentage points capacity factors of gas-fired plants. The results in Table 3 also suggest a ramp-up in capacity factors of plants running with diesel. However, this effect disappears once a stronger set of time-fixed effects is included.

derstanding how pollution travels over space. However, and to the best of our knowledge, more complex air transport models have not been developed or made public for Chile. This fact reduces our ability to incorporate issues such as the impact of mountain ranges on wind, or wind directions that may change across longer ranges.

[25] Further analysis using simple cycle turbine plants reveals that solar energy displaces coal-fired single-fuel engine generation at a larger magnitude (see Table A6 in the Appendix).

Table 3: The Effect of Daily Solar Energy on Daily Aggregated Fossil Fuel Generation

	Coal		Diesel		Fuel oil		Fuel oil #6		Natural gas	
	(1)	(2)	(1)	(2)	(1)	(2)	(1)	(2)	(1)	(2)
Panel A. Generation (GWh)										
Solar Gen_d	-0.656***	-0.483**	0.151	0.077	-0.011	-0.013	-0.016	-0.014	-0.215	-0.274**
	(0.175)	(0.159)	(0.094)	(0.092)	(0.019)	(0.024)	(0.017)	(0.013)	(0.150)	(0.134)
Solar Cap $Factor_d$	-0.041**	-0.066***	-0.003	-0.007	-0.0003	-0.0005	-0.002	-0.002	0.006	-0.015
	(0.015)	(0.013)	(0.007)	(0.012)	(0.001)	(0.001)	(0.001)	(0.002)	(0.009)	(0.010)
Panel B. Capacity Factor										
Solar Gen_d	-0.021***	-0.014***	0.015**	0.012	0.047	0.018	-0.018	-0.006	-0.063***	-0.049***
	(0.003)	(0.003)	(0.006)	(0.007)	(0.041)	(0.064)	(0.012)	(0.011)	(0.009)	(0.009)
Solar Cap $Factor_d$	-0.001***	-0.002***	0.0005	-0.0001	0.001	-0.0003	-0.001	-0.002*	-0.003***	-0.001**
	(0.0003)	(0.0003)	(0.0005)	(0.0004)	(0.001)	(0.001)	(0.001)	(0.001)	(0.001)	(0.0005)
Obs.	1,915	1,915	1,915	1,915	910	910	1,915	1,915	1,915	1,915
Controls	✓	✓	✓	✓	✓	✓	✓	✓	✓	✓
τ_1 fixed effects	✓		✓		✓		✓		✓	
τ_2 fixed effects		✓		✓		✓		✓		✓

Notes: This table displays estimation results from regressions of daily aggregated fossil fuels' generation (panel A) and fossil fuels' daily capacity factors (panel B) on daily solar power generation and daily solar capacity factors. Each row is a separate regression. Solar generation is in GWh. Solar capacity factor is between 0 and 100. Estimation results are marginal effects from an OLS (daily aggregated generation), and from a fractional logit response model (daily capacity factors). All estimations include plants with both single- and dual-fuel engines. All regressions include daily temperature, humidity, load, and price ratios as controls. Vector τ_1 includes year, month, and weekend fixed effects. Vector τ_2 includes year, seasons, year × seasons, and weekend fixed effects. Bootstrapped standard errors using 50 repetitions appear in parentheses. Significance levels: $^{*}p < 0.10$, $^{**}p < 0.05$, $^{***}p < 0.001$.

This solar-induced displacement of fossil fuel sources, particularly coal, is corroborated by the use of daily solar capacity factor instead of solar generation. These results in panel A show as more solar comes online (leading to an increase in solar capacity factor), coal generation is displaced. In particular, a 1-pp increase in solar capacity factor reduces daily coal-fired generation by .066 GWh, equivalent to a .16% decrease relative to the daily average coal power generation. Smaller estimated marginal effects attributable to solar capacity factor are not surprising because a 1-pp increase in daily average solar capacity factor is equivalent to a 0.062-GWh increase in daily solar generation. We also observe a reduction in other fuels, yet, we lose precision in estimating this displacement. For robustness checks, we first replace $FuelUse_m^f$ with lagged fuel consumption by using $FuelUse_{m-1}^f$, and then we completely remove $FuelUse$ from the estimation of our displacement equation (see Appendix Table A4), mostly for coal displacement. In the latter case, when $FuelUse_m^f$ is removed from the displacement specification, our findings reveal a stronger coal displacement, meaning that a 1-GWh extra of solar generation goes almost exclusively to displacing coal power generation. Relative to this result, we consider our baseline displacement estimates in Table 6.1 as conservative estimates.

The thermal displacement due to additional solar energy is also found in hydro, a dispatchable power source (Appendix Table A5). The result in column (2) (panel A) indicates

that, on average, a 1-GWh increase in daily solar generation displaces 0.007 GWh of hydro generation (equivalent to 3.3% of the average hydropower generated in a single day) and hydro capacity by 1.8%. Similarly, a 1-pp increase in solar capacity reduces hydro generation by .03 GWh and hydro capacity by .1%. An analogous effect is found on daily geothermal generation (column (1)), although the statistical significance of this effect disappears when stronger fixed effects are used. The results on geothermal capacity factors are stronger and statistically significant, demonstrating a reduction of 4 pp from increases in solar generation, and a reduction of 0.6 pp from increases in solar capacity.

It is important to note that geothermal displacement attenuates the potential benefits of a reduction in fossil fuels found in Table 3. Because geothermal energy is a non-emitting source of electricity, its displacement reduces some of the health benefits associated with the expansion of solar generation. Hydropower, on the other hand, is mostly utilized as a storage resource, dispatching in response to high price times; thus, we are unable to directly identify the environmental impacts of its displacement. Despite this potential attenuation, this effect is smaller in magnitude compared to the displacement of daily coal generation. Moreover, this effect is likely to be minor given the relatively small share of electricity that is produced by hydro and geothermal sources (both of which contribute only 0.4% of mean daily generation; see Table 1). In summary, we expect any attenuation effect from reduced hydro and geothermal generation to be small compared to the benefits of displaced coal and natural gas, which account for 83% and 11% of mean daily generation, respectively.

Finally, we find a positive coefficient of solar generation on wind generation, a non-dispatchable (but curtailable) power source. The result for wind in column (2) of Appendix Table A5 indicates that 1-GWh of daily solar generation ramps up wind generation by 0.099 GWh and that a 1-pp increase in solar capacity increases wind generation by .7 GWh. Similarly, an increase in solar generation and capacity results in a 1.3% and .2%, respectively, increase in wind capacity. Due to the non-dispatchability of wind generation, this likely reflects an underlying correlation between wind and solar, given the thermally driven wind systems that characterize the Atacama Desert (Jacques-Coper et al., 2015).[26] An additional source of positive correlation between wind and solar generation likely come from the ERNC policy itself, which boosts the adoption of renewable energy sources, mostly solar and wind energy. In any case, given that wind generation is not dispatchable but curtailable, the fact that we are not getting a negative coefficient weakly suggests that wind is not curtailed in response to greater solar output, or that, if curtailment exists, it is not large enough to

[26]Thermally driven winds are caused by local differences in radiational heating and cooling systems, which in the case of the Atacama favor the complementarity between wind energy and solar energy (Jacques-Coper et al., 2015; Muñoz et al., 2018).

overcome the positive correlation between the two sources.

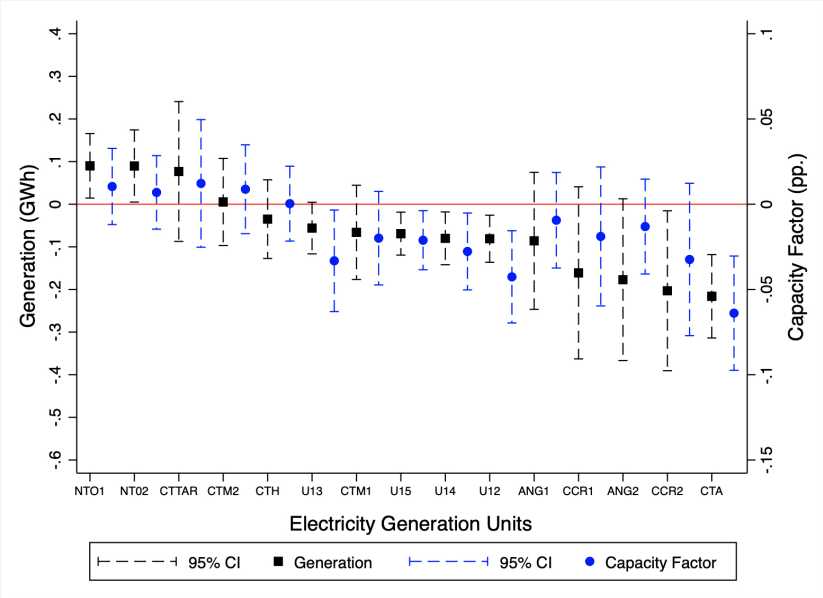

Figure 6: The Effect of Daily Solar Energy on Coal Combustion by Generation Units

Notes: The figure shows estimation results from regressions of daily coal-fired generation (squares) and coal capacity factors (circles) on daily solar power generation at the electricity generation unit (EGU) level. Point estimates are marginal effects of daily solar generation (in GWh) derived from an OLS regression on daily aggregated generation (left y-axis), and from a fractional logit response model on daily capacity factors (right y-axis). The estimation equations are identical to the ones in columns (2) of Table 3. Dashed lines represent 95% confidence intervals obtained with bootstrapped standard errors using 50 repetitions. The reference line in red is at the zero mark. All estimations use EGUs that report coal (and its derivatives) as their primary fuel source.

To delve deeper into the fossil fuel displacement found in Table 3, we estimate Equation (2) at the plant level to individually identify affected plants. We plot the marginal effects of solar generation on daily generation levels and capacity factors by coal-fired EGUs in Figure 6.[27] Squares represent point estimates of solar generation on daily coal generation (left y-axis), and circles represent marginal displacements of capacity factors (right y-axis). The negative impact of solar generation on coal combustion indicated in Table 3 is mostly explained by the shift in the generation of six units: U13 (statistically significant at the 10% level), U15, U14, U12, CCR2, and CTA. Indeed, CTA is the unit with the higher estimated displacement. In fact, considering this plant alone, solar-induced displacement translates into more than 200 MWh of avoided daily coal-fired generation. On average, our estimates reveal that a 1-GWh of solar generation displaces 203 MWh of generation from this particular unit on a given day.

In addition to the displacement of several coal-fired units, Figure 6 also reveals a statistically significant ramp-up in coal generation of two facilities: NTO1 and NTO2, located in the city of Tocopilla. On average, 1-GWh of daily solar generation increases their generation

[27]Similar graphs for diesel- and gas-fired units are in Appendix Figures A8 and A9, respectively.

by 90 and 89 MWh, respectively, jointly equivalent to 0.46% of the daily coal-fired generation (see Table 1). Although the generation ramp-up of these two coal-fired units is significantly lower than the displacement of other facilities, the increase slightly attenuates the potential health impact of the overall set of displaced plants in Tocopilla. Later in the paper, we use the proximity of cities to ramped-up plants as a robustness check of our results.

6.2 Solar Generation and Health Outcomes

The results on the effect of additional solar energy on the rate of daily hospital admissions using Equation (3) are displayed in Table 4 for cardiovascular (panel A) and respiratory (panel B) conditions, including the detail between upper (panel C) and lower (panel D) respiratory diseases. Each row of the table represents marginal effects from different regressions; in these, we either use daily solar generation or daily solar capacity factor as the main regressor. Furthermore, we also subset our results based on alternative sets of downwind cities as defined in Section 5. Column (1) presents the results of our regressions without controls. We then include controls in Columns (2) and (3) to capture time variation (year, seasons, year $\times$ seasons, and weekend fixed effects), weather conditions, and city-level demographics and mining production. In addition, columns (2) include city fixed effects, while columns (3) include city $\times$ year fixed effects. Because this final set of fixed effects is the most robust, it represents our preferred specification.

Altogether, the results in Table 4 indicate that solar generation leads to a reduction in hospital admissions. The results for our preferred specification (columns (3)) show that, across all cities, a 1-GWh increase in solar generation leads to an 11.4 percentage point (pp) reduction in the daily rate of hospital admissions due to all respiratory conditions (panel B), with the majority of this reduction coming from lower respiratory hospitalizations (roughly 8.5 pp). Considering the sample average of admissions, these effects are equivalent to a 9.38% reduction in daily hospital admissions due to all respiratory diseases, and to a 10.80% reduction of admissions due to lower respiratory diseases. Results for cardiovascular (panel A) and upper respiratory (panel C) hospitalizations are also negative but statistically insignificant at the conventional levels. Equivalent - albeit smaller, given the differences in magnitudes between capacity and generation- results are found when leveraging variation in daily solar capacity factors.

Though the results in the first three columns of Table 4 have the expected sign, they could be underestimating the true health effect of solar power generation if emissions from displaced fossil fuel plants are not equally distributed across space. Thus, to better capture the air quality effect of the solar-induced displacement of dirty plants, we redefine our sample to

Table 4: The Effect of Daily Solar Energy on the Daily Rate of Hospital Admissions

	All Cities			Downwind of Displaced Units					
				$< 10km$		$< 50km$		$< 100km$	
	(1)	(2)	(3)	(2)	(3)	(2)	(3)	(2)	(3)
Panel A. Cardiovascular									
Solar_d	0.008	-0.003	0.0003	-0.038	-0.039	-0.035	-0.036	-0.020	-0.017
	(0.025)	(0.065)	(0.049)	(0.085)	(0.070)	(0.085)	(0.074)	(0.068)	(0.059)
$\text{Solar Cap Factor}_d$	-0.001	-0.002	-0.002	-0.005	-0.005	-0.007	-0.006	-0.009*	-0.009
	(0.002)	(0.003)	(0.003)	(0.008)	(0.007)	(0.005)	(0.005)	(0.005)	(0.006)
Panel B. All Respiratory									
Solar_d	-0.057***	-0.115**	-0.114**	-0.324**	-0.325**	-0.184**	-0.188**	-0.253**	-0.251**
	(0.016)	(0.057)	(0.054)	(0.138)	(0.099)	(0.083)	(0.089)	(0.080)	(0.079)
$\text{Solar Cap Factor}_d$	-0.007**	-0.010**	-0.010**	-0.022**	-0.022**	-0.010	-0.010	-0.013*	-0.0136**
	(0.002)	(0.005)	(0.005)	(0.010)	(0.009)	(0.007)	(0.007)	(0.007)	(0.007)
Panel C. Upper Respiratory									
Solar_d	-0.019***	-0.027	-0.027	-0.080	-0.080	-0.044	-0.046	-0.053	-0.054
	(0.006)	(0.017)	(0.018)	(0.081)	(0.099)	(0.069)	(0.054)	(0.051)	(0.048)
$\text{Solar Cap Factor}_d$	-0.001	-0.001	-0.001	-0.003	-0.003	-0.001	-0.001	-0.002	-0.002
	(0.001)	(0.002)	(0.002)	(0.005)	(0.005)	(0.004)	(0.004)	(0.003)	(0.003)
Panel D. Lower Respiratory									
Solar_d	-0.025*	-0.085	-0.085*	-0.263**	-0.263**	-0.152**	-0.151**	-0.193**	-0.190**
	(0.013)	(0.054)	(0.048)	(0.101)	(0.085)	(0.064)	(0.074)	(0.061)	(0.063)
$\text{Solar Cap Factor}_d$	-0.004**	-0.009**	-0.009**	-0.021**	-0.021***	-0.010*	-0.010**	-0.011**	-0.011**
	(0.002)	(0.004)	(0.004)	(0.008)	(0.006)	(0.006)	(0.005)	(0.004)	(0.005)
Observations	36442	36385	36385	3830	3830	5745	5745	7660	7660
Number of cities	19	19	19	2	2	3	3	4	4
Sample Mean Y - Panel A	1.043	1.043	1.043	2.244	2.244	1.822	1.822	1.565	1.565
Sample Mean Y - Panel B	1.215	1.216	1.216	2.522	2.522	2.013	2.013	1.699	1.699
Sample Mean Y - Panel C	0.279	0.279	0.279	0.484	0.484	0.378	0.378	0.317	0.317
Sample Mean Y - Panel D	0.789	0.789	0.789	1.817	1.817	1.458	1.458	1.244	1.244
Controls		✓	✓	✓	✓	✓	✓	✓	✓
City fixed effects		✓		✓		✓		✓	
City × year fixed effects			✓		✓		✓		✓

Notes: This table displays estimation results from OLS regressions of daily hospital admissions on daily solar power generation or daily solar capacity factor. Each row is a separated regression. Solar generation is in GWh. Solar capacity factor is between 0 and 100. Daily hospital admissions are per 100,000 people. Controls include weather, mining production, and demographic covariates. All regressions include controls, year, seasons, year × seasons, and weekend fixed effects. Bootstrapped standard errors using 50 repetitions appear in parentheses. Significance levels: $^*p < 0.10$, $^{**}p < 0.05$, $^{***}p < 0.001$.

include cities located downwind of and at different distances from displaced fossil fuel plants identified in Section 6.1. These are the results in the last six columns of Table 4.

We obtain stronger and larger health effects when we incorporate wind exposure to air pollution from dirty, displaced plants. This is particularly true for the rate of admissions due to respiratory conditions near displaced plants ($< 10km$), although the coefficients on cardiovascular conditions continue to lack statistical significance. For cities within $10km$ downwind of displaced plants, the results in column (2) indicate that a 1-GWh increase in daily solar generation results in a 32.5 pp reduction in the rate of hospital admissions due to respiratory diseases in general, and in a 26.3 pp reduction in admissions due to lower respiratory diseases in particular. These effects correspond to a 12.9% and a 14.5%

daily reduction in each case. The signs and statistical significance of the estimated effects are slightly similar for cities within $50km$ and within $100km$ of distance from the displaced facilities, albeit with decreasing magnitudes. For instance, the 14.5% reduction in admissions due to all respiratory diseases found within $10km$ of displaced thermal plants decreases roughly to a 10% within $50km$ and to 11% within $100km$. The decay between the first group of cities is fairly consistent with the identifying assumption that the health benefits from thermal generation displacement decrease with distance from the displaced sources. Yet, this is not the case as we move from within-$50km$ cities to within-$100km$ cities. When we move between the first and second group of cities, we add a city that is small in terms of population, and likely attenuates the effect towards zero in the second group. We test and confirm this hypothesis in Section 7 by running alternative (count) estimation methods that take this possibility into account. In any event, the results in Table 4 suggest that solar power generation leads to better health outcomes, particularly in the immediate vicinity of displaced thermal plants, likely attributable to improvements in local air quality (a result we are able to demonstrate more directly in Section 6.2.2).

Health Effects Across Age Groups. Figure 7 illustrates the results of estimating Equation (3) across different age groups using our preferred specification. Full estimation results are given in Appendix Tables A7, A8, A9, A10, and A11, for infants, toddlers, kids, adults, and seniors, respectively. Similar to our baseline results, we also include the results of replacing daily solar generation with daily solar capacity factor for added robustness.

The results in Figure 7 show additional solar power generation leads to health benefits among infants and toddlers, some of the most vulnerable age groups. Figure 7(b) indicates a clear reduction in respiratory-related hospital admissions of infants and toddlers, especially in cities downwind of displaced dirty power plants. In particular, our exercise reveals strong and statistically significant reductions in admissions of infants and toddlers into hospitals due to lower respiratory diseases (see Figure 7(d)), which are equivalent to a 30.63% and a 27.58% decrease, respectively, relative to the daily rate of admissions in downwind cities within $10km$ of distance from displaced plants.[28] These reductions are maintained as we move farther away from curtailed thermal plants, although they decrease in magnitude. Reductions in lower respiratory-related hospital admissions vary between 14.99%-19.11% in the case of infants and between 16.17%-24.89% in the case of toddlers from downwind cities within $50km$ and $100km$. We also observe a reduction in respiratory-related hospital admissions among adults and seniors, but these are weak effects and are estimated with

[28] Percentage reductions are $0.081/0.264 = 30.63\%$ for infants, and $0.084/0.305 = 27.58\%$ for toddlers. See Appendix Tables A7 and A8.

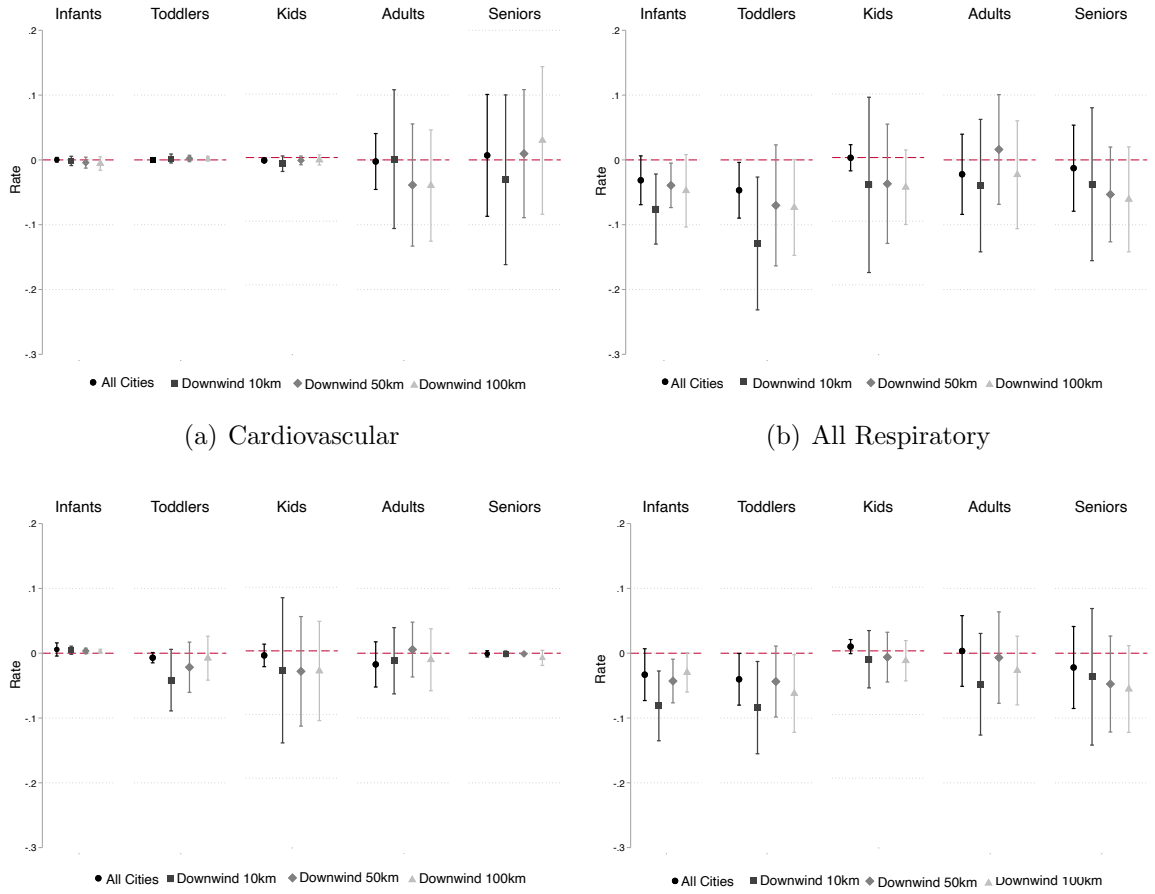

(a) Cardiovascular (b) All Respiratory

(c) Upper Respiratory (d) Lower Respiratory

Figure 7: The Effect of Daily Solar Energy on the Daily Rate of Hospital Admissions by Age Group

Notes: This figure plots estimation results from OLS regressions of daily hospital admissions on daily solar power generation by age group. Solar generation is in GWh. Daily hospital admissions are per 100,000 people. All regressions include controls (weather, mining production, and demographics), year, seasons, year × seasons, and weekend fixed effects. Dashed lines are 95% confidence intervals obtained with bootstrapped standard errors using 50 repetitions.

less precision. In any case, the results obtained for all respiratory diseases, mainly lower respiratory diseases, confirm the health benefits of increased solar power generation among vulnerable groups such as infants and toddlers, which become stronger in cities downwind of and in close proximity to displaced thermal plants.

Short- Versus Long-Term Health Effects. The results in Table 4 and Figure 7 both offer a general perspective of the net effect that day-to-day variation in solar generation has on day-to-day variation in hospital admissions, suggesting the existence of short-term benefits of additional solar generation on health. Additional evidence of the immediate co-benefit of solar is found in the results for infants in Figure 7 and Appendix Table A7. As

stated in Currie and Neidell (2005), the link between cause and effect is immediate in the case of infants, whereas diseases today in adults, for instance, may reflect pollution exposure from years ago. The negative effects of solar on respiratory-related hospital admissions of infants, particularly lower respiratory diseases, found in panels D of Figure 7 illustrate this immediate link. Considering that infants are less than one year old, these findings corroborate the contemporaneous feature of the co-benefits of solar power generation.

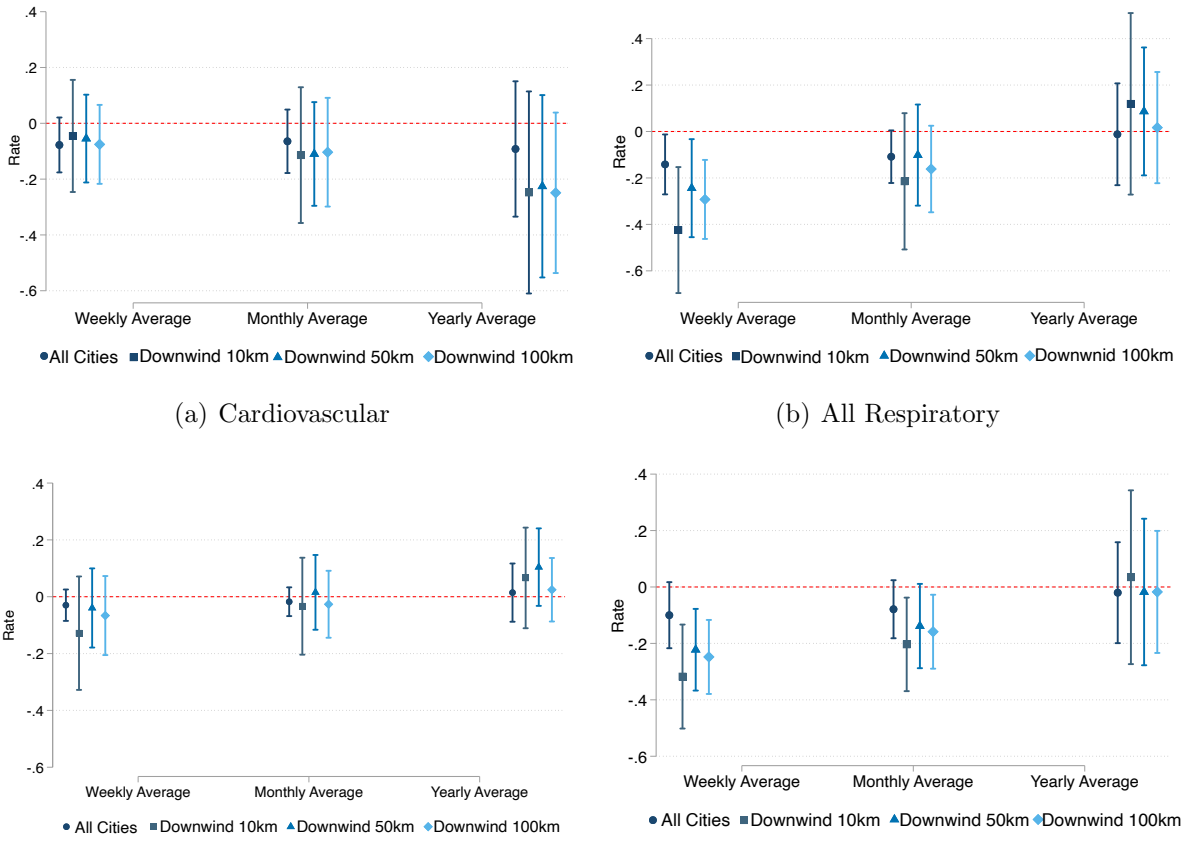

(a) Cardiovascular

(b) All Respiratory

(c) Upper Respiratory

(d) Lower Respiratory

Figure 8: The Long-Term Effect of Solar Energy on the Daily Rate of Hospital Admissions

Notes: This figure shows estimation results from OLS regressions of daily hospital admissions on weekly, monthly, and yearly average solar power generation across groups of cities. Solar generation is in GWh. Daily hospital admissions are per 100,000 people. Controls include weather, mining production, and demographic covariates. All regressions include controls, year, seasons, year × seasons, and weekend fixed effects. Dashed lines are 95% confidence intervals obtained by bootstrapping standard errors using 50 repetitions.

As an additional test on whether these co-benefits are masking some longer-run effects, we estimate Equation (4) where the main explanatory variable is allowed to reflect the moving weekly, monthly, or yearly average solar generation in the system. Equation (4) also allows taking into account the potential lagged effects of solar generation on contemporaneous health outcomes, albeit indirectly. To that end, we replace S_d by S_t, where $t = \{w, m, y\}$.

Modeled in this way, δ_t gives us the average marginal effect of 1 GWh of either weekly, monthly, or yearly average solar generation on the rate of daily relevant hospitalizations. The results using our strongest specification are displayed in Figure 8 for solar generation (see Appendix Figure A10 for solar capacity factor), with point estimates and corresponding standard errors shown in Appendix Table A12.

The results using long-term variation in solar power in Figure 8 (see Appendix Table A12 for point estimates) show reductions in hospitalizations due to respiratory diseases attributable to weekly average variation in solar generation, across all cities and cities downwind of displaced power plants. Similar effects are found when leveraging variation in solar capacity factor in Appendix Figure A10. These benefits, however, become smaller and generally less significant as we move toward longer times of exposure (monthly and yearly). We take these estimates together with our previous results among infants as compelling evidence of the immediate respiratory-related health effects of increased solar power generation.

Interestingly, the exercise in Figure 8 reveals weakly significant reductions in hospital admissions due to cardiovascular diseases that show an opposite pattern relative to respiratory diseases. These findings turn statistically significant when using capacity factors in Appendix Table A12. This time, the health benefits from increased solar generation (and the displacement of dirty generation) exhibit a long-term pattern when it comes to cardiovascular diseases, which likely originated from extended exposure to reduced air pollution.[29] We also find that these long-term cardiovascular health benefits are significant regardless of how we measure solar power (generation or capacity factor), are mostly present in downwind cities, and they decrease with distance as we move farther away from the pollution source; thus further supporting our identification strategy.

6.2.1 Solar-Induced Predicted Fossil Fuel Displacement and Health

Thus far, our results show reductions in hospital admissions due to daily increasing variation in solar generation. We link both the displacement and the health analyses using distances to displaced, dirty plants and wind direction, to pose that the curtailing of fossil fuel power generation, as a response to frequent and increasing injections of solar generation to the system, is likely driving the results.

In this section, we offer an additional test to this hypothesis based on predicted generation displacement, $\hat{G}_d^f$ from Equation (1). Using the estimated marginal effect of daily solar generation on daily aggregated fossil fuel generation, $\hat{\beta}_1$, and assuming a marginal

[29] This result is supported by epidemiological evidence that cardiovascular illnesses due to air pollution are exacerbated more from longer-term (i.e., years) exposure than from shorter-term exposure (see, for example, Newby et al. (2015) and Brook et al. (2010))

effect that is constant over the magnitude of daily generation, we predict the daily fossil fuel displacement in the system that comes exclusively from variation in solar power generation. Next, we re-estimate our health analysis using predicted displacement $\hat{G}_d^f$, instead of S_d in Equation (3), for all cities and cities downwind of displaced plants, respectively.[30] For simplicity, we predict displacement using only coal-fired generation as this is the main displaced fossil fuel identified in Section 6.1. To avoid predicted daily displacement being a mere linear combination of daily solar generation, we re-estimate Equations (1) and (2) allowing for heterogeneous effects by year. Thus, our predicted displacement variables, $\hat{G}_{dt}^f$ and $\hat{G}_{dt}^{\text{disp plants}}$, are calculated as follow:

$$\text{Aggregated (All Cities) Displacement} = \hat{G}_{dt}^f = \hat{\beta}_{1t} \times S_{dt}, \tag{5}$$

$$\text{Displacement in Downwind Cities} = \hat{G}_{dt}^{\text{disp plants}} = \hat{\gamma}_{1t} \times S_{dt}, \tag{6}$$

where $t = \{2012, ...2017\}$, $\hat{\beta}_{1t}$ is the estimated marginal effect of S_d on daily aggregated generation by fuel f on year t, and $\hat{\gamma}_{1t}$ is the estimated marginal effect of S_d on aggregated generation by displaced plants on year t. Because the variables $\hat{G}_{dt}^f$ and $\hat{G}_{dt}^{\text{disp plants}}$ come from a first-step estimation process, we bootstrap this analysis using 500 replications. Appendix Table A13 illustrates the estimated marginal effect of solar-induced predicted fossil fuel displacement of dirty generation on morbidity.

The estimated health benefits from solar-induced predicted displacement are consistent with our baseline health results for lower respiratory diseases, especially across downwind cities. Because in this exercise we include as the regressor the full amount of fossil fuel displacement, we obtain effects that are larger in magnitude relative to the findings in Table 2. Yet, the sign and statistical significance of these effects remain. Though we obtain negative estimates for all respiratory diseases, they are less precise. The consistency of the results for lower respiratory diseases relative to our baseline health estimates strongly supports our findings of health benefits from daily solar power generation.

6.2.2 $PM_{2.5}$, Solar Generation, and Health

Our previous results systematically indicate significant reductions in air pollution-related hospitalizations due to fossil fuel displacement as a response to increased solar power generation, mostly in cities downwind of displaced fossil fuel plants. While this strategy helps us to incorporate the air transport of pollutants emitted by the displaced thermal plants, it

[30] Because downwind cities are defined as such based on proximity from and location of displaced fossil fuel plants, we estimate an average displacement coefficient for these cities using variation coming from previously identified displaced plants.

constitutes an indirect test of the mechanism through which solar generation affects health. In this section, we employ a more direct test on the channel through which solar power generation decreases pollution-related morbidity by using available data on $PM_{2.5}$ concentrations. As mentioned in Section 3.2, station-based pollution data in Chile is scarce outside Santiago. However, we gathered publicly available daily $PM_{2.5}$ records for some of the cities hosting fossil fuel plants, some of which are downwind of these plants' emissions.[31]

With these data, we first re-estimate our baseline health equations but replace solar generation with city-level daily average $PM_{2.5}$ concentrations. We do so to estimate the direct effect of pollution concentrations on our morbidity outcomes. In doing this, we have to consider the role of omitted variables. For instance, $PM_{2.5}$ can be formed due to chemical reactions of secondary particles from SO_2 and NO_X, pollutants that not only are common to coal combustion but also have a direct impact on health (World Health Organization, 2006). In addition, other factors such as economic conditions may have a simultaneous impact on both health outcomes and air pollution concentrations. Thus, while informative, this regression may give us an inconsistent estimator of the air pollution impact on health. To address this, we also include a specification in which we use day-to-day variation in solar generation or capacity factor as two different instruments for $PM_{2.5}$. Table 5 presents the results from these regressions, including first-stage results from regressing daily $PM_{2.5}$ on daily solar power or daily solar capacity factor. Our initial OLS regression is presented in columns (1) for all cities and downwind cities within $10km$. In columns (2) and (3), we present results from an instrumental-variables (IV) approach using a Two-Stage Least Square (2SLS) estimator.

The results in column (1) of Table 5 indicate $PM_{2.5}$ concentrations increase morbidity, particularly those associated with respiratory diseases. We also find a positive effect on cardiovascular outcomes, but they are very small and not statistically significant at the conventional levels. These findings support our results related to the direct impact of solar on health, namely, more solar power and less fossil fuel generation reduce emissions and in turn, hospitalizations. Furthermore, the fact that we do not find a direct effect of pollution on cardiovascular hospitalizations explains our lack of significance on cardiovascular hospitalizations in our baseline health analysis. Instrumenting for $PM_{2.5}$ in columns (2) and (3) results in significantly larger coefficients, suggesting a downward bias of the OLS estimates in column (1). At the same time, these larger-in-magnitude estimates signal that the use

[31]Specifically, we have data for Arica (2013-2017), Antofagasta (2013-2017), Tocopilla (2012-2017) and Alto Hospicio (2016-2017). The last two cities, namely Tocopilla and Alto Hospicio, are part of the group of downwind cities within $10km$ of displaced fossil fuel plants. Data are daily records averaged across stations and come from the National Air Quality Information System (SINCA)'s website, https://sinca.mma.gob.cl. Descriptive statistics for this variable are in Appendix Table A14.

Table 5: The Effect of Solar-Induced Changes in $PM_{2.5}$ on the Daily Rate of Hospital Admissions

	All Cities			Cities $< 10km$ Downwind of Displaced Fossil Fuel Plants		
	OLS	IV using S_d	IV using CF_d^{solar}	OLS	IV using S_d	IV using CF_d^{solar}
	(1)	(2)	(3)	(1)	(2)	(3)
Panel A. Cardiovascular						
$PM_{2.5}$	0.0002	-0.012	0.030	-0.002	0.029	0.038
	(0.007)	(0.053)	(0.044)	(0.013)	(0.071)	(0.059)
Panel B. All Respiratory						
$PM_{2.5}$	0.038***	0.193***	0.158**	0.045**	0.249**	0.205**
	(0.009)	(0.058)	(0.064)	(0.018)	(0.078)	(0.089)
Panel C. Upper Respiratory						
$PM_{2.5}$	0.006	0.054	0.055	0.010	0.087	0.060
	(0.006)	(0.042)	(0.053)	(0.011)	(0.090)	(0.074)
Panel D. Lower Respiratory						
$PM_{2.5}$	0.031***	0.143***	0.126**	0.036**	0.157**	0.157**
	(0.007)	(0.041)	(0.041)	(0.011)	(0.079)	(0.059)
Obs.	5,174	5,174	5,174	2,288	2,288	2,288
Number of Cities	4	4	4	2	2	2
Sample Mean - Panel A	2.146	2.146	2.146	2.756	2.756	2.756
Sample Mean - Panel B	2.206	2.206	2.206	2.206	3.113	3.113
Sample Mean - Panel C	0.515	0.515	0.515	0.589	0.589	0.589
Sample Mean - Panel D	1.422	1.422	1.422	2.239	2.239	2.239
First-Stage Results:						
$Solar_d$	-	-0.044***	-	-	-0.051**	-
	-	(0.012)	-	-	(0.018)	-
Cap Fac $Solar_d$	-	-	-0.004***	-	-	-0.007***
	-	-	(0.001)	-	-	(0.001)
F Test	-	98.278	80.811	-	48.743	79.752

Notes: This table displays estimation results from regressions of daily hospital admissions by disease on daily average $PM_{2.5}$ concentrations. Estimation results are marginal effects from OLS (column (1)) and 2SLS IV regressions using daily solar generation (column (2)) or daily solar capacity factor (column (3)) as instruments for $PM_{2.5}$. Daily $PM_{2.5}$ are measured in $\mu g/m^3$. Solar generation is in GWh. Solar capacity factor is between 0 and 100. All regressions include weather controls (minimum and maximum temperature, humidity, wind speed), mining production, demographic covariates, and year and weekend fixed effects. To facilitate the bootstrapping procedure of standard errors, we remove seasons and year × seasons fixed effects. Bootstrapped standard errors using 50 replications appear in parentheses. Significance levels: $^{*}p < 0.10$, $^{**}p < 0.05$, $^{***}p < 0.001$.

of day-to-day variation in solar generation allows us to fully capture variation in hospital admissions due to changes in daily $PM_{2.5}$ concentrations. We take the results in Table 5 as strong evidence that the co-benefits of solar power generation on hospital admissions found throughout our analysis are largely due to reductions in local airborne pollution from displaced thermal generation.

7 Additional Robustness Checks

Alternative Groups of Cities. Our results are robust to several alternative specifications. First, we check the robustness of our wind direction analysis by using cities with fossil fuel plants as a proxy for cities with pollution exposure. From our displacement analysis, we are also able to consider: 1) cities upwind of displaced plants, 2) cities downwind of non-displaced plants,[32] and 3) cities downwind of ramped-up plants (see Figure 6 in Section 6.1). This latter group, however, is quite restrictive as it ultimately limits the cities to just one. Results are in Appendix Table A15.

Reductions in hospitalizations attributable to solar generation are primarily found in places with fossil fuel generation. The results in the first two columns of Table A15 suggest that additional solar generation predominantly curtails respiratory admissions in cities where displacement is possible. Namely, an additional 1-GWh of solar generation results in a 23.6 pp reduction in the rate of all respiratory hospitalizations in cities that house fossil fuel plants, of which the majority of these effects are reductions in lower respiratory hospitalizations. Similar to our findings with all cities and downwind cities, we do not find a statistically significant impact on cardiovascular-related hospitalizations.

We also find that cities upwind of displaced plants or downwind of non-displaced plants are not generally affected by solar, as almost all coefficients are statistically insignificant and very small. We do find a negative effect, albeit small in magnitude, in cities upwind of displaced plants. This is not unusual as we define downwind cities assuming a radius of exposure of 45 degrees, which is quite conservative. In any case, we find no results in cities downwind of non-displaced plants, which validates our identification strategy of using distance to displaced thermal plants to more accurately identify the impact of solar on health. Finally, we find large positive effects of solar on lower respiratory hospitalizations in cities that are downwind of plants that have ramped up in response to solar generation (column (1)). Our plant-level analysis shows that two coal-fired plants and one gas-fired unit ramp up their production in response to the injection of this renewable (see Figure 6 and Appendix Figure A9). Thus, it is not surprising that respiratory hospitalizations increase in this subsample. Yet this effect disappears once we utilize our preferred set of time-fixed effects in column (2).

Alternative Estimation Methods. We also test the robustness of our OLS health estimation by utilizing alternative estimators and models: a Poisson estimator (Appendix Table A16), and a Zero-Inflated Negative Binomial (ZINB, Appendix Table A17) and a Negative

[32] Defined as plants for whom the displacement regressions were insignificant.

Binomial model (Appendix Table A18). Unlike OLS, the Poisson estimator takes into account the structure of the hospital admissions data by considering the number of counts of the event (admissions) a day. Thus, we estimate Equation (3) by replacing the outcome variable $Health_{jd}$ for the number of admissions a day. The ZINB and Negative Binomial specifications are variations of the Poisson estimator in which the zero-inflation of the outcomes, i.e., the pile-up at zero, and the overdispersion of the data, respectively, are allowed.[33] To interpret our coefficient estimates as rates, we restrict the coefficient of the population size in Equation (3) to one.

Our Poisson results in Appendix Table A16 are very similar to the results obtained by utilizing OLS. Specifically, we find that a 1-GWh increase in daily solar generation reduces the daily rate of all respiratory hospitalizations by 6.7% in all cities, by 14.4% downwind $10km$ cities, by 9.3% in downwind $50km$ cities, and by 7.8% in downwind $100km$. A similar effect is found for hospital admissions due to lower respiratory diseases: an additional 1-GWh increase in daily solar generation leads to a 12.5% reduction in hospitalizations due to lower respiratory diseases in cities downwind within $10km$ of distance, an effect that decreases monotonically as we move farther away to cities downwind within $50km$ and $100km$. Notice here that this feature was not evident in Table 4 as OLS obscures the fact that downwind cities in our sample within $50km$ and $100km$ of distance from displaced plants are small in population, and thus, counts of hospital admissions are less disperse as compared to the distribution of admissions in all cities or downwind cities within $10km$. This data structure is taken into account by the Poisson estimator, and thus, consistently with one of our identifying assumptions, the estimated marginal effect of solar on health consistently decreases with distance to the pollution source. We obtain very similar results with the ZINB and the Negative Binomial specifications in A17 and A18. These findings demonstrate that our results are robust to the choice of estimator, and support the intuitive nature of a health effect that monotonically decreases with distance to displaced power plants.

Placebo Health Outcomes Additionally, we test whether solar generation affects health outcomes that are, presumably, unrelated to pollution. Appendix Table A19 displays the ZINB results of this falsification test using infections (panel A) and blood diseases (excluding anemia) (panel B). We also include Schlenker and Walker (2016)'s placebo outcomes: strokes (panel C), bone fractures (panel D) and appendicitis (panel E).[34] These results are small and

[33] It is important to note here that some cities in northern Chile are very small in size, which means that many of them report zero daily hospital admissions. Alternative estimation methods to deal with this, such as a Hurdle estimation, resulted in the lack of convergence in many of our regressions.

[34] The exact ICD-10 codes are A00/A099, A200/A799 and B50/B999 for infections (we exclude tuberculosis A15/A19 and viral infections B00/B499); D65/D899 for blood disorders (excluding anemia); I60/I699 for

mostly statistically insignificant, regardless of the group of cities considered, which indicates that our previous findings are not sensitive to the choice of health disease.

8 Discussion

The remarkable and rapid expansion of solar generation capacity in Chile has provided a natural experiment to test the impact of renewable electricity sources on morbidity in a developing country. We run a variety of different tests to quantify the health benefits of almost 600 MW of new solar generation capacity. Overall, our results tell a positive story about how we can employ solar energy to bring about improved health outcomes in settings with elevated pollution exposure and reduced healthcare access.

We first demonstrate that solar energy can effectively displace fossil fuel plants, notably plants that rely on coal and natural gas. These heavy emitters are displaced by increases in solar generation, although the benefits may be attenuated by the ramp-up of a subset of fossil fuel generators and the reductions in hydro and geothermal electricity. However, given the relatively small shares of these fuel types in total generation, the attenuation of displacement is not enough to offset the positive health benefits.

We next show that the day-to-day operation of solar plants reduces daily hospitalizations of respiratory diseases, particularly those related to the lower airways. When taking into account the transport of pollutants using cities downwind of fossil fuel plants displaced by solar generation, we find significant morbidity reductions associated with all types of respiratory diseases, particularly lower respiratory diseases. The effect size is larger in towns in the immediate vicinity of displaced fossil fuel plants (within $10km$), yet the effect is still noticeable up to $100km$ from the displaced facilities. This result demonstrates the geographic heterogeneous effect of solar generation and simultaneously suggests that areas with intense fossil fuel generation will benefit more from an expansion of renewable, clean energy sources. Across different age groups, we find the largest statistically significant impacts on hospitalizations of infants and toddlers, the most vulnerable age groups. Furthermore, we show that the health co-benefits of solar generation are strongest in the short-term and are distinguishable after immediate exposure to reduced pollution from curtailed fossil fuel generation, mostly when it comes to respiratory diseases. Our findings also reveal that long-term displacement of fossil fuel sources may also lead to benefits in cardiovascular diseases.

Our results remain unaltered after using several robustness checks, which include the use of cities without thermal generation, upwind cities, cities downwind of non-displaced plants, and cities downwind of plants that have ramped up. Our results are also robust to alternative

strokes; S000/S999 for bone fractures; and K350/K389 for appendicitis.

estimation approaches, including utilizing Poisson and negative binomial models, and to the use of hospital admissions due to other conditions presumably not related to pollution.

Our study provides important evidence that solar generation can bring about positive health outcomes in developing nations, increasing the social benefits of investment in power generation capacity for these clean resources. A simple back-of-the-envelope calculation considering an overnight hospital average stay cost of USD 706 for the case of respiratory diseases in this country (Alvear et al., 2013), an average length of stay of 5.6 nights in our sample, and total annual reductions in hospital admissions of 25.45 (9.38% of an average of 0.743 daily hospitalizations), we obtain an average reduction of 142.75 respiratory-related hospital nights a year.[35] This translates into over CH$80 million in savings per year, roughly equivalent to USD 100,000 or 212 Chilean monthly minimum salaries (as of 2022). These numbers scale up to more than CH$255 million savings a year, equivalent to USD 319,000 or 672 minimum salaries, for downwind cities within $10km$ of distance from displaced dirty plants. It is important to point out that this number underestimates the total costs associated with pollution exposure for two reasons. First, we do not estimate mortality, which generally results in significantly larger costs than morbidity (for example, in Muller and Mendelsohn (2007), the mortality costs are 5.5 times larger than the morbidity costs of air pollution exposure). Furthermore, countries such as Chile that suffer from limited healthcare infrastructure would be forced to adjust their healthcare provision during spikes in air pollution (Guidetti et al., 2021). Thus, our results should be considered as a lower bound of the true co-benefits that solar generation can bring to developing countries.

This work can be expanded upon in several ways. First, our results suggest that solar generation may have a long-term effect on cardiovascular-related morbidity. Estimating whether solar generation reduces mortality from pollution exposure, particularly cardiovascular-related mortality, would help identify the full benefits of a cleaner grid in Chile. This is something to explore in future research. Second, we lacked comprehensive data to explore the impact of solar power on global and local pollutants beyond $PM_{2.5}$. Future research could employ satellite data to conduct this analysis. Furthermore, our work estimates the impact of solar generation prior to the northern and southern grid interconnection in Chile; identifying the effect once these two grids are interconnected is another potential avenue of research outside the scope of this paper.[36] These avenues remain open for future research.

[35]The daily rate of daily hospital admissions due to respiratory diseases across all cities is 1.216 per 100,000 people. Considering the average sample population across all cities of 61,154 inhabitants, we obtain 0.743 average hospitalizations per day.

[36]The *a priori* effect of the interconnection on the health benefits of solar generation is unclear, due to different factors. First, Chile's major population centers are in the south, which would imply greater impacts of solar generation on health. However, solar generation is more likely to occur in the north, given the region's massive solar irradiation compared to southern Chile. Thus, transmission constraints would likely attenuate

Acknowledgements

We thank Andrew Bibler, Janet Currie, Harrison Fell, Maria Harris, Sarah Jacobson, Nicolai Kuminoff, Lucija Muehlenbachs, Subhrendu K. Pattanayak, and Brett Watson for their helpful comments and suggestions. We also thank seminar participants at CAF, CERE-Umeå University, Environmental Defense Fund, FGV-EESP, Grantham Workshop, Insper, Manhattan College, Adolfo Ibañez University, North Catholic University, PUC-Chile, University of Chile, University of São Paulo, University of Talca, and workshop and conference participants at the 21st Annual CU Environmental and Resource Economics Workshop, the 25th Annual Conference of the European Association of Environmental and Resource Economists, the 2021 Association of Environmental and Resource Economists Annual Summer Conference, Camp Resources XXVI, the 7th Canadian Resource and Environmental Economics Association Workshop, the 2020 Eastern Economic Association Annual Meeting, the 2021 Empirical Methods in Energy Economics Summer Workshop, 2021 SETI Annual Meetings, Tercer Workshop Sobre Economía del Medio Ambiente y Cambio Climático, the 2021 Western Economic Association International Annual Conference, and the 2022 PDRI Conference on Climate Change the Environment, for helpful comments and suggestions. All errors are ours.

References

Abel, D., Holloway, T., Harkey, M., Rrushaj, A., Brinkman, G., Duran, P., Janssen, M., and Denholm, P. (2018). Potential air quality benefits from increased solar photovoltaic electricity generation in the eastern United States. *Atmospheric Environment*, 175:65–74.

Alvear, S., Canteros, J., Jara, J., and Rodríguez, P. (2013). Costos reales de tratamientos intensivos por paciente y día cama. *Revista médica de Chile*, 141(2):202–208.

Anenberg, S. C., Schwartz, J., Shindell, D., Amann, M., Faluvegi, G., Klimont, Z., Janssens-Maenhout, G., Pozzoli, L., Van Dingenen, R., Vignati, E., et al. (2012). Global air quality and health co-benefits of mitigating near-term climate change through methane and black carbon emission controls. *Environmental Health Perspectives*, 120(6):831–839.

Arceo, E., Hanna, R., and Oliva, P. (2016). Does the effect of pollution on infant mortality

that benefit. Furthermore, because the southern grid is cleaner, the relative benefits of solar generation will be lower compared to that in northern Chile. Thus, the overall effect may be larger or smaller than the effect of solar only within SING.

differ between developing and developed countries? Evidence from Mexico City. *The Economic Journal*, 126(591):257–280.

Baker, E., Fowlie, M., Lemoine, D., and Reynolds, S. S. (2013). The economics of solar electricity. *Annu. Rev. Resour. Econ.*, 5(1):387–426.

Banzhaf, S., Ma, L., and Timmins, C. (2019). Environmental justice: The economics of race, place, and pollution. *Journal of Economic Perspectives*, 33(1):185–208.

Barbose, G., Wiser, R., Heeter, J., Mai, T., Bird, L., Bolinger, M., Carpenter, A., Heath, G., Keyser, D., Macknick, J., et al. (2016). A retrospective analysis of benefits and impacts of US renewable portfolio standards. *Energy Policy*, 96:645–660.

Barrows, G., Garg, T., and Jha, A. (2018). The economic benefits versus environmental costs of India's coal-fired power plants. *Available at SSRN*.

Bell, M. L., Dominici, F., and Samet, J. M. (2005). A meta-analysis of time-series studies of Ozone and mortality with comparison to the national morbidity, mortality, and air pollution study. *Epidemiology*, 16(4):436–445.

Bell, M. L., McDermott, A., Zeger, S. L., Samet, J. M., and Dominici, F. (2004). Ozone and short-term mortality in 95 US urban communities, 1987-2000. *JAMA*, 292(19):2372–2378.

Bharadwaj, P., Gibson, M., Zivin, J. G., and Neilson, C. (2017). Gray matters: Fetal pollution exposure and human capital formation. *Journal of the Association of Environmental and Resource Economists*, 4(2):505–542.

Bonilla, J. A., Lopez-Feldman, A., Pereda, P., Rivera, N. M., Ruiz-Tagle, J. C., et al. (2021). Long-term air pollution exposure and covid-19 mortality in latin america. Technical report, University of São Paulo (FEA-USP).

Brook, R. D., Rajagopalan, S., Pope III, C. A., Brook, J. R., Bhatnagar, A., Diez-Roux, A. V., Holguin, F., Hong, Y., Luepker, R. V., Mittleman, M. A., et al. (2010). Particulate matter air pollution and cardiovascular disease: an update to the scientific statement from the American Heart Association. *Circulation*, 121(21):2331–2378.

Buonocore, J. J., Luckow, P., Norris, G., Spengler, J. D., Biewald, B., Fisher, J., and Levy, J. I. (2016). Health and climate benefits of different energy-efficiency and renewable energy choices. *Nature Climate Change*, 6(1):100–105.

Burney, J. A. (2020). The downstream air pollution impacts of the transition from coal to natural gas in the United States. *Nature Sustainability*, pages 1–9.

Bushnell, J. and Novan, K. (2021). Setting with the sun: The impacts of renewable energy on conventional generation. *Journal of the Association of Environmental and Resource Economists*, 8(4):759–796.

Callaway, D. S., Fowlie, M., and McCormick, G. (2018). Location, location, location: The variable value of renewable energy and demand-side efficiency resources. *Journal of the Association of Environmental and Resource Economists*, 5(1):39–75.

Casey, J. A., Gemmill, A., Karasek, D., Ogburn, E. L., Goin, D. E., and Morello-Frosch, R. (2018a). Increase in fertility following coal and oil power plant retirements in California. *Environmental Health*, 17(1):44.

Casey, J. A., Karasek, D., Ogburn, E. L., Goin, D. E., Dang, K., Braveman, P. A., and Morello-Frosch, R. (2018b). Retirements of coal and oil power plants in California: Association with reduced preterm birth among populations nearby. *American Journal of Epidemiology*, 187(8):1586–1594.

Chauhan, A. J., Inskip, H. M., Linaker, C. H., Smith, S., Schreiber, J., Johnston, S. L., and Holgate, S. T. (2003). Personal exposure to Nitrogen Dioxide (NO_2) and the severity of virus-induced asthma in children. *The Lancet*, 361(9373):1939–1944.

Chay, K. Y. and Greenstone, M. (2003a). Air quality, infant mortality, and the Clean Air Act of 1970. Technical report, National Bureau of Economic Research.

Chay, K. Y. and Greenstone, M. (2003b). The impact of air pollution on infant mortality: Evidence from geographic variation in pollution shocks induced by a recession. *The Quarterly Journal of Economics*, 118(3):1121–1167.

Chen, Y., Ebenstein, A., Greenstone, M., and Li, H. (2013). Evidence on the impact of sustained exposure to air pollution on life expectancy from China's Huai River policy. *Proceedings of the National Academy of Sciences of the United States of America*, 110(32):12936–12941.

Chile Environmental Ministry (2017). Informe Consolidado de Emisiones y Transferencia de Contaminantes 2005-2017. Retrieved from RETC, Ministerio de Medio Ambiente: ttps://retc.mma.gob.cl.

Chile Environmental Ministry (2018). Tercer Informe Bienal de Actualización de Chile sobre Cambio Climático. Retrieved from Ministerio de Medio Ambiente: https://www.mma.gob.cl.

Cullen, J. (2013). Measuring the environmental benefits of wind-generated electricity. *American Economic Journal: Economic Policy*, 5(4):107–33.

Cullen, J. A. and Mansur, E. T. (2017). Inferring carbon abatement costs in electricity markets: A revealed preference approach using the shale revolution. *American Economic Journal: Economic Policy*, 9(3):106–33.

Currie, J. and Neidell, M. (2005). Air pollution and infant health: What can we learn from California's recent experience? *Quarterly Journal of Economics*, 120(3):1003–1030.

Currie, J., Neidell, M., and Schmieder, J. F. (2009). Air pollution and infant health: Lessons from New Jersey. *Journal of Health Economics*, 28(3):688–703.

Currie, J. and Walker, R. (2011). Traffic congestion and infant health: Evidence from E-ZPass. *American Economic Journal: Applied Economics*, 3(1):65–90.

Currie, J., Zivin, J. G., Mullins, J., and Neidell, M. (2014). What do we know about short-and long-term effects of early-life exposure to pollution? *Annu. Rev. Resour. Econ.*, 6(1):217–247.

Dardati, E., de Elejalde, R., and Giolito, E. P. (2021). On the short-term impact of pollution: The effect of PM 2.5 on emergency room visits.

Edenhofer, O., Hirth, L., Knopf, B., Pahle, M., Schlömer, S., Schmid, E., and Ueckerdt, F. (2013). On the economics of renewable energy sources. *Energy Economics*, 40:S12–S23.

Fell, H. and Kaffine, D. T. (2018). The fall of coal: Joint impacts of fuel prices and renewables on generation and emissions. *American Economic Journal: Economic Policy*, 10(2):90–116.

Fell, H., Kaffine, D. T., and Novan, K. (2021). Emissions, transmission, and the environmental value of renewable energy. *American Economic Journal: Economic Policy*, 13(2):241–72.

Fell, H. and Linn, J. (2013). Renewable Electricity Policies, Heterogeneity, and Cost Effectiveness. *Journal of Environmental Economics and Management*, 66(3):688–707.

Fell, H. and Morrill, M. S. (2022). The impact of wind energy on air pollution and emergency department visits.

Franklin, B. A., Brook, R., and Pope III, C. A. (2015). Air pollution and cardiovascular disease. *Current Problems in Cardiology*, 40(5):207–238.

Galetovic, A. and Muñoz, C. M. (2011). Regulated electricity retailing in Chile. *Energy Policy*, 39(10):6453–6465.

Gauderman, W. J., Avol, E., Lurmann, F., Kuenzli, N., Gilliland, F., Peters, J., and McConnell, R. (2005). Childhood asthma and exposure to traffic and Nitrogen Dioxide. *Epidemiology*, 16(6):737–743.

Guidetti, B., Pereda, P., and Severnini, E. (2021). " placebo tests" for the impacts of air pollution on health: The challenge of limited health care infrastructure. In *AEA Papers and Proceedings*, volume 111, pages 371–75.

Gupta, A. and Spears, D. (2017). Health externalities of India's expansion of coal plants: Evidence from a national panel of 40,000 households. *Journal of Environmental Economics and Management*, 86:262–276.

Haas, J., Palma-Behnke, R., Valencia, F., Araya, P., Díaz-Ferrán, G., Telsnig, T., Eltrop, L., Díaz, M., Püschel, S., Grandel, M., et al. (2018). Sunset or sunrise? understanding the barriers and options for the massive deployment of solar technologies in Chile. *Energy Policy*, 112:399–414.

Hoek, G., Krishnan, R. M., Beelen, R., Peters, A., Ostro, B., Brunekreef, B., and Kaufman, J. D. (2013). Long-term air pollution exposure and cardio-respiratory mortality: a review. *Environmental Health*, 12(1):43.

Holladay, J. S. and LaRiviere, J. (2017). The impact of cheap natural gas on marginal emissions from electricity generation and implications for energy policy. *Journal of Environmental Economics and Management*, 85:205–227.

Hollingsworth, A. and Rudik, I. (2019). External impacts of local energy policy: The case of renewable portfolio standards. *Journal of the Association of Environmental and Resource Economists*, 6(1):187–213.

Jacques-Coper, M., Falvey, M., and Muñoz, R. C. (2015). Inter-daily variability of a strong thermally-driven wind system over the Atacama Desert of South America: synoptic forcing and short-term predictability using the GFS global model. *Theoretical and Applied Climatology*, 121(1-2):211–223.

Johnsen, R., LaRiviere, J., and Wolff, H. (2019). Fracking, coal, and air quality. *Journal of the Association of Environmental and Resource Economists*, 6(5):1001–1037.

Kaffine, D. T., McBee, B. J., and Lieskovsky, J. (2013). Emissions savings from wind power generation in Texas. *The Energy Journal*, 34(1).

Knittel, C. R., Metaxoglou, K., and Trindade, A. (2015). Natural gas prices and coal displacement: Evidence from electricity markets. Technical report, National Bureau of Economic Research.

Knittel, C. R., Miller, D. L., and Sanders, N. J. (2016). Caution, drivers! Children present: Traffic, pollution, and infant health. *Review of Economics and Statistics*, 98(2):350–366.

Kopas, J., York, E., Jin, X., Harish, S., Kennedy, R., Shen, S. V., and Urpelainen, J. (2020). Environmental justice in India: Incidence of air pollution from coal-fired power plants. *Ecological Economics*, 176:106711.

Lavaine, E. and Neidell, M. (2017). Energy production and health externalities: Evidence from oil refinery strikes in France. *Journal of the Association of Environmental and Resource Economists*, 4(2):447–477.

Linn, J., Mastrangelo, E., and Burtraw, D. (2014). Regulating greenhouse gases from coal power plants under the Clean Air Act. *Journal of the Association of Environmental and Resource Economists*, 1(1/2):97–134.

Linn, J. and Muehlenbachs, L. (2018). The heterogeneous impacts of low natural gas prices on consumers and the environment. *Journal of Environmental Economics and Management*, 89:1–28.

Mei, Y., Gao, L., Zhang, W., and Yang, F.-A. (2021). Do homeowners benefit when coal-fired power plants switch to natural gas? evidence from beijing, china. *Journal of Environmental Economics and Management*, 110:102566.

Millstein, D., Wiser, R., Bolinger, M., and Barbose, G. (2017). The climate and air-quality benefits of wind and solar power in the United States. *Nature Energy*, 2(9):17134.

Ministry of Energy (2013). Ley 20.698: Propicia la ampliación de la matriz energética mediante fuentes renovables no convencionales. Retrieved from Congreso Nacional de Chile.

Muller, N. Z. and Mendelsohn, R. (2007). Measuring the damages of air pollution in the United States. *Journal of Environmental Economics and Management*, 54(1):1–14.

Muller, N. Z. and Mendelsohn, R. (2009). Efficient pollution regulation: getting the prices right. *American Economic Review*, 99(5):1714–39.

Muñoz, R. C., Falvey, M. J., Arancibia, M., Astudillo, V. I., Elgueta, J., Ibarra, M., Santana, C., and Vásquez, C. (2018). Wind energy exploration over the Atacama Desert: A numerical model–guided observational program. *Bulletin of the American Meteorological Society*, 99(10):2079–2092.

Neidell, M. (2009). Information, avoidance behavior, and health the effect of Ozone on asthma hospitalizations. *Journal of Human Resources*, 44(2):450–478.

Newby, D. E., Mannucci, P. M., Tell, G. S., Baccarelli, A. A., Brook, R. D., Donaldson, K., Forastiere, F., Franchini, M., Franco, O. H., Graham, I., et al. (2015). Expert position paper on air pollution and cardiovascular disease. *European heart journal*, 36(2):83–93.

Novan, K. (2015). Valuing the wind: Renewable energy policies and air pollution avoided. *American Economic Journal: Economic Policy*, 7(3):291–326.

Pershagen, G., Rylander, E., Norberg, S., Eriksson, M., and Nordvall, S. L. (1995). Air pollution involving Nitrogen Dioxide exposure and Wheezing Bronchitis in children. *International Journal of Epidemiology*, 24(6):1147–1153.

Programa Chile Sustentable (2017). Termoelétricas a Carbón en Chile. http://www.chilesustentable.net. Retrieved in March, 2020.

Rau, T., Urzúa, S., and Reyes, L. (2015). Early exposure to hazardous waste and academic achievement: evidence from a case of environmental negligence. *Journal of the Association of Environmental and Resource Economists*, 2(4):527–563.

Rivera, N. M. (2020). Is mining an environmental disamenity? evidence from resource extraction site openings. *Environmental and Resource Economics*, 75(3):485–528.

Rivera, N. M. and Loveridge, S. (2022). Coal-to-gas fuel switching and its effects on housing prices. *Energy Economics*, 106:105733.

Rondanelli, R., Molina, A., and Falvey, M. (2015). The Atacama surface solar maximum. *Bulletin of the American Meteorological Society*, 96(3):405–418.

Schlenker, W. and Walker, W. R. (2016). Airports, air pollution, and contemporaneous health. *The Review of Economic Studies*, 83(2):768–809.

Schwartz, J. (1996). Air pollution and hospital admissions for respiratory disease. *Epidemiology*, pages 20–28.

Schwartz, J. and Morris, R. (1995). Air pollution and hospital admissions for cardiovascular disease in Detroit, Michigan. *American Journal of Epidemiology*, 142(1):23–35.

Sergi, B., Adams, P. J., Muller, N., Robinson, A. L., Davis, S., Marshall, J. D., and Azevedo, I. M. L. (2020). Optimizing emissions reductions from the US power sector for climate and health benefits. *Environmental Science & Technology*.

Siler-Evans, K., Azevedo, I. L., Morgan, M. G., and Apt, J. (2013). Regional variations in the health, environmental, and climate benefits of wind and solar generation. *Proceedings of the National Academy of Sciences*, 110(29):11768–11773.

Spiller, E., Proville, J., Roy, A., and Muller, N. Z. (2021). Mortality risk from pm 2.5: a comparison of modeling approaches to identify disparities across racial/ethnic groups in policy outcomes. *Environmental health perspectives*, 129(12):127004.

Spiller, E., Sopher, P., Martin, N., Mirzatuny, M., and Zhang, X. (2017). The environmental impacts of green technologies in TX. *Energy Economics*, 68:199–214.

Thakrar, S. K., Balasubramanian, S., Adams, P. J., Azevedo, I. M., Muller, N. Z., Pandis, S. N., Polasky, S., Pope III, C. A., Robinson, A. L., Apte, J. S., et al. (2020). Reducing mortality from air pollution in the united states by targeting specific emission sources. *Environmental Science & Technology Letters*, 7(9):639–645.

U.S. Energy Information Administration (2019). International Energy Outlook 2019. Retrieved in November, 2019.

U.S. Environmental Protection Agency (2006). Air quality criteria document for Ozone. https://cfpub.epa.gov/ncea/risk/recordisplay.cfm?deid=149923. Retrieved in December, 2020.

U.S. Environmental Protection Agency (2014). EPA's Report on the Environment (ROE): Sulfur Dioxide Emissions. https://cfpub.epa.gov/roe/indicator.cfm?i=22. Last Updated: 2014.

U.S. Environmental Protection Agency (2019). Local Renewable Energy Benefits and Resources. https://www.epa.gov/statelocalenergy/local-renewable-energy-benefits-and-resources. Retrieved in November, 2019.

Wiser, R., Mai, T., Millstein, D., Barbose, G., Bird, L., Heeter, J., Keyser, D., Krishnan, V., and Macknick, J. (2017). Assessing the costs and benefits of US renewable portfolio standards. *Environmental Research Letters*, 12(9):094023.

World Health Organization (2006). *Air Quality Guidelines*. Global Update 2005. World Health Organization.

Appendix

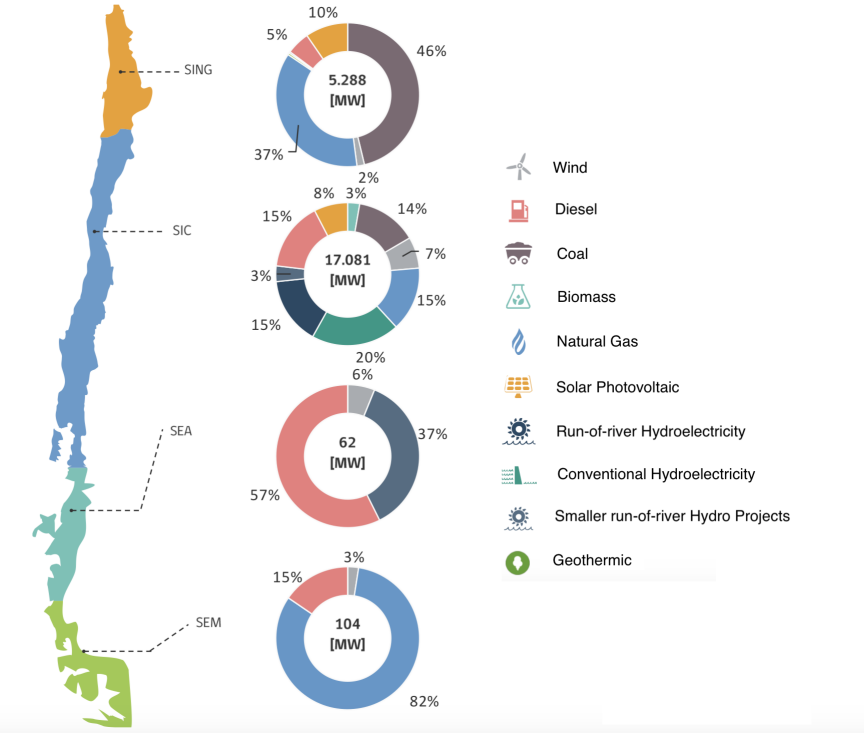

Figure A1: Bulk Power Systems in Chile

Notes: This figure depicts the four bulk power system that existed in Chile until 2018. It also displays the fuel source composition of each system: the Northern Interconnected System (SING), the Central Interconnected System (SIC), the Aysen Electric System (SEA), and the Magallanes Electric System (SEM). SING and SIC interconnected in 2018, and the whole system was renamed as the National Electric System (SEC). This figure was adapted from the *National Energy Commission Monthly Report*, dated December 2017. https://www.cne.cl/wp-content/uploads/2015/06/RMensual_v201712.pdf

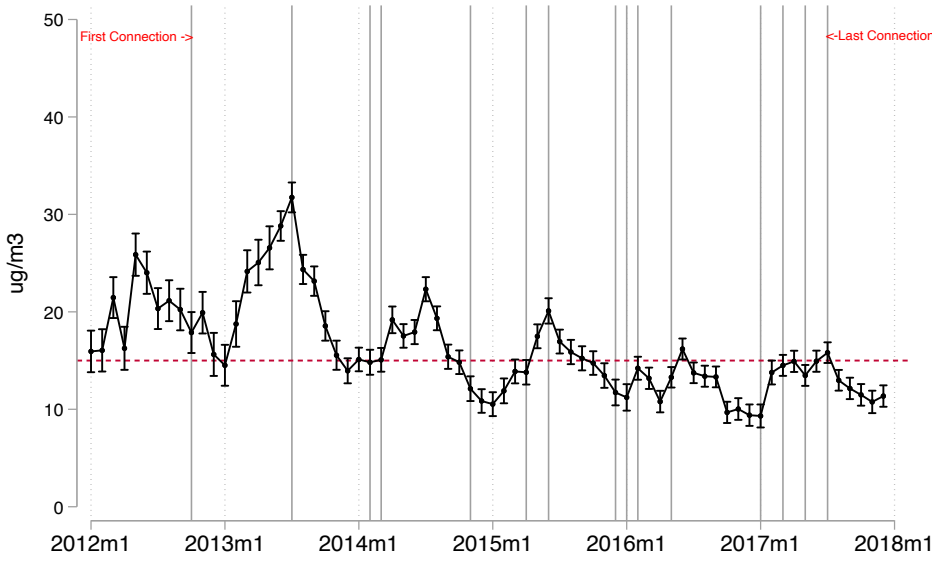

Figure A2: Monthly Average $PM_{2.5}$ Concentrations at SING and Dates of Solar Connections

Notes: This figure shows monthly average fine particle matter ($PM_{2.5}$) concentrations across cities at SING hosting thermal power plants from 2012 to 2017. Observations are in $\mu g/m^3$. Gray lines represent the date (month and year) of connection of the solar plants included in the sample (there are some solar plants connecting to the system during the same month). The dashed-red reference line represents the World Health Organization's 24-hour mean guideline of 15 $\mu g/m^3$. We trim the top and bottom 1% of all observations. Data come from the National Air Quality Information System (Sistema de Información Nacional de Calidad del Aire — SINCA) from 2012 to 2017.

Table A1: Monthly Fuel Use and Prices

Variable	Mean	Std. Dev.	Min.	Max.	Obs.
Panel A. Fuel Use					
Coal	34,931.76	3,210.30	25,949.25	42,148.77	2,192
Diesel	1,020.77	684.61	26.08	2,602.4	2,192
Fuel oil	369.33	301.059	1	1,219	1,187
Fuel oil #6	955.93	910.55	9	3,321.5	2,192
Natural gas	15,333.87	7,389.24	3,371.79	44,707.66	2,192
Panel B. Fuel Prices					
Coal	105.41	16.21	68.19	138.73	2,192
Diesel	620.94	200.63	288.5	908.7	2,192
Fuel oil	95.79	22.91	46.67	125.33	1,187
Fuel oil #6	446.96	175.40	157	728.41	2,192
Natural gas	3.15	0.79	1.7	5.94	2,192

Notes: This table displays main descriptive statistics of monthly fossil fuel uses and prices from 2012 to 2017. Descriptive statistics use main fuel source only. Coal, diesel and fuel oil are in tons, while natural gas is in thousands m^3. Prices are in US$/ton for coal, US$/m^3 for diesel and fuel oil #6, in US$/mm btu for natural gas, and in US$/bbl for fuel oil. Data come from the National Energy Commission.

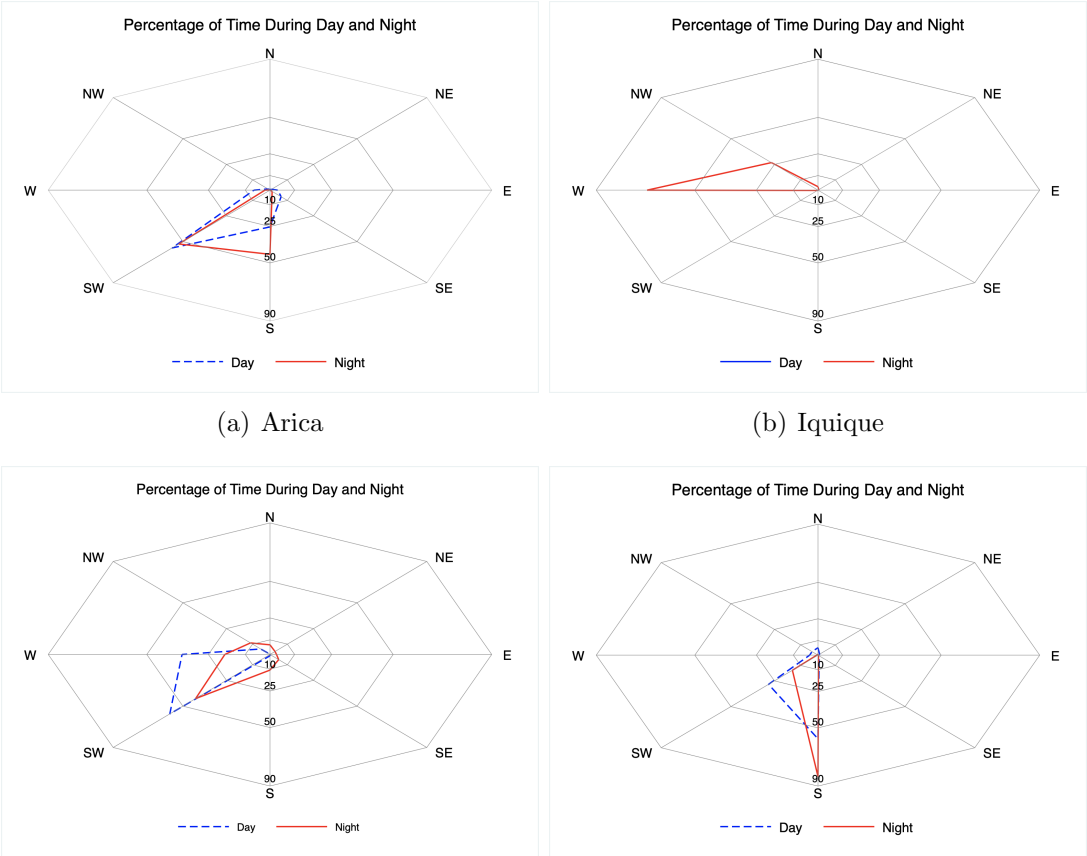

(a) Arica (b) Iquique

(c) Tocopilla (d) Antofagasta

Figure A3: Daily Wind Direction in Cities with Fossil Fuel Generation

Notes: This figure shows daily wind directions in four (out of five) cities that host fossil-fueled generators in our sample. "Daytime" (dashed line) encompasses average wind direction patterns during sunshine hours (7 a.m.–7 p.m.). "Night" (solid line) encompasses average wind direction between 7 p.m. and 7 a.m. the following day. Concentric circles represent the percentage of time in which the wind blows in that direction, namely 10%, 25%, 50% and 90%. Data come from the Meteorological Service and Air Quality System from 2012 to 2017. Data on daytime wind direction for Iquique (Panel 3(b)) are not available.

Table A2: Summary Statistics on the Daily Rate of Hospital Admissions by Age Group

Disease	Mean	Std. Dev.	Min.	Max.	Obs.
Panel A. Infants					
Cardiovascular	0.004	0.436	0	85.324	41,648
All respiratory	0.126	1.058	0	78.309	41,648
Upper respiratory	0.007	0.212	0	29.326	41,648
Lower respiratory	0.116	1.027	0	78.309	41,648
Panel B. Toddlers					
Cardiovascular	0.004	0.138	0	19.372	41,648
All respiratory	0.235	1.956	0	107.759	41,648
Upper respiratory	0.079	0.812	0	57.937	41,648
Lower respiratory	0.150	1.759	0	107.759	41,648
Panel C. Kids					
Cardiovascular	0.012	0.387	0	58.893	41,648
All respiratory	0.128	2.555	0	319.489	41,648
Upper respiratory	0.065	0.930	0	85.324	41,648
Lower respiratory	0.061	2.375	0	319.489	41,648
Panel D. Adults					
Cardiovascular	0.535	3.337	0	409.836	41,648
All respiratory	0.364	2.290	0	168.350	41,648
Upper respiratory	0.119	1.383	0	168.350	41,648
Lower respiratory	0.190	1.677	0	107.759	41,648
Panel E. Seniors					
Cardiovascular	0.489	3.418	0	322.581	41,648
All respiratory	0.350	3.728	0	409.836	41,648
Upper respiratory	0.006	0.339	0	56.465	41,648
Lower respiratory	0.27	2.457	0	107.759	41,648

Notes: This table displays main descriptive statistics of the daily rate of hospital admissions by age group from 2012 to 2017. Hospital admission rates are per 100,000 people. Observations are across all cities in the sample using patient's city of origin. Data come from the Ministry of Health, through the Department of Health Statistics and Information (DEIS) from 2012 to 2017.

Table A3: Descriptive Statistics - Other Covariates

Variable	Mean	Std. Dev.	Min.	Max.
Panel A. All cities (n= 19)				
Demographics:				
Population	61,802.89	104,603.38	244	395,453
Density	19.43	47.45	0.08	229.51
Poverty Rate	14.11	9.06	2	37
Fertility Rate	11.18	6.32	0	21.6
Weather:				
Min. Temp. (C)	7.10	6.34	-25	23
Max. Temp. (C)	10.72	8.65	-11.8	33.4
Humidity (%)	49.11	13.71	9.68	96.26
Panel B. Cities with fossil fuel generation (n= 5)				
Demographics:				
Population	167,575	140,344.43	11,090	395,453
Density	30.91	32.35	2.92	89.28
Poverty Rate	8.30	3.66	3.12	15.71
Fertility Rate	16.31	2.13	12.19	21.6
Weather:				
Min. Temp. (C)	9.03	6.67	-18.4	23
Max. Temp. (C)	13.46	8.72	-11.8	33.4
Humidity (%)	52.31	14.07	9.69	96.26
Panel C. Cities without fossil fuel generation (n = 13)				
Demographics:				
Population	25,041.19	51,812.2	244	184,543
Density	16.42	53.11	0.08	229.51
Poverty Rate	16.29	9.82	2	37
Fertility Rate	9.40	6.49	0	20.99
Weather:				
Min. Temp. (C)	6.40	6.09	-25	22
Max. Temp. (C)	9.98	8.52	-11.8	33
Humidity (%)	47.88	13.68	9.68	95.85

Notes: This table displays main descriptive statistics of covariates by groups of cities. Observations are at the city level. There is one city in our sample, Pica, that switches from panel C to panel B due to the opening of a new fossil fuel generator during our study period. We discard this city from panels B and C. Data comes from the National System of Municipalities Information (SINIM) from 2012 to 2017.

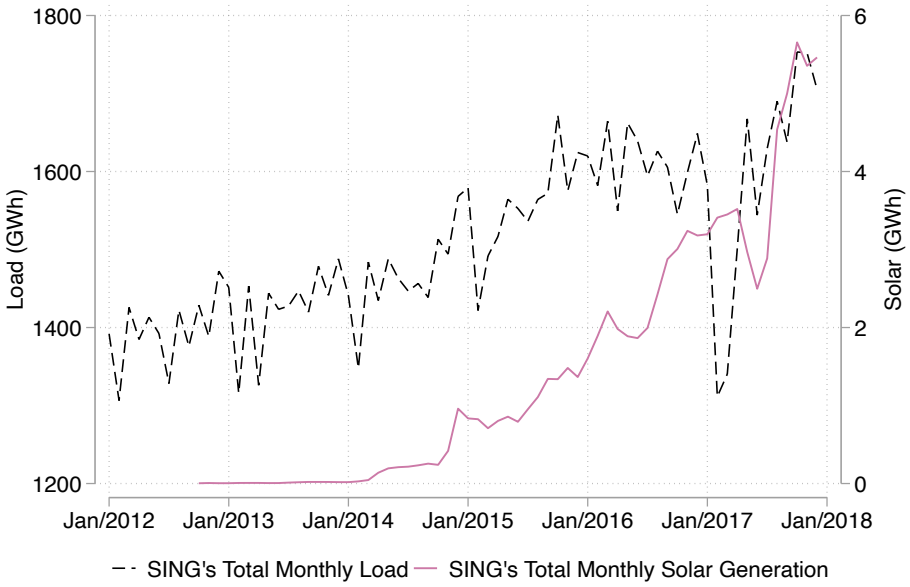

Figure A4: SING's Monthly Load and Solar Generation

Notes: This figure depicts the total monthly load and total monthly solar power generation at SING. Information is in gigawatts per hour (GWh). Monthly load is on the main y-axis. Monthly solar generation is on the secondary y-axis. Data comes from the National Electricity Coordinator from 2012 to 2017.

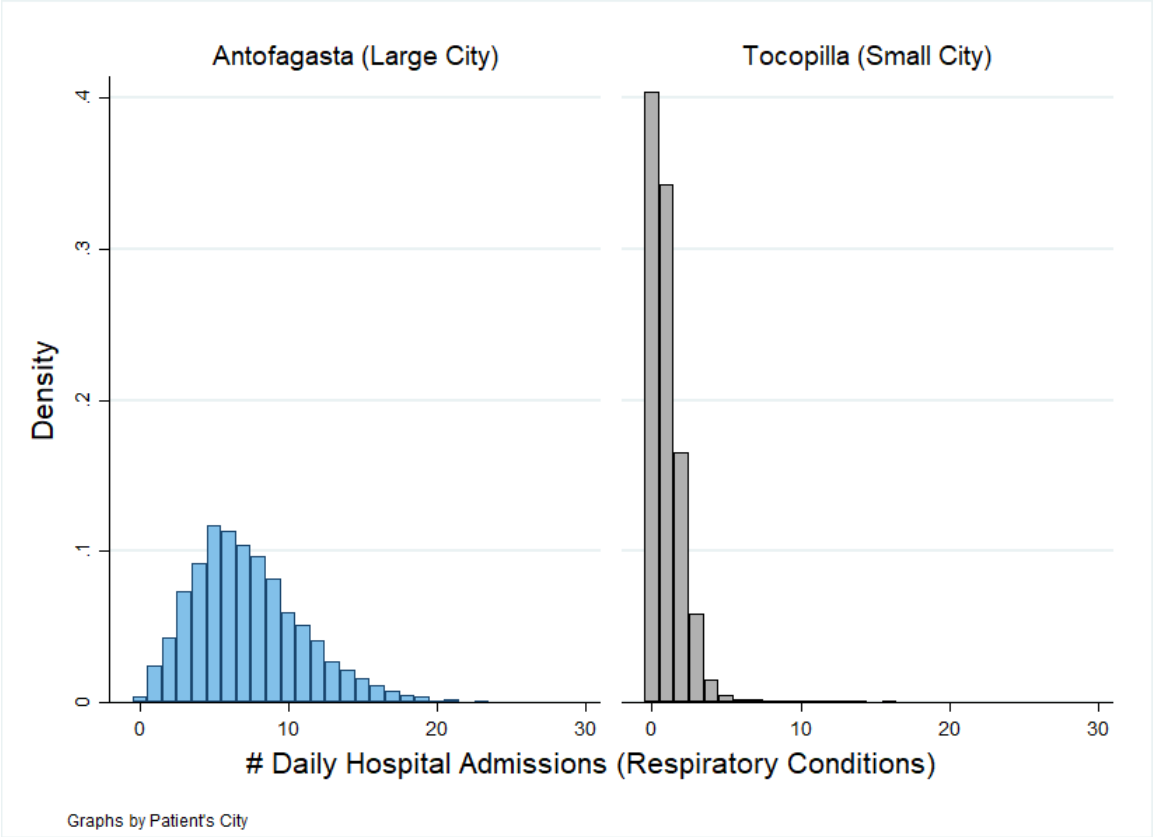

Figure A5: Overdispersion in the Health Outcome Variables

Notes: The left-hand panel exhibits the number of daily hospital admissions due to respiratory conditions for one of the largest cities in the sample, Antofagasta, while the right-hand panel shows the same variable for the case of a smaller city, Tocopilla. The overdispersion of this variable is evident in the case of the large city (left-hand side). The heterogeneity in the size of the pile-up at zero is also clear when comparing the two cities.

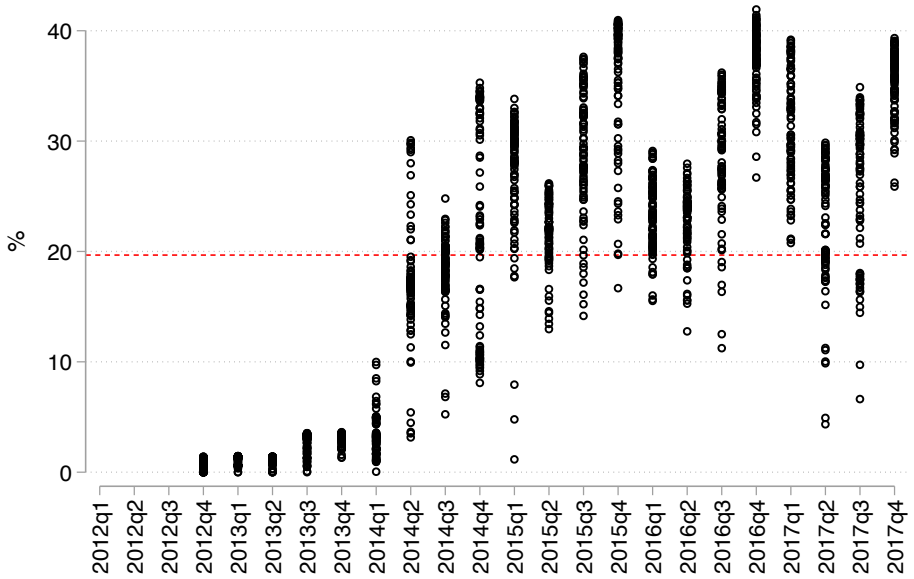

Figure A6: Within-Quarter Daily Solar Capacity Factor Over Time

Notes: The figure shows variation in daily solar capacity factor within quarters. Values represent percentages. Red dashed line represent the sample average. Data come from the National Electricity Coordinator from 2012 to 2017.

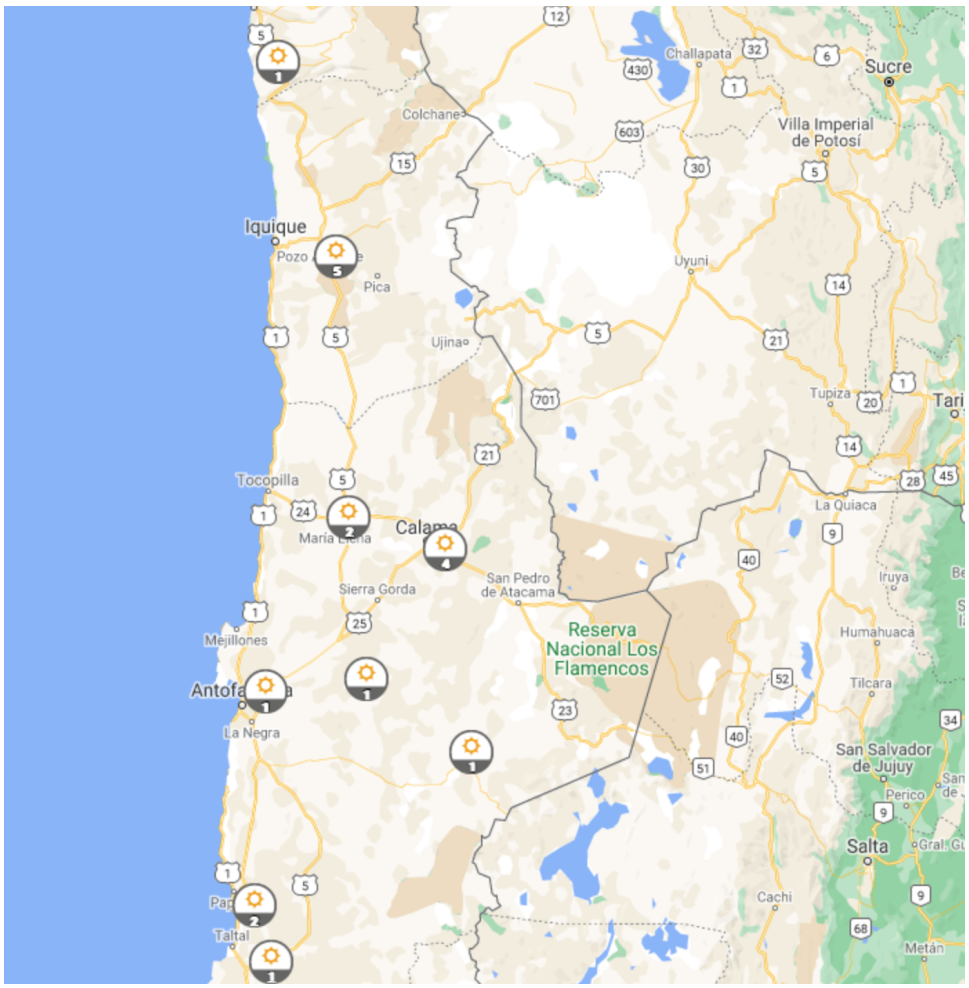

Figure A7: Location of Solar Generators at SING

Notes: This figure depicts the location of the solar generators at SING (northern Chile) included in our analysis. The figure was obtained from the National Energy Comission (CNE) from https://energiamaps.cne.cl

Table A4: The Effect of Daily Solar Energy on Daily Aggregated Fossil Fuel Generation

	Coal		Diesel		Fuel oil		Fuel oil #6		Natural gas	
	Fuel Use Lagged	No Fuel Use	Fuel Use Lagged	No Fuel Use	Fuel Use Lagged	No Fuel Use	Fuel Use Lagged	No Fuel Use	Fuel Use Lagged	No Fuel Use
Panel A. Generation (GWh)										
Solar Gen_d	-0.482**	-0.997***	-0.287**	0.002	0.009	-0.010	-0.037**	-0.039**	-0.144	-0.001
	(0.158)	(0.225)	(0.093)	(0.132)	(0.030)	(0.025)	(0.013)	(0.018)	(0.106)	(0.225)
Solar Cap $Factor_d$	-0.048**	-0.043**	-0.023**	-0.015	-0.0003	-0.001	-0.003	-0.004**	0.005	-0.008
	(0.016)	(0.020)	(0.0098)	(0.012)	(0.001)	(0.001)	(0.002)	(0.002)	(0.012)	(0.012)
Panel B. Capacity Factor										
Solar Gen_d	-0.016***	-0.016***	-0.018**	-0.0003	0.045	0.023	-0.014	-0.024	-0.038***	0.003
	(0.003)	(0.005)	(0.007)	(0.011)	(0.061)	(0.057)	(0.015)	(0.017)	(0.006)	(0.012)
Solar Cap $Factor_d$	-0.002***	-0.001**	-0.001**	-0.001	-0.0004	-0.0004	-0.001	-0.002	-0.001	-0.00005
	(0.0003)	(0.0003)	(0.0004)	(0.0005)	(0.002)	(0.001)	(0.001)	(0.001)	(0.001)	(0.001)
Obs.	1,824	1,915	1,824	1,915	667	910	1,824	1,915	1,824	1,915

Notes: This table displays estimation results from regressions of daily aggregated fossil fuels' generation (panel A) and fossil fuels' daily capacity factors (panel B) on daily solar power generation and daily solar capacity factors using alternative definitions of fuel use. Fuel use lagged is lagged one month. Each row is a separated regression. Solar generation is in GWh. Solar capacity factor is between 0 and 100. Estimation results are marginal effects from an OLS (daily aggregated generation), and from a fractional logit response model (daily capacity factors). All estimations include plants with both single- and dual-fuel engines. All regressions include daily temperature, humidity, load and price ratios as controls. Regressions using lagged fuel use also include year, seasons, year × seasons, and weekend fixed effects. Regressions excluding fuel use include year, months, year × months, and weekend fixed effects. Bootstrapped standard errors using 50 repetitions appear in parentheses. Significance levels: $^{*}p < 0.10$, $^{**}p < 0.05$, $^{***}p < 0.001$.

Table A5: The Effect of Daily Solar Energy on Daily Aggregated Renewable Generation

	Wind		Hydro		Geothermal	
	(1)	(2)	(1)	(2)	(1)	(2)
Panel A. Generation (GWh)						
Solar_d	0.015	0.099***	-0.008***	-0.007***	-0.071***	-0.026
	(0.020)	(0.019)	(0.001)	(0.002)	(0.019)	(0.016)
Solar Cap Factor_d	0.001	0.007***	-0.0001	-0.0003**	-0.010***	-0.005*
	(0.001)	(0.001)	(0.0001)	(0.0001)	(0.003)	(0.003)
Panel B. Capacity Factor						
Solar_d	-0.004	0.013**	-0.021***	-0.018***	-0.050***	-0.040***
	(0.005)	(0.004)	(0.004)	(0.005)	(0.013)	(0.011)
Solar Cap Factor_d	0.002***	0.002***	-0.0004	-0.001***	-0.007***	-0.006***
	(0.0004)	(0.0003)	(0.0003)	(0.0003)	(0.002)	(0.002)
Obs.	1,489	1,489	1,915	1,915	306	306
Controls	✓	✓	✓	✓	✓	✓
τ_1 fixed effects	✓		✓		✓	
τ_2 fixed effects		✓		✓		✓

Notes: This table displays estimation results from regressions of daily aggregated renewable generation (panel A) and renewables' daily capacity factors (panel B) on daily solar power generation and daily solar capacity factor. Each row is a separated regression. Estimation results are marginal effects from an OLS (daily aggregated generation), and from a fractional logit response model (daily capacity factors). Solar generation is in GWh. Solar capacity factor is between 0 and 100. All estimations include plants with both single- and dual-fuel engines. All regressions include daily temperature, humidity and load as controls (fuel price ratios are not included in this regression as these are renewable generators only). Vector τ_1 includes year, month, and weekend fixed effects. Vector τ_2 includes year, seasons, year × seasons, and weekend fixed effects. Bootstrapped standard errors using 50 repetitions appear in parentheses. Significance levels: $^{*}p < 0.10$, $^{**}p < 0.05$, $^{***}p < 0.001$.

Table A6: The Effect of Solar on Daily Aggregated Fossil Fuel Generation Using Single-Fuel Engines Only

	Coal		Diesel		Fuel oil		Fuel oil #6	
	(1)	(2)	(1)	(2)	(1)	(2)	(1)	(2)
Panel A. Generation (GWh)								
Solar_d	-0.813***	-0.813***	-0.017	-0.017	-0.011	-0.011	0.001	0.001
	(0.137)	(0.137)	(0.011)	(0.011)	(0.023)	(0.023)	(0.001)	(0.001)
Panel B. Capacity Factor								
Solar_d	-0.022***	-0.022***	-0.009**	-0.009**	0.047	0.047	0.029	0.029
	(0.004)	(0.004)	(0.004)	(0.004)	(0.047)	(0.047)	(0.018)	(0.018)
Obs.	1,915	1,915	1,915	1,915	910	910	1,825	1,825
Controls	✓	✓	✓	✓	✓	✓	✓	✓
τ_1 fixed effects	✓		✓		✓		✓	
τ_2 fixed effects		✓		✓		✓		✓

Notes: This table displays estimation results from regressions of daily aggregated fossil fuel generation (panel A) and fossil fuels' daily capacity factors (panel B) on daily solar power generation. Estimation results are marginal effects of daily solar generation (in GWh) derived from an OLS regression on daily aggregated generation, and from a fractional logit response model on daily capacity factors. All estimations include plants with both single- and dual-fuel engines. All regressions include daily temperature, humidity, load and price ratios as controls. Vector τ_1 includes year, month, and weekend fixed effects. Vector τ_2 includes year, seasons, year $\times$ seasons, and weekend fixed effects. Bootstrapped standard errors using 50 repetitions appear in parentheses. Significance levels: $^{*}p < 0.10$, $^{**}p < 0.05$, $^{***}p < 0.001$.

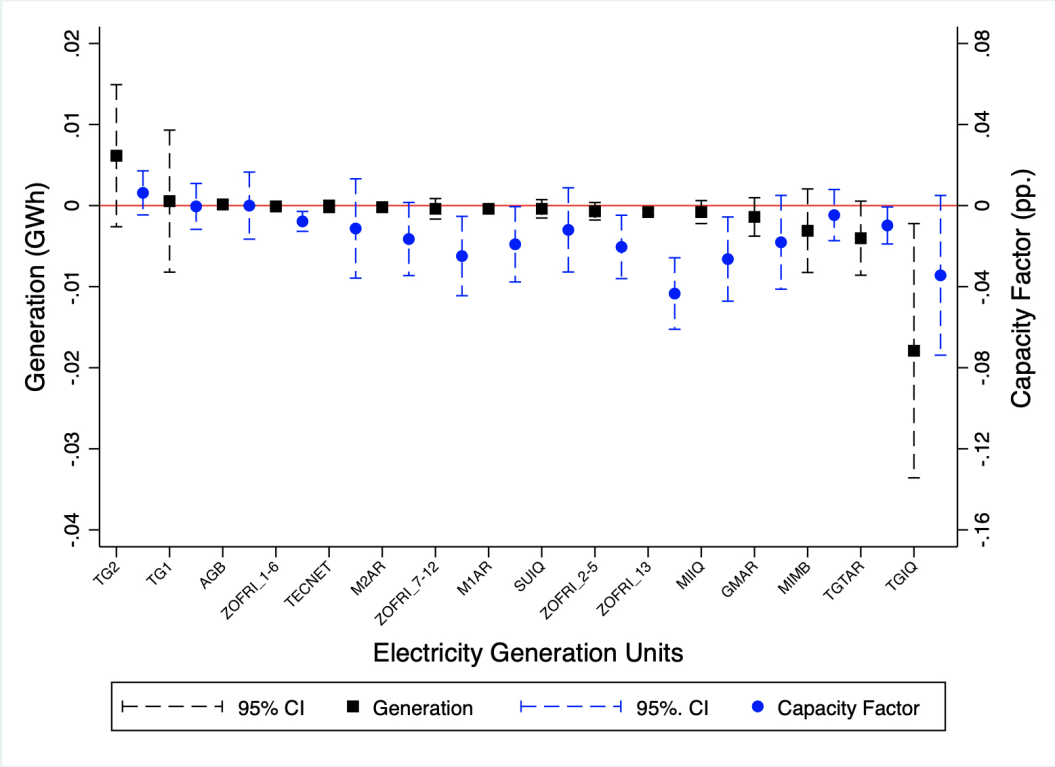

Figure A8: Diesel-Fired (Single-Fuel) EGUs and Displacement

Notes: The figure shows estimation results from regressions of daily diesel-fired generation (squares) and capacity factors (circles) on daily solar power generation at the electricity generation unit (EGU) level. Point estimates are marginal effects of daily solar generation (in GWh) derived from an OLS on daily aggregated generation (left y-axis), and from a fractional logit response model on daily capacity factors (right y-axis). The estimation equations are identical to the ones in columns (2) of Table 3. Dashed lines represent 95% confidence intervals obtained with bootstrapped standard errors using 50 repetitions. Reference line in red is at the zero mark. All estimations use combined-cycle EGUs that report diesel as their primary fuel source. We exclude units with dual engines that run with natural gas or that report using fuel oil as well.

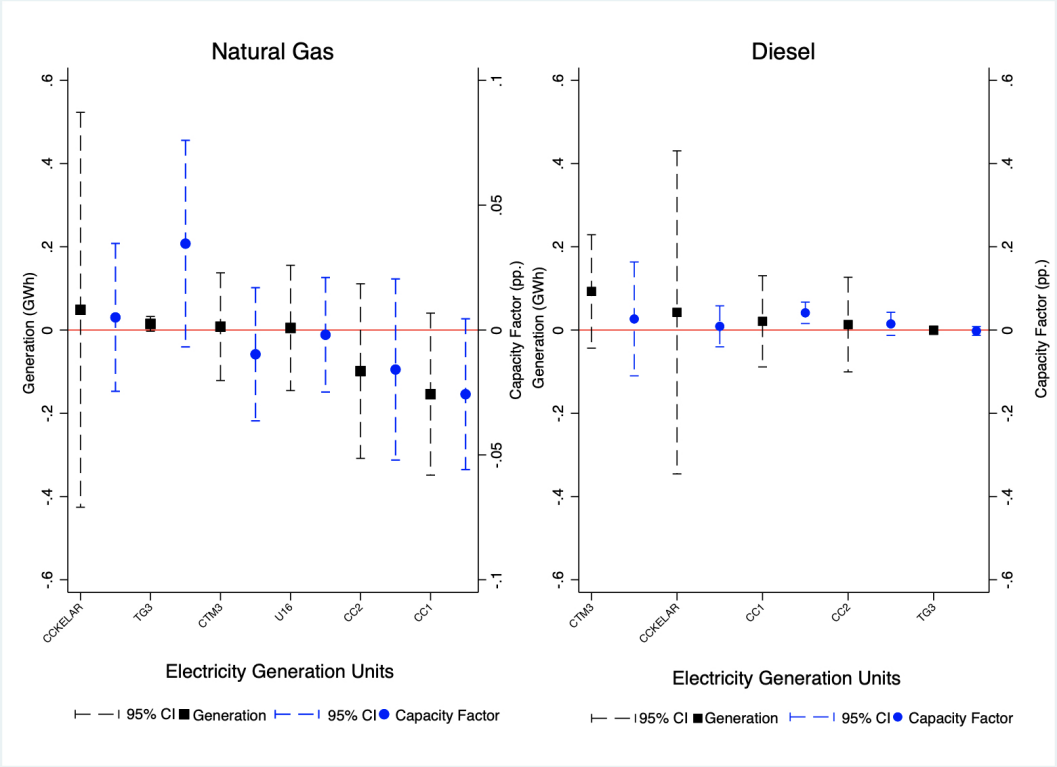

Figure A9: Natural Gas-Fired (Combined-Cycle) EGUs and Displacement

Notes: The figure shows estimation results from regressions of daily gas-fired generation (squares) and capacity factors (circles) on daily solar power generation at the electricity generation unit (EGU) level. Natural gas-fired plants in our sample are all combined-cycle plants. The left-hand side graph shows estimation results for gas plants. The right-hand side graph shows estimation results for diesel plants. Point estimates are marginal effects of daily solar generation (in GWh) derived from an OLS regression on daily aggregated generation (left y-axis), and from a fractional logit response model on daily capacity factors (right y-axis). The estimation equations are identical to the ones in columns (2) of Table 3. Dashed lines represent 95% confidence intervals obtained with bootstrapped standard errors using 50 repetitions. Reference line in red is at the zero mark. All estimations use combined-cycle EGUs that report natural gas as their primary fuel source.

Table A7: The Effect of Daily Solar Energy on the Daily Rate of Hospital Admissions by Age - Infants

	All Cities		Downwind of Displaced Units					
			$< 10km$		$< 50km$		$< 100km$	
	(1)	(2)	(1)	(2)	(1)	(2)	(1)	(2)
Panel A. Cardiovascular								
Solar_d	-0.00005	0.0002	-0.002	-0.002	-0.004	-0.004	-0.006	-0.006
	(0.001)	(0.002)	(0.003)	(0.004)	(0.005)	(0.004)	(0.004)	(0.005)
Solar Cap Factor_d	0.0001	0.0001	-0.0001	-0.0001	-0.0003	-0.0003	-0.0006	-0.0005
	(0.0002)	(0.0002)	(0.0002)	(0.0002)	(0.0004)	(0.0003)	(0.0006)	(0.0005)
Panel B. All Respiratory								
Solar_d	-0.032	-0.031	-0.076**	-0.076**	-0.042**	-0.039**	-0.051*	-0.048*
	(0.026)	(0.019)	(0.031)	(0.028)	(0.017)	(0.018)	(0.028)	(0.029)
Solar Cap Factor_d	-0.002	-0.002	-0.006**	-0.006**	-0.001	-0.001	-0.006	-0.002
	(0.001)	(0.001)	(0.002)	(0.002)	(0.002)	(0.002)	(0.002)	(0.002)
Panel C. Upper Respiratory								
Solar_d	0.006	0.006	0.005	0.005	0.004*	0.003	0.003*	0.003*
	(0.004)	(0.005)	(0.003)	(0.003)	(0.002)	(0.002)	(0.002)	(0.002)
Solar Cap Factor_d	0.0001	0.0001	0.0001	0.0001	0.0001	0.0001	0.0001	0.0001
	(0.0001)	(0.0001)	(0.0004)	(0.0003)	(0.0002)	(0.0002)	(0.0002)	(0.0002)
Panel D. Lower Respiratory								
Solar_d	-0.034	-0.033	-0.081**	-0.081**	-0.046**	-0.043**	-0.033	-0.030*
	(0.024)	(0.020)	(0.026)	(0.028)	(0.015)	(0.017)	(0.021)	(0.015)
Solar Cap Factor_d	-0.002	-0.002	-0.006**	-0.006**	-0.001	-0.001	-0.001	-0.001
	(0.001)	(0.001)	(0.002)	(0.002)	(0.002)	(0.002)	(0.002)	(0.002)
Observations	36,385	36,385	3,830	3,830	5,745	5,745	7,660	7,660
Number of cities	19	19	2	2	3	3	4	4
Sample Mean Y - Panel A	0.005	0.005	0.005	0.005	0.007	0.007	0.007	0.007
Sample Mean Y - Panel B	0.119	0.119	0.290	0.290	0.246	0.246	0.219	0.219
Sample Mean Y - Panel C	0.006	0.006	0.019	0.019	0.015	0.015	0.012	0.012
Sample Mean Y - Panel D	0.110	0.110	0.264	0.264	0.225	0.225	0.200	0.200
Controls	✓	✓	✓	✓	✓	✓	✓	✓
City fixed effects	✓		✓		✓		✓	
City × year fixed effects		✓		✓		✓		✓

Notes: This table displays estimation results from OLS regressions of infants' daily hospital admissions on daily solar power generation or daily solar capacity factor. Each row is a separated regression. Solar generation is in GWh. Solar capacity factor is between 0 and 100. Daily hospital admissions are per 100,000 people. Infants are less than 1 year old. Controls include weather, mining production, and demographic covariates. All regressions include controls, year, seasons, year × seasons, and weekend fixed effects. Bootstrapped standard errors using 50 repetitions appear in parentheses. Significance levels: $^{*}p < 0.10$, $^{**}p < 0.05$, $^{***}p < 0.001$.

Table A8: The Effect of Daily Solar Energy on the Daily Rate of Hospital Admissions by Age - Toddlers

	All Cities		Downwind of Displaced Units					
			$< 10km$		$< 50km$		$< 100km$	
	(1)	(2)	(1)	(2)	(1)	(2)	(1)	(2)
Panel A. Cardiovascular								
Solar_d	-0.00003	-0.00004	0.002	0.002	0.002	0.002	0.001	0.002
	(0.001)	(0.001)	(0.004)	(0.004)	(0.002)	(0.003)	(0.002)	(0.002)
Solar Cap Factor_d	-0.000001	0.000002	0.0001	0.0001	0.0001	0.0001	0.0000	-0.00002
	(0.0001)	(0.0001)	(0.001)	(0.001)	(0.0003)	(0.0003)	(0.0003)	(0.0002)
Panel B. All Respiratory								
Solar_d	-0.048**	-0.047**	-0.128**	-0.129**	-0.070**	-0.070	-0.073**	-0.074*
	(0.019)	(0.022)	(0.053)	(0.052)	(0.035)	(0.048)	(0.033)	(0.038)
Solar Cap Factor_d	-0.005**	-0.005**	-0.008**	-0.008**	-0.007**	-0.007**	-0.007**	-0.007**
	(0.002)	(0.001)	(0.003)	(0.003)	(0.002)	(0.003)	(0.003)	(0.003)
Panel C. Upper Respiratory								
Solar_d	-0.008	-0.007*	-0.041	-0.042*	-0.023	-0.022	-0.008	-0.008
	(0.006)	(0.004)	(0.030)	(0.024)	(0.018)	(0.020)	(0.013)	(0.017)
Solar Cap Factor_d	-0.001	-0.001	-0.003	-0.003	-0.002	-0.002	-0.0002	-0.0002
	(0.0005)	(0.001)	(0.003)	(0.002)	(0.001)	(0.002)	(0.002)	(0.002)
Panel D. Lower Respiratory								
Solar_d	-0.041**	-0.040**	-0.084**	-0.084**	-0.043	-0.044	-0.062**	-0.062**
	(0.020)	(0.020)	(0.033)	(0.036)	(0.036)	(0.028)	(0.030)	(0.031)
Solar Cap Factor_d	-0.004**	-0.004***	-0.006**	-0.006**	-0.005**	-0.005**	-0.007**	-0.007**
	(0.002)	(0.001)	(0.002)	(0.002)	(0.002)	(0.002)	(0.003)	(0.003)
Observations	36,385	36,385	3,830	3,830	5,745	5,745	7,660	7,660
Number of cities	19	19	2	2	3	3	4	4
Sample Mean Y - Panel A	0.004	0.004	0.011	0.011	0.008	0.008	0.008	0.008
Sample Mean Y - Panel B	0.239	0.239	0.436	0.436	0.374	0.374	0.334	0.334
Sample Mean Y - Panel C	0.079	0.079	0.127	0.127	0.097	0.097	0.082	0.082
Sample Mean Y - Panel D	0.153	0.153	0.305	0.305	0.272	0.272	0.249	0.249
Controls	✓	✓	✓	✓	✓	✓	✓	✓
City fixed effects	✓		✓		✓		✓	
City × year fixed effects		✓		✓		✓		✓

Notes: This table displays estimation results from OLS regressions of toddlers' daily hospital admissions on daily solar power generation or daily solar capacity factor. Each row is a separated regression. Solar generation is in GWh. Solar capacity factor is between 0 and 100. Daily hospital admissions are per 100,000 people. Toddlers are between 1-5 years old. Controls include weather, mining production, and demographic covariates. All regressions include controls, year, seasons, year × seasons, and weekend fixed effects. Bootstrapped standard errors using 50 repetitions appear in parentheses. Significance levels: $^{*}p < 0.10$, $^{**}p < 0.05$, $^{***}p < 0.001$.

Table A9: The Effect of Daily Solar Energy on the Daily Rate of Hospital Admissions by Age - Kids

	All Cities		Downwind of Displaced Units					
			$< 10km$		$< 50km$		$< 100km$	
	(1)	(2)	(1)	(2)	(1)	(2)	(1)	(2)
Panel A. Cardiovascular								
Solar_d	-0.004	-0.004	-0.010	-0.010	-0.004	-0.004	-0.003	-0.004
	(0.003)	(0.003)	(0.006)	(0.006)	(0.005)	(0.003)	(0.004)	(0.004)
Solar Cap Factor_d	-0.001	-0.001	-0.001	-0.001	-0.00004	-0.00004	-0.001	-0.001
	(0.001)	(0.001)	(0.001)	(0.001)	(0.0004)	(0.0004)	(0.001)	(0.001)
Panel B. All Respiratory								
Solar_d	-0.001	-0.0003	-0.043	-0.043	-0.044	-0.041	-0.048	-0.047
	(0.010)	(0.011)	(0.063)	(0.070)	(0.035)	(0.048)	(0.031)	(0.030)
Solar Cap Factor_d	0.001	0.001	-0.001	-0.001	-0.002	-0.002	-0.001	-0.001
	(0.002)	(0.002)	(0.004)	(0.003)	(0.002)	(0.002)	(0.002)	(0.002)
Panel C. Upper Respiratory								
Solar_d	-0.008	-0.007	-0.031	-0.031	-0.034	-0.032	-0.032	-0.032
	(0.007)	(0.009)	(0.057)	(0.058)	(0.046)	(0.044)	(0.028)	(0.040)
Solar Cap Factor_d	-0.0001	-0.0001	0.001	0.001	0.00001	0.0001	-0.0004	-0.0004
	(0.001)	(0.0004)	(0.003)	(0.003)	(0.002)	(0.002)	(0.001)	(0.001)
Panel D. Lower Respiratory								
Solar_d	0.006	0.007	-0.013	-0.013	-0.010	-0.010	-0.016	-0.016
	(0.006)	(0.006)	(0.025)	(0.023)	(0.015)	(0.020)	(0.017)	(0.016)
Solar Cap Factor_d	0.001	0.001	-0.002	-0.002	-0.002	-0.002*	-0.001	-0.001
	(0.002)	(0.002)	(0.001)	(0.002)	(0.001)	(0.001)	(0.001)	(0.001)
Observations	36,385	36,385	3,830	3,830	5,745	5,745	7,660	7,660
Number of cities	19	19	2	2	3	3	4	4
Sample Mean Y - Panel A	0.012	0.012	0.019	0.019	0.017	0.017	0.019	0.019
Sample Mean Y - Panel B	0.136	0.136	0.303	0.303	0.225	0.225	0.195	0.195
Sample Mean Y - Panel C	0.066	0.066	0.159	0.159	0.116	0.116	0.095	0.095
Sample Mean Y - Panel D	0.067	0.067	0.138	0.138	0.105	0.105	0.098	0.098
Controls	✓	✓	✓	✓	✓	✓	✓	✓
City fixed effects	✓		✓		✓		✓	
City × year fixed effects		✓		✓		✓		✓

Notes: This table displays estimation results from OLS regressions of kids' daily hospital admissions on daily solar power generation or daily solar capacity factor. Each row is a separated regression. Solar generation is in GWh. Solar capacity factor is between 0 and 100. Daily hospital admissions are per 100,000 people. Kids are between 6-14 years old. Controls include weather, mining production, and demographic covariates. All regressions include controls, year, seasons, year × seasons, and weekend fixed effects. Bootstrapped standard errors using 50 repetitions appear in parentheses. Significance levels: $^{*}p < 0.10$, $^{**}p < 0.05$, $^{***}p < 0.001$.

Table A10: The Effect of Daily Solar Energy on the Daily Rate of Hospital Admissions by Age - Adults

	All Cities		Downwind of Displaced Units					
			$< 10km$		$< 50km$		$< 100km$	
	(1)	(2)	(1)	(2)	(1)	(2)	(1)	(2)
Panel A. Cardiovascular								
Solar_d	-0.003	-0.002	0.001	0.001	-0.041	-0.039	-0.044	-0.040
	(0.022)	(0.022)	(0.055)	(0.055)	(0.042)	(0.048)	(0.043)	(0.044)
$\text{Solar Cap Factor}_d$	-0.0002	-0.0002	-0.0003	-0.0002	-0.003	-0.003	-0.004	-0.004
	(0.002)	(0.002)	(0.006)	(0.005)	(0.004)	(0.004)	(0.005)	(0.004)
Panel B. All Respiratory								
Solar_d	-0.021	-0.022	-0.040	-0.040	0.017	0.016	-0.025	-0.023
	(0.032)	(0.032)	(0.053)	(0.052)	(0.039)	(0.043)	(0.038)	(0.043)
$\text{Solar Cap Factor}_d$	-0.003	-0.003*	-0.009**	-0.009**	-0.001	-0.0005	-0.004	-0.004
	(0.002)	(0.002)	(0.004)	(0.004)	(0.004)	(0.004)	(0.004)	(0.004)
Panel C. Upper Respiratory								
Solar_d	-0.016	-0.017	-0.012	-0.012	0.009	0.006	-0.009	-0.010
	(0.017)	(0.018)	(0.032)	(0.026)	(0.024)	(0.022)	(0.024)	(0.024)
$\text{Solar Cap Factor}_d$	-0.001	-0.001	-0.001	-0.001	0.001	0.001	-0.001	-0.001
	(0.001)	(0.002)	(0.003)	(0.002)	(0.002)	(0.003)	(0.002)	(0.002)
Panel D. Lower Respiratory								
Solar_d	0.004	0.003	-0.048	-0.048	-0.010	-0.007	-0.030	-0.027
	(0.030)	(0.028)	(0.040)	(0.040)	(0.037)	(0.036)	(0.031)	(0.027)
$\text{Solar Cap Factor}_d$	-0.001	-0.001	-0.007	-0.007**	-0.001	-0.001	-0.002	-0.002
	(0.001)	(0.001)	(0.004)	(0.004)	(0.003)	(0.003)	(0.003)	(0.002)
Observations	36,385	36,385	3,830	3,830	5,745	5,745	7,660	7,660
Number of cities	19	19	2	2	3	3	4	4
Sample Mean Y - Panel A	0.531	0.531	1.120	1.120	0.919	0.919	0.752	0.752
Sample Mean Y - Panel B	0.369	0.369	0.756	0.756	0.604	0.604	0.473	0.473
Sample Mean Y - Panel C	0.122	0.122	0.173	0.173	0.145	0.145	0.122	0.122
Sample Mean Y - Panel D	0.191	0.191	0.466	0.466	0.367	0.367	0.281	0.281
Controls	✓	✓	✓	✓	✓	✓	✓	✓
City fixed effects	✓		✓		✓		✓	
City × year fixed effects		✓		✓		✓		✓

Notes: This table displays estimation results from OLS regressions of adults' daily hospital admissions on daily solar power generation or daily solar capacity factor. Each row is a separated regression. Solar generation is in GWh. Solar capacity factor is between 0 and 100. Daily hospital admissions are per 100,000 people. Adults are between 15-64 years old. Controls include weather, mining production, and demographic covariates. All regressions include controls, year, seasons, year × seasons, and weekend fixed effects. Bootstrapped standard errors using 50 repetitions appear in parentheses. Significance levels: $^{*}p < 0.10$, $^{**}p < 0.05$, $^{***}p < 0.001$.

Table A11: The Effect of Daily Solar Energy on the Daily Rate of Hospital Admissions by Age - Seniors

	All Cities		Downwind of Displaced Units					
			$< 10km$		$< 50km$		$< 100km$	
	(1)	(2)	(1)	(2)	(1)	(2)	(1)	(2)
Panel A. Cardiovascular								
Solar_d	0.004	0.007	-0.030	-0.031	0.013	0.010	0.032	0.030
	(0.055)	(0.048)	(0.082)	(0.067)	(0.056)	(0.050)	(0.049)	(0.058)
Solar Cap Factor_d	-0.001	-0.001	-0.004	-0.004	-0.003	-0.003	-0.004	-0.003
	(0.003)	(0.003)	(0.005)	(0.007)	(0.004)	(0.004)	(0.005)	(0.004)
Panel B. All Respiratory								
Solar_d	-0.013	-0.013	-0.038	-0.038	-0.046	-0.053	-0.056	-0.061
	(0.025)	(0.034)	(0.058)	(0.060)	(0.041)	(0.037)	(0.047)	(0.041)
Solar Cap Factor_d	-0.002	-0.002	0.002	0.002	0.001	0.001	0.001	0.001
	(0.002)	(0.002)	(0.004)	(0.005)	(0.003)	(0.003)	(0.003)	(0.003)
Panel C. Upper Respiratory								
Solar_d	-0.001	-0.001	-0.001	-0.001	-0.001	-0.001	-0.008	-0.007
	(0.002)	(0.002)	(0.003)	(0.002)	(0.001)	(0.001)	(0.007)	(0.006)
Solar Cap Factor_d	-0.0001	-0.0001	-0.0001	-0.0001	-0.0001	-0.0001	-0.0004	-0.0004
	(0.0001)	(0.0001)	(0.0003)	(0.0002)	(0.0002)	(0.0002)	(0.0003)	(0.0004)
Panel D. Lower Respiratory								
Solar_d	-0.021	-0.022	-0.037	-0.036	-0.043	-0.048	-0.052	-0.055
	(0.030)	(0.032)	(0.053)	(0.054)	(0.032)	(0.038)	(0.039)	(0.034)
Solar Cap Factor_d	-0.003	-0.003	0.0004	0.0004	-0.0002	-0.0004	0.0001	0.00002
	(0.002)	(0.002)	(0.004)	(0.003)	(0.003)	(0.003)	(0.003)	(0.003)
Observations	36,385	36,385	3,830	3,830	5,745	5,745	7,660	7,660
Number of cities	19	19	2	2	3	3	4	4
Sample Mean Y - Panel A	0.491	0.491	1.089	1.089	0.870	0.870	0.780	0.780
Sample Mean Y - Panel B	0.352	0.352	0.736	0.736	0.564	0.564	0.477	0.477
Sample Mean Y - Panel C	0.006	0.006	0.006	0.006	0.004	0.004	0.006	0.006
Sample Mean Y - Panel D	0.267	0.267	0.643	0.643	0.489	0.489	0.416	0.416
Controls	✓	✓	✓	✓	✓	✓	✓	✓
City fixed effects	✓		✓		✓		✓	
City × year fixed effects		✓		✓		✓		✓

Notes: This table displays estimation results from OLS regressions of seniors' daily hospital admissions on daily solar power generation or daily solar capacity factor. Each row is a separated regression. Solar generation is in GWh. Solar capacity factor is between 0 and 100. Daily hospital admissions are per 100,000 people. Seniors are 65 years old or more. Controls include weather, mining production, and demographic covariates. All regressions include controls, year, seasons, year × seasons, and weekend fixed effects. Bootstrapped standard errors using 50 repetitions appear in parentheses. Significance levels: $^{*}p < 0.10$, $^{**}p < 0.05$, $^{***}p < 0.001$.

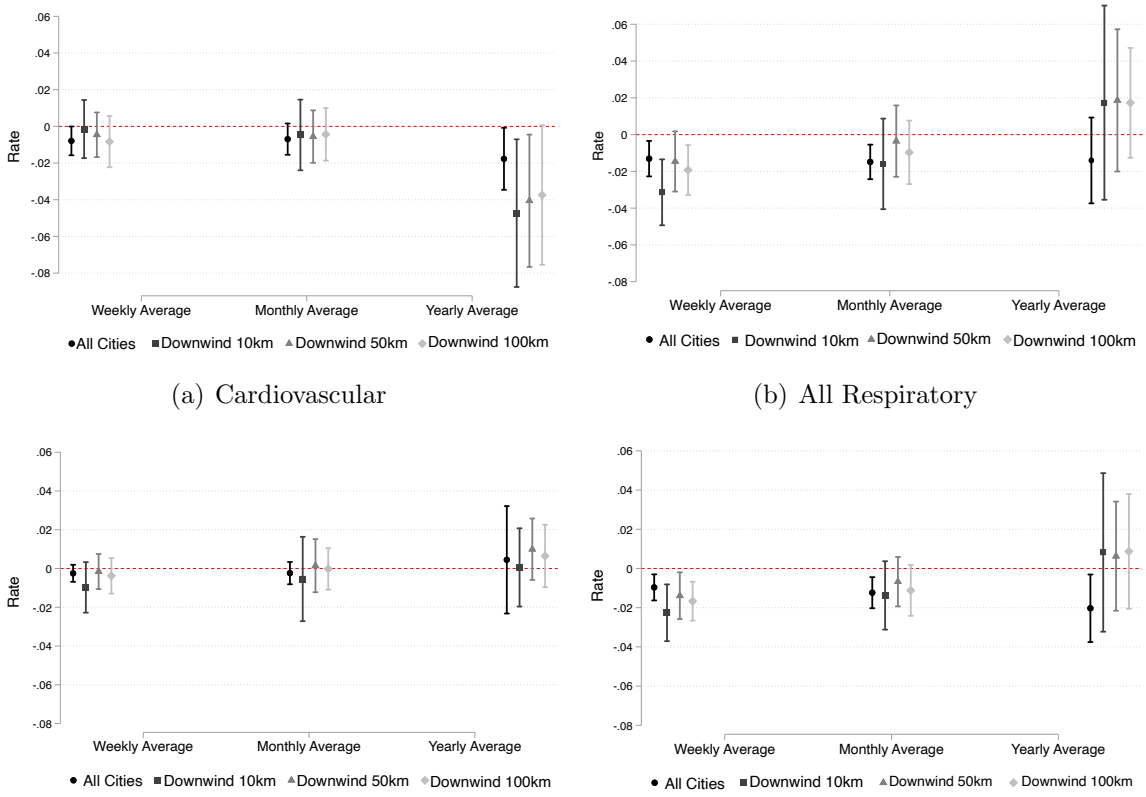

(a) Cardiovascular

(b) All Respiratory

(c) Upper Respiratory

(d) Lower Respiratory

Figure A10: The Long-Term Effect of Solar Capacity Factors on the Daily Rate of Hospital Admissions

Notes: This figure shows estimation results of regressing daily hospital admissions on weekly, monthly, and yearly average solar capacity factor across groups of cities. Capacity factor is between 0 and 100. Daily hospital admissions are per 100,000 people. Controls include weather, mining production, and demographic covariates. All regressions include controls, year, seasons, year $\times$ seasons, and weekend fixed effects in both the main and the inflate equations. Dashed lines are 95% confidence intervals obtained by bootstrapping standard errors using 50 repetitions.

Table A12: The Long-Term Effect of Average Solar Generation on the Daily Rate of Hospital Admissions

	t =week				t =month				t =year			
	All	Downwind			All	Downwind			All	Downwind		
	Cities	$< 10km$	$< 50km$	$< 100km$	Cities	$< 10km$	$< 50km$	$< 100km$	Cities	$< 10km$	$< 50km$	$< 100km$
Panel A. Cardiovascular												
Solar_t	-0.078	-0.045	-0.055	-0.076	-0.065	-0.114	-0.110	-0.104	-0.092	-0.248	-0.226	-0.249*
	(0.056)	(0.120)	(0.087)	(0.081)	(0.072)	(0.114)	(0.098)	(0.091)	(0.085)	(0.197)	(0.161)	(0.137)
Solar Cap Factor_t	-0.008*	-0.001	-0.005	-0.008	-0.007	-0.005	-0.006	-0.004	-0.018**	-0.047**	-0.041**	-0.037*
	(0.004)	(0.008)	(0.006)	(0.007)	(0.005)	(0.011)	(0.008)	(0.009)	(0.008)	(0.021)	(0.017)	(0.020)
Panel B. All Respiratory												
Solar_t	-0.142**	-0.425***	-0.244**	-0.293***	-0.109	-0.215	-0.102	-0.162*	-0.012	0.119	0.087	0.017
	(0.053)	(0.128)	(0.099)	(0.087)	(0.070)	(0.141)	(0.120)	(0.088)	(0.101)	(0.199)	(0.121)	(0.128)
Solar Cap Factor_t	-0.013**	-0.031**	-0.015*	-0.019**	-0.015**	-0.016	-0.004	-0.010	-0.014	0.017	0.019	0.017
	(0.005)	(0.011)	(0.008)	(0.007)	(0.005)	(0.013)	(0.010)	(0.009)	(0.016)	(0.023)	(0.022)	(0.016)
Panel C. Upper Respiratory												
Solar_t	-0.030	-0.128	-0.040	-0.066	-0.018	-0.033	0.015	-0.027	0.014	0.066	0.104*	0.025
	(0.025)	(0.095)	(0.073)	(0.055)	(0.024)	(0.101)	(0.061)	(0.052)	(0.042)	(0.100)	(0.061)	(0.054)
Solar Cap Factor_t	-0.003	-0.010	-0.002	-0.004	-0.002	-0.005	0.001	-0.0002	0.004	0.001	0.010	0.006
	(0.002)	(0.006)	(0.006)	(0.005)	(0.003)	(0.011)	(0.008)	(0.005)	(0.012)	(0.010)	(0.011)	(0.008)
Panel D. Lower Respiratory												
Solar_t	-0.100**	-0.318***	-0.222**	-0.248***	-0.079*	-0.203**	-0.138*	-0.159*	-0.020	0.035	-0.018	-0.018
	(0.051)	(0.087)	(0.088)	(0.074)	(0.048)	(0.101)	(0.080)	(0.083)	(0.073)	(0.158)	(0.121)	(0.115)
Solar Cap Factor_t	-0.010**	-0.023**	-0.014**	-0.017***	-0.012**	-0.014*	-0.007	-0.011*	-0.020**	0.008	0.006	0.009
	(0.004)	(0.007)	(0.006)	(0.005)	(0.005)	(0.008)	(0.007)	(0.006)	(0.009)	(0.023)	(0.018)	(0.016)
Obs.	36,385	3,830	5,745	7,660	36,385	3,830	5,745	7,660	36,385	3,830	5,745	7,660
Number of cities	19	2	3	4	19	2	3	4	19	2	3	4
Controls	×	×	×	×	×	×	×	×	×	×	×	×
City × year fixed effects	×	×	×	×	×	×	×	×	×	×	×	×

Notes: This table displays estimation results of regressing daily hospital admissions on weekly, monthly, and yearly average solar power generation or average solar capacity factor across groups of cities. Solar generation is in GWh. Solar capacity factor is in between 0 and 100. Daily hospital admissions are per 100,000 people. Controls include weather, mining production, and demographic covariates. All regressions include controls, year, seasons, year × seasons, and weekend fixed effects in both the main and the inflate equations. Bootstrapped standard errors using 50 repetitions appear in parentheses. Significance levels: $^{*}p < 0.10$, $^{**}p < 0.05$, $^{***}p < 0.001$.

Table A13: The Effect of Daily Solar-Induced Predicted Fossil Fuel Displacement on the Daily Rate of Hospital Admissions

	All Cities		Downwind of Displaced Units					
			$< 10km$		$< 50km$		$< 100km$	
	(1)	(2)	(1)	(2)	(1)	(2)	(1)	(2)
Panel A. Cardiovascular								
$\hat{G}_d$	0.033	0.035	-0.107	-0.108	-0.049	-0.042	-0.074	-0.065
	(0.052)	(0.056)	(0.193)	(0.202)	(0.165)	(0.177)	(0.149)	(0.149)
Panel B. All Respiratory								
$\hat{G}_d$	-0.072	-0.138**	-0.207	-0.208	-0.145	-0.141	-0.386*	-0.379*
	(0.053)	(0.060)	(0.294)	(0.293)	(0.209)	(0.200)	(0.203)	(0.198)
Panel C. Upper Respiratory								
$\hat{G}_d$	-0.003	-0.018	0.202	0.201	0.176	0.174	0.067	0.065
	(0.017)	(0.017)	(0.177)	(0.177)	(0.131)	(0.130)	(0.108)	(0.111)
Panel D. Lower Respiratory								
$\hat{G}_d$	-0.045	-0.049	-0.483**	-0.482**	-0.376**	-0.366**	-0.510**	-0.501**
	(0.035)	(0.034)	(0.226)	(0.224)	(0.158)	(0.151)	(0.162)	(0.166)
Observations	36,442	36,385	3,830	3,830	5,745	5,745	7,660	7,660
Controls	✓	✓	✓	✓	✓	✓	✓	✓
City fixed effects	✓		✓		✓		✓	
City × year fixed effects		✓		✓		✓		✓

Notes: This table displays estimation results from OLS regressions of daily hospital admissions on daily predicted displacement of fossil fuel generation. Predicted displacement is in GWh. Daily hospital admissions are per 100,000 people. Controls include weather, mining production, and demographic covariates. Bootstrapped standard errors appear in parentheses. Significance levels: $^{*}p < 0.10$, $^{**}p < 0.05$, $^{***}p < 0.001$.

Table A14: Descriptive Statistics on Fine Particulate Matter ($PM_{2.5}$) Concentrations

Variable	Mean	Std. Dev.	Min.	Max.	Obs.
Panel A. All Cities					
$PM_{2.5}$	14.74	6.89	3.39	47.80	5,780
Panel B. Cities $\leq$ 10km Downwind of Displaced Fossil Fuel Plants					
$PM_{2.5}$	17.49	7.51	3.58	47.80	2,784

Notes: This table displays main descriptive statistics of fine particle matter concentrations for cities with available data. Panel A corresponds to data from four cities hosting fossil-fueled power plants (Alto Hospicio, Antofagasta, Arica, and Tocopilla. Panel B corresponds to data from two cities near and downwind of displaced fossil fuel plants (Alto Hospicio and Tocopilla). Data are daily records averaged across stations from 2012 to 2017, and come from the National Air Quality Information System (SINCA)'s website https://sinca.mma.gob.cl.

Table A15: The Effect of Daily Solar Energy on the Daily Rate of Hospital Admissions Using Alternative Cities

	With Fossil Fuel Generation		Upwind of Displaced Plants		Downwind of Non-displaced Plants		Downwind of Ramping-Up Plants	
	(1)	(2)	(1)	(2)	(1)	(2)	(1)	(2)
Panel A. Cardiovascular								
$Solar_d$	0.016	0.025	-0.040	-0.037	-0.034	-0.014	0.032	-0.017
	(0.065)	(0.056)	(0.118)	(0.155)	(0.147)	(0.134)	(0.050)	(0.057)
Solar Cap Fac_d	-0.003	-0.003	-0.0004	0.00001	0.014	0.016	-0.002	-0.006
	(0.004)	(0.005)	(0.008)	(0.007)	(0.011)	(0.013)	(0.004)	(0.005)
Panel B. All Respiratory								
$Solar_d$	-0.233***	-0.236***	-0.127	-0.128	0.101	0.110	0.222**	-0.085
	(0.053)	(0.062)	(0.134)	(0.165)	(0.115)	(0.135)	(0.073)	(0.087)
Solar Cap Fac_d	-0.014**	-0.014**	-0.028**	-0.029**	-0.002	-0.002	0.014**	-0.005
	(0.006)	(0.004)	(0.009)	(0.009)	(0.012)	(0.015)	(0.006)	(0.007)
Panel C. Upper Respiratory								
$Solar_d$	-0.084*	-0.081	-0.009	-0.014	0.068	0.065	0.050	-0.009
	(0.045)	(0.049)	(0.028)	(0.024)	(0.101)	(0.090)	(0.045)	(0.039)
Solar Cap Fac_d	-0.004	-0.004	-0.002	-0.003	0.004	0.004	-0.001	-0.003
	(0.003)	(0.003)	(0.002)	(0.003)	(0.010)	(0.011)	(0.005)	(0.004)
Panel D. Lower Respiratory								
$Solar_d$	-0.145**	-0.156***	-0.105	-0.101	0.026	0.038	0.183***	-0.075
	(0.046)	(0.046)	(0.137)	(0.143)	(0.061)	(0.049)	(0.054)	(0.060)
Solar Cap Fac_d	-0.013***	-0.013***	-0.022**	-0.021**	-0.005	-0.003	0.012**	-0.004
	(0.003)	(0.004)	(0.009)	(0.010)	(0.006)	(0.005)	(0.004)	(0.003)
Obs.	9,575	9,575	11,490	11,490	5,745	5,745	1,915	1,915
Number of Cities	5	5	6	6	3	3	1	1
τ_1 fixed effects							✓	
τ_2 fixed effects	✓	✓	✓	✓	✓	✓		✓
City fixed effects	✓		✓		✓			
City × Year fixed effects		✓		✓		✓		

Notes: This table displays estimation results from OLS regressions of daily hospital admissions on daily solar power generation and daily solar capacity factors using alternative cities. Each row is a separated regression. Solar generation is in GWh. Solar capacity factor is between 0 and 100. Daily hospital admissions are per 100,000 people. All regressions include controls (weather, mining production, and demographics). Vector τ_1 includes year, month, and weekend fixed effects. Vector τ_2 includes year, seasons, year × seasons, and weekend fixed effects. Bootstrapped standard errors using 50 repetitions appear in parentheses. Significance levels: $^*p < 0.10$, $^{**}p < 0.05$, $^{***}p < 0.001$.

Table A16: The Effect of 1 GWh of Solar Generation on the Daily Rate of Hospital Admissions Using a Poisson Estimator

	All Cities			Cities Downwind of Displaced Fossil Fuel Plants					
				$< 10km$		$< 50km$		$< 100km$	
	(1)	(2)	(3)	(2)	(3)	(2)	(3)	(2)	(3)
Panel A. Cardiovascular									
Solar_d	-0.032***	-0.024*	-0.022	-0.060*	-0.059*	-0.044	-0.040	-0.033	-0.030
	(0.004)	(0.013)	(0.013)	(0.036)	(0.036)	(0.035)	(0.029)	(0.021)	(0.018)
Solar Cap Factor_d	-0.004***	-0.002**	-0.002*	-0.004	-0.004	-0.003	-0.003	-0.003*	-0.003*
	(0.0005)	(0.001)	(0.001)	(0.003)	(0.003)	(0.002)	(0.002)	(0.002)	(0.002)
Panel B. All respiratory									
Solar_d	-0.041***	-0.066***	-0.067***	-0.144**	-0.144***	-0.094**	-0.093**	-0.080***	-0.078***
	(0.005)	(0.013)	(0.013)	(0.048)	(0.036)	(0.033)	(0.036)	(0.021)	(0.021)
Solar Cap Factor_d	-0.005***	-0.004***	-0.004***	-0.010**	-0.010**	-0.006**	-0.006**	-0.005**	-0.005**
	(0.001)	(0.001)	(0.001)	(0.004)	(0.004)	(0.002)	(0.003)	(0.002)	(0.002)
Panel C. Upper respiratory									
Solar_d	-0.022***	-0.027**	-0.027**	-0.032	-0.033	-0.021	-0.021	-0.017	-0.017
	(0.003)	(0.009)	(0.010)	(0.020)	(0.020)	(0.018)	(0.015)	(0.011)	(0.012)
Solar Cap Factor_d	-0.002***	-0.002**	-0.002***	-0.001	-0.001	-0.001	-0.001	-0.001	-0.001
	(0.0004)	(0.001)	(0.001)	(0.002)	(0.002)	(0.001)	(0.001)	(0.001)	(0.001)
Panel D. Lower respiratory									
Solar_d	-0.016***	-0.039***	-0.040***	-0.127**	-0.125**	-0.084**	-0.081***	-0.070***	-0.067***
	(0.003)	(0.012)	(0.010)	(0.040)	(0.041)	(0.026)	(0.024)	(0.018)	(0.020)
Solar Cap Factor_d	-0.003***	-0.002**	-0.002**	-0.010***	-0.010***	-0.006**	-0.006**	-0.005**	-0.005**
	(0.0003)	(0.001)	(0.001)	(0.003)	(0.003)	(0.003)	(0.002)	(0.002)	(0.002)
Obs.	36,442	36,385	36,385	3,830	3,830	5,745	5,745	7,660	7,660
Controls		✓	✓	✓	✓	✓	✓	✓	✓
City-fixed effects		✓		✓		✓		✓	
City × year-fixed effects			✓		✓		✓		✓

Notes: This table displays estimation results from regressions of daily hospital admissions on daily solar power generation or daily solar capacity factor using a Poisson estimator (offsetting by population). Each row is a separated regression. Solar generation is in GWh. Solar capacity factor is between 0 and 100. Controls include weather, mining production, and demographic covariates. All regressions include year, seasons, year × seasons, and weekend fixed effects. Bootstrapped standard errors using 50 repetitions appear in parentheses. Significance levels: $^{*}p < 0.10$, $^{**}p < 0.05$, $^{***}p < 0.001$.

Table A17: The Effect of 1 GWh of Solar Generation on the Daily Rate of Hospital Admissions Using a ZINB Estimator

	All Cities			Cities Downwind of Displaced Fossil Fuel Plants					
				$< 10km$		$< 50km$		$< 100km$	
	(1)	(2)	(3)	(2)	(3)	(2)	(3)	(2)	(3)
Panel A. Cardiovascular									
Solar_d	-0.038***	-0.028**	-0.021	-0.050	-0.050	-0.038	-0.038	-0.033	-0.031
	(0.004)	(0.014)	(0.013)	(0.042)	(0.038)	(0.037)	(0.032)	(0.021)	(0.021)
Solar Cap Factor_d	-0.005***	-0.002*	-0.002**	-0.004	-0.004	-0.003	-0.003	-0.003	-0.003*
	(0.0005)	(0.001)	(0.001)	(0.003)	(0.003)	(0.002)	(0.004)	(0.003)	(0.002)
Panel B. All respiratory									
Solar_d	-0.049***	-0.067**	-0.068***	-0.140**	-0.140**	-0.094**	-0.092**	-0.077**	-0.077***
	(0.005)	(0.026)	(0.014)	(0.045)	(0.045)	(0.030)	(0.035)	(0.024)	(0.023)
Solar Cap Factor_d	-0.006***	-0.004*	-0.004***	-0.010**	-0.010**	-0.005**	-0.005*	-0.005**	-0.005**
	(0.001)	(0.002)	(0.001)	(0.004)	(0.004)	(0.002)	(0.003)	(0.002)	(0.002)
Panel C. Upper respiratory									
Solar_d	-0.015***	-0.028**	-0.027***	-0.024	-0.024	-0.015	-0.014	-0.014	-0.018
	(0.003)	(0.009)	(0.008)	(0.209)	(0.217)	(0.142)	(0.099)	(0.182)	(0.284)
Solar Cap Factor_d	-0.001**	-0.002**	-0.002**	-0.001	-0.001	-0.0004	-0.001	-0.0005	-0.001
	(0.0004)	(0.001)	(0.001)	(0.008)	(0.006)	(0.003)	(0.005)	(0.007)	(0.014)
Panel D. Lower respiratory									
Solar_d	-0.023***	-0.038*	-0.041***	-0.130**	-0.127**	-0.076**	-0.072**	-0.067***	-0.068**
	(0.003)	(0.019)	(0.012)	(0.051)	(0.040)	(0.036)	(0.030)	(0.018)	(0.023)
Solar Cap Factor_d	-0.004**	-0.002	-0.002**	-0.010	-0.010**	-0.006**	-0.006**	-0.005**	-0.005**
	(0.001)	(0.002)	(0.001)	(0.007)	(0.003)	(0.003)	(0.002)	(0.002)	(0.002)
Obs.	36,442	36,385	36,385	3,830	3,830	5,745	5,745	7,660	7,660
Controls		✓	✓	✓	✓	✓	✓	✓	✓
City-fixed effects		✓		✓		✓		✓	
City × year-fixed effects			✓		✓		✓		✓

Notes: This table displays estimation results from regressions of daily hospital admissions on daily solar power generation or daily solar capacity factor using a Zero-Inflated Negative Binomial model (offsetting by population). Each row is a separated regression. Solar generation is in GWh. Solar capacity factor is between 0 and 100. Controls include weather, mining production, and demographic covariates in both the main and the inflate equation. All regressions include year, seasons, year × seasons, and weekend fixed effects. Bootstrapped standard errors using 50 repetitions appear in parentheses. Significance levels: $^{*}p < 0.10$, $^{**}p < 0.05$, $^{***}p < 0.001$.

Table A18: The Effect of 1 GWh of Solar Generation on the Daily Rate of Hospital Admissions Using a Negative Binomial Regression Model

	All Cities			Cities Downwind of Displaced Fossil Fuel Plants					
				$< 10km$		$< 50km$		$< 100km$	
	(1)	(2)	(3)	(2)	(3)	(2)	(3)	(2)	(3)
Panel A. Cardiovascular									
Solar_d	-0.030***	-0.025**	-0.022*	-0.060	-0.059	-0.044	-0.040	-0.033	-0.030
	(0.004)	(0.012)	(0.012)	(0.041)	(0.039)	(0.027)	(0.029)	(0.023)	(0.020)
Solar Cap Factor_d	-0.003***	-0.002**	-0.002**	-0.004	-0.004	-0.003*	-0.003	-0.003	-0.003*
	(0.001)	(0.001)	(0.001)	(0.003)	(0.003)	(0.002)	(0.002)	(0.002)	(0.001)
Panel B. All respiratory									
Solar_d	-0.038***	-0.067***	-0.068***	-0.142**	-0.142***	-0.091***	-0.090**	-0.079***	-0.077***
	(0.005)	(0.012)	(0.016)	(0.048)	(0.040)	(0.026)	(0.029)	(0.021)	(0.022)
Solar Cap Factor_d	-0.005***	-0.004**	-0.004***	-0.010**	-0.010**	-0.005**	-0.005**	-0.005**	-0.005**
	(0.001)	(0.001)	(0.001)	(0.004)	(0.003)	(0.003)	(0.003)	(0.002)	(0.002)
Panel C. Upper respiratory									
Solar_d	-0.019***	-0.030**	-0.030***	-0.037*	-0.040*	-0.023	-0.023	-0.020**	-0.019*
	(0.003)	(0.010)	(0.009)	(0.020)	(0.020)	(0.015)	(0.018)	(0.010)	(0.012)
Solar Cap Factor_d	-0.001***	-0.002***	-0.002***	-0.002	-0.002	-0.001	-0.001	-0.001	-0.001
	(0.0004)	(0.001)	(0.001)	(0.002)	(0.001)	(0.001)	(0.001)	(0.001)	(0.001)
Panel D. Lower respiratory									
Solar_d	-0.016***	-0.038***	-0.039***	-0.125***	-0.123**	-0.082***	-0.079**	-0.069***	-0.066***
	(0.003)	(0.011)	(0.009)	(0.033)	(0.039)	(0.022)	(0.025)	(0.018)	(0.018)
Solar Cap Factor_d	-0.003***	-0.002**	-0.002**	-0.010***	-0.010**	-0.006**	-0.006**	-0.005**	-0.005**
	(0.0003)	(0.001)	(0.001)	(0.003)	(0.003)	(0.002)	(0.002)	(0.002)	(0.002)
Obs.	36,442	36,385	36,385	3,830	3,830	5,745	5,745	7,660	7,660
Controls		✓	✓	✓	✓	✓	✓	✓	✓
City-fixed effects		✓		✓		✓		✓	
City × year-fixed effects			✓		✓		✓		✓

Notes: This table displays estimation results from regressions of daily hospital admissions on daily solar power generation or daily solar capacity factor using a Negative Binomial model (offsetting by population). Each row is a separated regression. Solar generation is in GWh. Solar capacity factor is between 0 and 100. Controls include weather, mining production, and demographic covariates. All regressions include year, seasons, year × seasons, and weekend fixed effects. Bootstrapped standard errors using 50 repetitions appear in parentheses. Significance levels: $^{*}p < 0.10$, $^{**}p < 0.05$, $^{***}p < 0.001$.

Table A19: The Effect of Daily Solar Energy on Placebo Health Outcomes

	All Cities		Cities Downwind of Displaced Fossil Fuel Plants					
			$< 10km$		$< 50km$		$< 100km$	
	(1)	(2)	(1)	(2)	(1)	(2)	(1)	(2)
Panel A. Infections								
Solar Gen_d	0.018	0.019	-0.003	-0.003	-0.009	-0.012	-0.041	-0.040*
	(0.025)	(0.026)	(0.024)	(0.028)	(0.036)	(0.032)	(0.030)	(0.023)
Solar Cap Fac_d	0.003*	0.003	0.001	0.001	-0.0004	-0.0004	-0.002	-0.002
	(0.002)	(0.002)	(0.002)	(0.002)	(0.003)	(0.003)	(0.002)	(0.002)
Panel B. Blood-Related Diseases								
Solar Gen_d	-0.003	-0.003	0.021	0.021	0.002	0.002	0.002	0.002
	(0.005)	(0.008)	(0.015)	(0.017)	(0.014)	(0.016)	(0.012)	(0.010)
Solar Cap Fac_d	-0.001	-0.001	0.001	0.001	0.001	0.001	0.001	0.001
	(0.001)	(0.001)	(0.001)	(0.001)	(0.001)	(0.001)	(0.001)	(0.001)
Panel C. Strokes								
Solar Gen_d	-0.024	-0.025	0.005	0.005	-0.018	-0.022	0.007	0.005
	(0.022)	(0.025)	(0.034)	(0.029)	(0.032)	(0.032)	(0.030)	(0.031)
Solar Cap Fac_d	-0.0002	-0.0003	-0.002	-0.002	-0.002	-0.002	0.001	0.001
	(0.002)	(0.002)	(0.002)	(0.002)	(0.003)	(0.003)	(0.003)	(0.003)
Panel D. Bone Fractures								
Solar_d	0.004	-0.001	0.056	0.057	-0.020	-0.011	-0.040	-0.036
	(0.047)	(0.049)	(0.054)	(0.061)	(0.065)	(0.072)	(0.076)	(0.078)
Solar Cap Fac_d	0.002	0.001	0.009*	0.009*	0.002	0.002	0.001	0.0002
	(0.004)	(0.004)	(0.005)	(0.005)	(0.004)	(0.006)	(0.005)	(0.006)
Panel E. Appendicitis								
Solar_d	0.005	0.005	0.019	0.019	0.045	0.048	0.037	0.039
	(0.023)	(0.022)	(0.024)	(0.032)	(0.034)	(0.039)	(0.035)	(0.033)
Solar Cap Fac_d	0.001	0.001	0.001	0.001	0.001	0.001	0.001	0.001
	(0.002)	(0.002)	(0.002)	(0.003)	(0.003)	(0.003)	(0.003)	(0.003)
Obs.	36,385	36,385	3,830	3,830	5,745	5,745	7,660	7,660
Number of Cities	19	19	2	2	3	3	4	4
City fixed effects	✓		✓		✓		✓	
City×year fixed effects		✓		✓		✓		✓

Notes: This table displays estimation results from OLS regressions of daily hospital admissions on daily solar power generation and daily solar capacity factor using placebo health outcomes. Each row is a separated regression. Solar generation is in GWh. Solar capacity factor is between 0 and 100. Daily hospital admissions are per 100,000 people. Controls include weather, mining production, and demographic covariates. All regressions include controls, year, seasons, year × seasons, and weekend fixed effects. Bootstrapped standard errors using 50 repetitions appear in parentheses. Significance levels: $^{*}p < 0.10$, $^{**}p < 0.05$, $^{***}p < 0.001$.